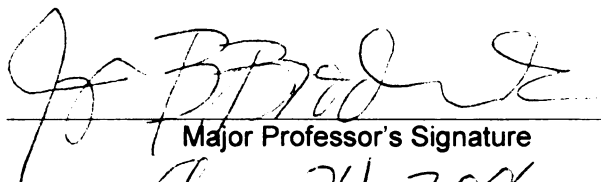This is to certify that the
dissertation entitled

SPORE PHOTOPRODUCT LYASE: INVESTIGATIONS OF A
RADICAL DNA REPAIR ENZYME
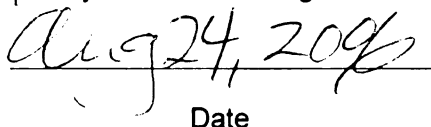
presented by

Jeffrey Michael Buis

has been accepted towards fulfillment
of the requirements for the

__Ph.D.__   degree in   _____Chemistry_____

_____
Major Professor's Signature

Aug 24, 2006
_____
Date

MSU is an Affirmative Action/Equal Opportunity Institution

PLACE IN RETURN BOX to remove this checkout from your record.
TO AVOID FINES return on or before date due.
MAY BE RECALLED with earlier due date if requested.

DATE DUE	DATE DUE	DATE DUE

SPORE PHOTOPRODUCT LYASE: INVESTIGATIONS OF A RADICAL DNA
REPAIR ENZYME

By

Jeffrey Michael Buis

A DISSERTATION

Submitted to
Michigan State University
in partial fulfillment of the requirements
for the degree of

DOCTOR OF PHILOSOPHY

Department of Chemistry

2006

ABSTRACT

SPORE PHOTOPRODUCT LYASE: INVESTIGATIONS OF A RADICAL DNA REPAIR ENZYME

By

Jeffrey Michael Buis

Exposure to ultra-violet light in sporulating bacteria creates a unique form of DNA damage known as the spore photoproduct (SP). Sporulating bacteria contain a novel direct reversal repair enzyme to repair this damage called spore photoproduct lyase (SPL), which catalyzes the repair of SP dimers to thymine monomers. Presented here is the first detailed characterization of catalytically active SPL, which has been anaerobically purified from overexpressing *Escherichia coli*. Anaerobically purified SPL is monomeric and is red-brown in color. The purified enzyme contains ~3.1 iron and 3.0 acid labile S^{2-} per protein and has a UV-visible spectrum characteristic of an iron sulfur proteins ((410 nm 11.9 mM^{-1} cm^{-1}) and 450 nm (10.5 mM^{-1} cm^{-1})). The X-band EPR spectrum of the purified enzyme shows a nearly isotropic signal (g = 2.02) characteristic of a [3Fe-4S]$^{1+}$ cluster; reduction of SPL with sodium dithionite results in the appearance of a new EPR signal (g = 2.03, 1.93, and 1.89) consistent with assignment to a [4Fe-4S]$^{1+}$ cluster. Mössbauer results confirm the presence of a mixture of cluster states in the isolated protein with assignment to [2Fe-2S]$^{2+}$ and [3Fe-4S]$^{1+}$ clusters. Reduction with sodium dithionite yields primarily a [4Fe-4S]$^{1+}$ cluster. The reduced purified enzyme is active in SP repair, with a specific activity of 0.33 μmol/min/mg. This can be increased to 1.33 μmol/min/mg by

using SPL that has been reduced prior to the assay and correlates to 2.4 μmol/min/mg of SPL with a $[4Fe-4S]^{1+}$ cluster. Only a catalytic amount of SPL is required for DNA repair and no irreversible cleavage of S-adenosylmethionine into methionine and 5'-deoxyadenosine is observed during the reaction. Label transfer from $[5'-^3H]$ S-adenosylmethionine to repaired thymine is observed, providing evidence to support a mechanism in which a 5'-deoxyadenosyl radical intermediate directly abstracts a hydrogen from SP C-6 to generate a substrate radical, and subsequent to radical mediated β-scission, a product radical abstracts a hydrogen from 5'-deoxyadenosine to regenerate the 5'-deoxyadenosyl radical. An isotope affect of ~15-17 can be calculated from C-6 - ^3H label transfer experiments, suggesting initial H atom abstraction to be a slow step in the repair reaction. Gel shift assays show SPL binding DNA in the presence and absence of the iron sulfur cluster.

This work is dedicated to my beautiful wife Lorraine Buis who has loved and supported me during all of the endeavors of my life and has put up with me no matter what. I never would have made it without you and look forward to many more adventures together. I would also like to dedicate this work to my parents John and Judith Buis who have always been there to help me in anyway possible.

Austin, Brian Facione and everyone else whose presence had made this such great experience for me.

TABLE OF CONTENTS

CHAPTER VI
MECHANISTIC CONSIDERATIONS FOR SPORE PHOTOPRODUCT LYASE102

CHAPTER VII
DNA BINDING PROPERTIES OF SPORE
PHOTOPRODUCT LYASE 124

CHAPTER VIII

LIST OF TABLES

Table VIII.1. Table of dissociation constants calculated from varying amounts of SPL during equilibrium dialysis. This yielded an average K_d = 200 µM ± 25 µM.150

LIST OF FIGURES

LIST OF SCHEMES

LIST OF ABBREVIATIONS

5'dAdo .... 5'-deoxyadenosine

AdoCbl .... adenosylcobalamin

AdoMet .... S-adenosyl-L-methionine

anRNR .... anaerobic ribonucleotide reductase

ATP .... adenosine triphosphate

APS .... ammonium persulfate

B. subtilus .... *Bacillus subtilis*

BioB .... Biotin Synthase

β-ME .... β-mercaptoethanol

BSA .... bovine serum albumin

CPD .... cyclobutane photodimer

CPM .... counts per minute

DFT .... density functional theory

DNA .... deoxyribonucleic acid

DPM .... disintegrations per minute

DTT .... dithiothreitol

EDTA .... Ethylenedinitrolo)tetra-acetic acid disodium salt dehydrate

ENDOR .... electron nuclear double resonance

EPR .... electron paramagnetic resonance

EXAFS .... extended x-ray absorbtion fine structure

FAD .... flavin adenine dinucleotide

FPLC .... fast protein liquid chromatography

hemN .... oxygen independent coproporphyrinogen-III-oxidase

HPLC .... high performance liquid chromatography

E.coli .... *Escherichia coli*

iMAC .... immobilized metal affinity chromatography

IPTG .... isopropyl-β-D-thioglactopyranoside

LAM .... lysine 2,3 –aminomutase

LB .... Luria-Bertani

LMCT .... ligand to metal charge transfer

NMR... nuclear magnetic resonance

MM... minimal media

MOPS .... 3-(N-morpholino) propanesulfonic acid

PFL.. pyruvate formate lyase

PFL-AE .... pyruvate formate lyase activating enzyme

PMSF.. phenylmethyl sulfonyl fluoride

RNA .... ribonucleic acid

SAM.. S-adenosyl-L-methionine

SDS-PAGE .... sodium dodecyl sulfate-polyacrylamide gel electrophoresis

SP .... spore photoproduct

SPL.. spore photoproduct lyase

SASP .... small acid soluble protein

T.. thymine

TEMED .... N,N,N',N'-tetra-methyl-ethylendiamine

TFA... triflouroacetic acid

CHAPTER I

INTRODUCTION

I.1   Iron Sulfur Clusters in Biology

Iron sulfur clusters are among the most versatile and ubiquitous metal-containing structures found in biology. The most obvious and most well known role for these clusters is electron transport, with most types of iron sulfur clusters possessing at least two readily accessible redox states. The flexible protein environment surrounding the cluster creates a wide range of redox potentials in different proteins. This role as an electron transporter is most notably found in ferredoxins, the mitochondrial electron transport chain, rubredoxin, and the proteins of photosynthesis.[1, 2] There are three types of iron sulfur clusters found commonly in biology in addition to numerous modifications such as the active site centers in hydrogenase and nitrogenase.[3, 4] The three common cluster types are shown in Figure I.1 are the $[2Fe-2S]^{2+/1+}$, $[3Fe-4S]^{1+/0}$ and the $[4Fe-4S]^{3+/2+/1+}$ clusters.[1, 2]

While most of the initial work on iron-sulfur clusters focused on their roles in electron transport, a number of other roles have emerged for these clusters reflecting their diverse and elegant chemistry. For example, iron sulfur clusters

function in regulatory roles,[5] turning gene expression on or off in response to the

level of iron (the iron-responsive element-binding protein),[6, 7] oxygen (the
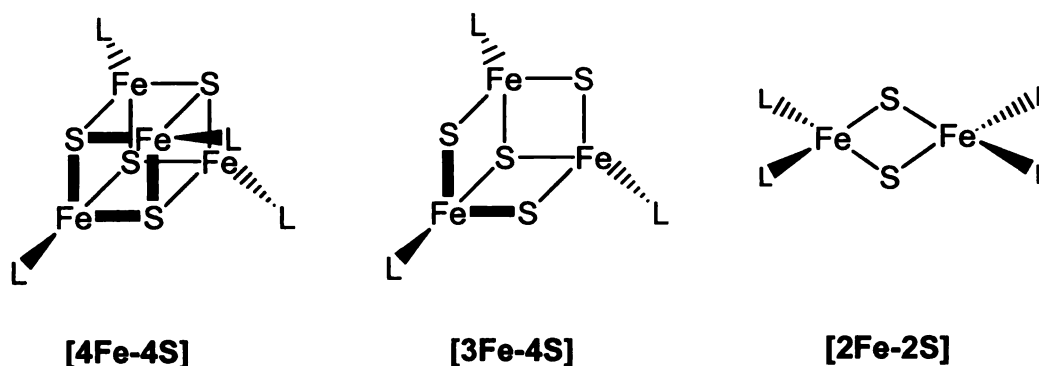
[4Fe-4S]   **[3Fe-4S]**   **[2Fe-2S]**

Figure I.1.   The three major categories of iron sulfur clusters are illustrated including the [4Fe-4S], [3Fe-4S], [2Fe-2S] from left to right.

fumarate-nitrate reduction protein),[8-10] and superoxide (SoxR).[11-13] Iron-sulfur

clusters have also been implicated in both redox (nitrogenase,[14] carbon

monoxide dehydrogenase,[15] hydrogenase[16]) and non-redox (aconitase)

catalysis.[17] In addition there is evidence of a purely structural role for the cluster

in several enzymes including the DNA repair enzymes endonuclease III[18] and

MutY.[19] One of the most intriguing new roles for iron sulfur clusters has been

their involvement in the initiation of radical catalysis in the radical SAM

superfamily.[20-27] This role will be discussed in greater detail later.
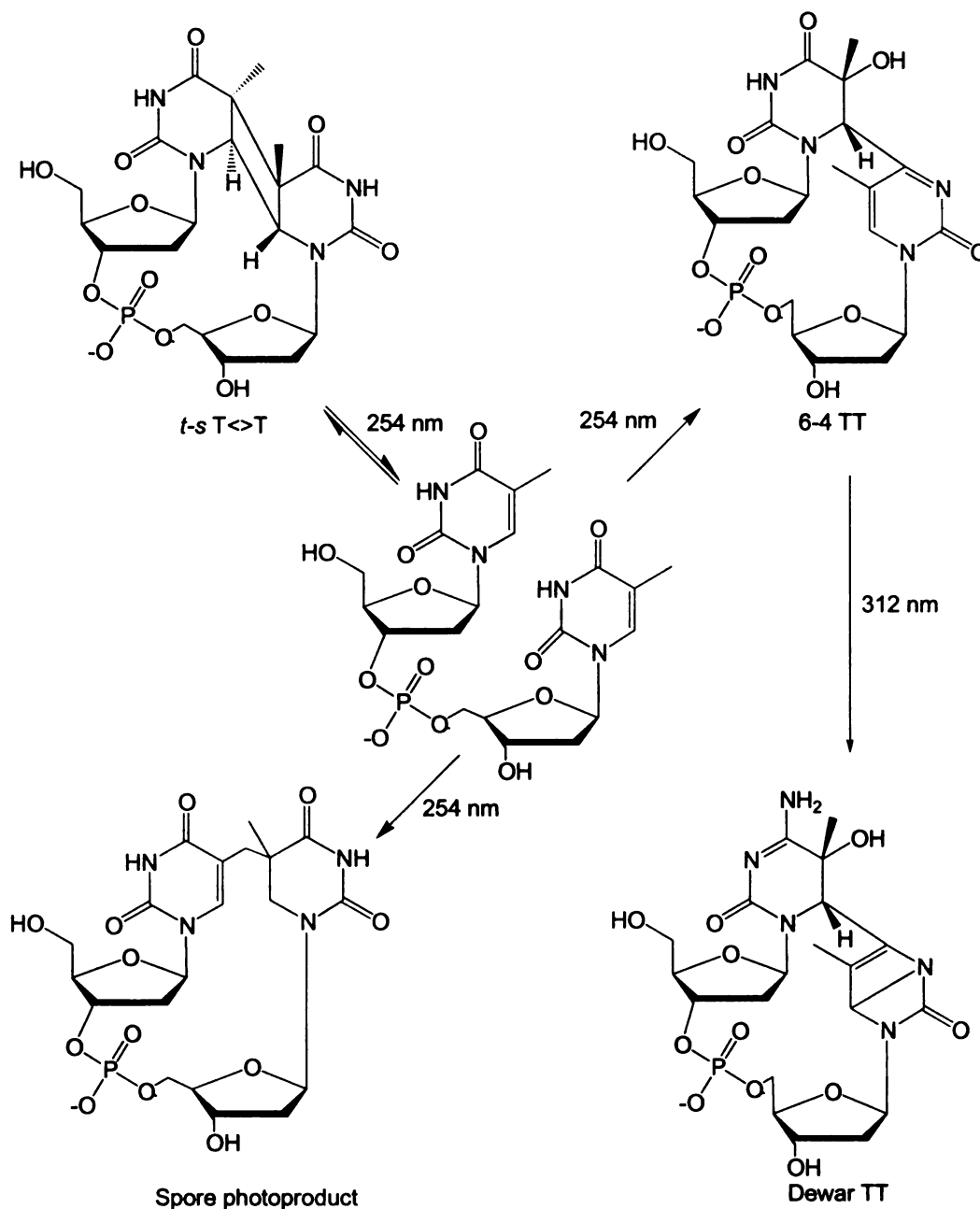
Scheme I.1. An pair of adjacent thymine bases (center) can undergo conversion to a variety of photoproducts when exposed to UV light at 254nm including, a *cis, syn* cyclobutane dimer (*t-s* T<>T, upper left), a spore photoproduct (lower left), and a 6-4 photoproduct (6-4 TT, upper right) which can undergo further conversion to a dewar photoproduct (dewar TT, lower right).

3

I.2   DNA Damage, Spore Photoproduct and Small, Acid Soluble Protein

Recognized as the informationally active component of almost all genetic material, deoxyribonucleic acid (DNA) was first thought to be an extremely stable macromolecule capable of passing the information required for life from generation to generation with little change.[28] It is now know that DNA is not as stable as once thought and is, in fact, subject to constant mutation and damage. These mutations can occur during the replication or recombination of the DNA, from the inherent instability of specific chemical bonds or from environmental factors including chemical (cross-linking agents) and physical (ionizing or UV radiation) sources.[28] Specific types of DNA damage include mismatched base pairs during replication, strand breakage by reactive oxygen species, deamination, depurination, and interstrand crosslinking by a variety of chemical agents.[28] Whatever form of DNA damage that occurs, all of them are harmful to cell viability. Without repair, DNA replication as well as gene transcription will be blocked, inhibiting the cell from producing the proteins and enzymes necessary for cellular function.

As noted above, DNA can be damaged in a number of ways; one such example is by exposure to ultraviolet (UV) light. It has been shown that DNA exposed to ultraviolet light contains a number of damaged DNA photoproducts involving the pyrimidine bases.[29] [30]Among these photoproducts, the primary type of damage is the cyclobutane dimer (CPD), shown in Scheme I.1. However, secondary photoproducts are also produced such as 6-4 photoproducts.[29] In the mid 1960's, an intriguing phenomenon was discovered among sporulating

4

bacteria such as *Bacillus* and *Clostridium*. When exposed to large amounts of

ultraviolet light, most types of bacteria cannot survive; Bacillus and Clostridium

spore were however shown to have a high resistance towards UV light, being 5

to 50 times more resistant to UV light than normal vegetative cells.[31] A clue to

this increased resistance was found by examining the type of DNA damage in UV

exposed spores. It was discovered that the major photoproduct in irradiated

spores was not cyclobutane dimers, as found in vegetative cells, but 5-thyminyl-

5,6-dihydrothymine (now known as spore photoproduct, SP) (Scheme I.1). [29, 32]

In addition to the different type of DNA damage incurred, the protein

composition of bacterial spores is unique. Up to 20% of protein in the spores of

various *Bacillus* species is a group of proteins called small, acid soluble protein

(SASP).[33] The small, acid soluble proteins are so named because the proteins

were found to be soluble in acidic mixtures and thus could be dissolved in acidic

solutions while other proteins precipitated, allowing for easier purification. These

proteins range from 60-73 amino acids (5-7kDa) and appear approximately 3-4

hours after the onset of sporulation.[33] The SASPs can be divided into two types,

the γ and the α/β SASPs.[33] Significant properties of the γ-type SASPs include:

1) They are encoded by a single gene in all species.

2) Their amino acid sequences are highly conserved but not as highly as
   the α/β SASP.

3) They are not associated with spore DNA *in vivo*.[34]

4) Their only known role is as an amino acid reserve for spores during
   germination.

Characteristics of the α/β-type SASP include:

1) They are encoded by a family of seven genes.

2) Their amino acid sequence is highly conserved across families.

3) They are associated with spore DNA in vivo.[34]

4) They play a major role in determining the properties of spore DNA *in vivo* and resistance of spores to UV light.[35]

During spore germination, the SASPs are rapidly degraded to amino acids with their degradation initiated by a novel endonuclease termed the germination protease.[36] The presence of the α/β-type SASP is associated with the spores UV resistance and spores that contain deletion mutants for SASPs show a markedly lower UV resistance.[37] *In vivo* studies have shown that α/β-type SASPs are associated with the spore's chromosomal DNA and this may protect the DNA from damage.[38, 39] It has been proposed that the SASP promotes a conformational change in the DNA when it binds.[40, 41, 42] Cells in the vegetative state are found in the B conformation while spectroscopic evidence suggests the DNA in spores is best described as being in an A conformation. The A conformation of DNA has more bases per helix turn and a wider diameter than the B conformation, which may promote the formation of the methylene bridge in SP as opposed to the cyclobutane dimer.[40-42] SASP has also been shown to bind DNA *in vitro* and overexpression in *E. coli.* can partially change the properties of a cell to be more spore like.[43] However, the mechanism by which SASP promotes the conformational change in DNA or why this causes the major

photoproduct to be changed from the cyclobutane dimer to the spore

photoproduct remains unclear.

I.3   Spore Photoproduct Lyase

Damage to a cell's DNA is extremely harmful and can lead to mutations in

enzymes crucial for cellular function, causing reduced cell viability and increased

cell apoptosis.[28] It is therefore important that a cell has a method for repairing

this damage either by a direct reversal pathway or by nucleotide excision repair.

In nucleotide excision repair the specific base and those around it are cut out of

the DNA strand and replaced by new base pairs leaving the strand repaired.[44, 45]

The direct reversal pathway on the other hand requires an enzyme to specifically

repair the one or more bases that are damaged. An example of this occurs with

the aforementioned cyclobutane dimer. An enzyme known as DNA photolyase

utilizes light to cleave the two bonds forming the thymine bridge.[46] This light

driven enzyme contains two cofactors; one is always a flavin-adenine

dinucleotide (FAD) and the other is a folate, methenyltetrahydrofolate (MTHF) or

a deazaflavin, 8-hydroxy-7, 8-didemethyl-5-deazariboflavin (8-HDF).[47]

Accordingly, the enzymes have been classified into folate class and deazaflavin

class photolyases. The reaction occurs by the DNA photolyase binding to the

damaged DNA and flipping the CPD out of the helix and into the active site cavity

of DNA photolyase.[46, 47] The folate then absorbs a blue light photon and

transfers the excitation energy to the flavin, which then transfers an electron to

the CPD; the 5-5 and 6-6 bonds of the cyclobutane ring are now in violation of

Huckel rules, and therefore, the CPD is split to form two pyrimidines.[46, 47]

Concomitantly, an electron is transferred back to the nascently formed FADH to regenerate the FADH⁻ form.

DNA photolyase is one of the most studied DNA repair proteins; when the initial spore photoproduct was discovered, it was hypothesized that a novel type of DNA photolyase might exist in sporulating bacteria utilizing a similar pathway to cleave the spore photoproduct.[47, 48] Sequence homology studies found that there was gene (*splB*) that showed some C-terminal homology to the DNA photolyases (Table I.1).[49, 50] Another study of this gene found that deletion mutants did not have as high of survival capabilities when exposed to UV light.[48, 51]

- N.c. WSYNVDHFHAWTQGRTGFPIIDAAMRQVLSTGYMHNRLRMI   477
- S.c. WENNPVAFEKWCTGNTGIPIVDAIMRKLLYTGYINNRSRMI   454
- E.c. WQSNPAHLQAWQEGKTGYPIVDAAMRQLNSTGWNHNRLRMI   346
- H.h. WRDDPAALQAWKDGETGYPIVDAGMRQLRAEAYMHNRVRMI   353
- A.n. WENREALFTAWTQAQTGYPIVDAAMRQLTETGWMHNRCRMI   353
- S.g. WRSDADEMHAWKSGLTGYPLVDAAMRQLAHEGWMHNRARML   334

- B.s. SPLDKRIEAAVKVAKAGYPLGFIVAPIYIHEGWEEGYRHLF   250

Table I.1. C-terminal sequence homology between DNA photolyases from different organisms (above) and spore photoproduct lyase from *Bacillus subtilis* (below) shows several conserved residues.
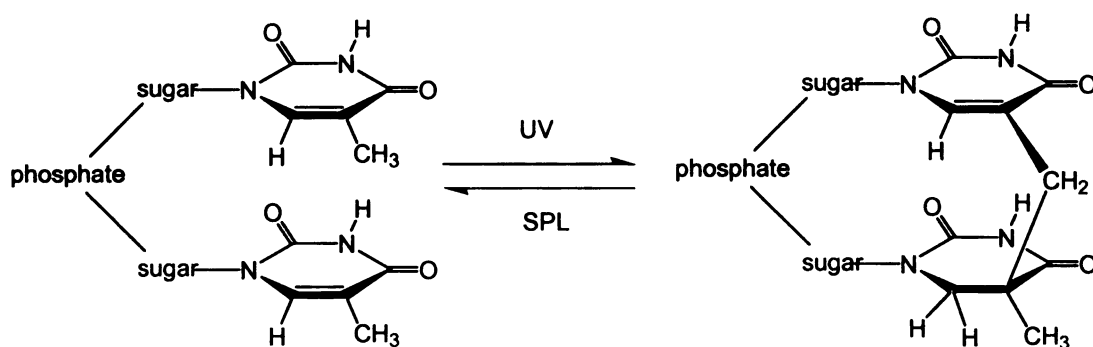
Scheme I.2. The UV induced spore photoproduct is repaired directly by spore photoproduct lyase. The methyl bridge of SP is cleaved by SPL reverting the thymine dimer back to two adjacent thymines.

Dark repair of SP with the new enzyme spore photoproduct lyase (SPL, Scheme I.2) was later demonstrated, differentiating it from the DNA photolyases by functioning independent of light.[45] If SPL does not utilize light to carry out DNA repair, then it must have a different and novel repair mechanism. In fact, sequence homology studies show that it contains a specific sequence, CXXXCXXC (Table I.2), which places it with a group of enzymes known as the radical SAM superfamily.[52] Work carried out by the Nicholson lab confirmed that like other members of the radical SAM superfamily SPL requires the presence of S-adenosylmethionine (SAM) and contains an iron-sulfur cluster. Unlike the DNA photolyases, no flavin is present as a cofactor and no light is needed to initiate DNA repair.[52, 53]

- SP Lyase   86   IPFATGCMGHCHYCYLQTT
- PFL-AE   24   ITFFQGCLMRCLYCHNRDT
- aRNR-AE   20   VLFVTGCLHKCEGCYNRST
- Biotin Synthase 47   SIKTGACPQDCKYCPQTSR
- Lipoate Synthase 48   MILGAICTRRCPFCDVAHG
- LAM   132   LLITDMCSMYCRHCTRRRF
- HemN   53   YFHIPFCQSMCLYCGCSIH
- ThiH   90   LYLSNYCNSKCVYCGFQIL
- MoaA   15   IAVTPECNLDCFFCHMEFK
- BssD   68   TIFLKGCNYKCGFCFHTIN

Table I.2 CX_3CX_2C conserved binding motif of the radical SAM superfamily.

I.4   Radical SAM Superfamily

The radical SAM superfamily is composed of a wide range of proteins with different functionalities and is thought to be composed of over 600 different enzymes.[20] These enzymes range in function from the sulfur insertions of biotin synthase (BioB) [54, 55] and lipoate synthase (LipA)[56] to the protein radical activation of pyruvate formate lyase activating enzyme (PFL-AE) ,[57, 58] anaerobic ribonucleotide reductase activating enzyme (anRNR),[59, 60] and benzylsuccinate synthase activating enzyme.[61] The superfamily contains enzymes that catalyze rearrangement reactions such as lysine 2,3-aminomutase (LAM)[62] and proteins like oxygen-independent coproporphyrinogen-III oxidase (HemN) involved in heme biosynthesis.[63] More recently they have been implicated in the formation of iron sulfur clusters in hydE and hydG[64, 65] and the formation of molybdoterin by moaA.[66] Given the diversity of reactions catalyzed above, it is then not

surprising that the radical SAM superfamily would contain an enzyme capable of DNA repair such as spore photoproduct lyase.[52, 53] The diversity of the superfamily is summarized in Scheme I.3 and illustrates the wide ranging chemistry of its members.

The radical SAM superfamily is a composed of a group of protein with several unique characteristics. First, all members of the radical SAM superfamily share a cysteine motif, CX_3CX_2C. (Table I.2)[20-25] This amino acid sequence coordinates an iron-sulfur cluster as demonstrated by several members of the superfamily.[62, 67, 68] Among proteins with iron sulfur clusters, this sequence is unique because it only has 3 cysteinal ligands capable of coordinating the cluster.[20-25] This leaves open the possibility of either a [3Fe-4S] cluster or a [4Fe-4S] cluster with one non-cysteinal ligand being present. In addition to having the conserved sequence motif, all members in the family coordinate an iron sulfur cluster and all members of the family utilize the small molecule S-adenosyl-L-methionine.[20-25] S-Adenosyl-L-methionine is a naturally occurring molecule distributed in virtually all body tissues and fluids. It is of fundamental importance in a number of biochemical reactions involving enzymatic transmethylation, contributing to the synthesis, activation and/or metabolism of such compounds as hormones, neurotransmitters, nucleic acids, proteins, phospholipids and certain drugs.[69] Its most prominent role has been that of a methyl donor involved in reactions such as the methylation of DNA and RNA.[69] Its role in the radical SAM superfamily is both new and unexpected.[20-25]

11
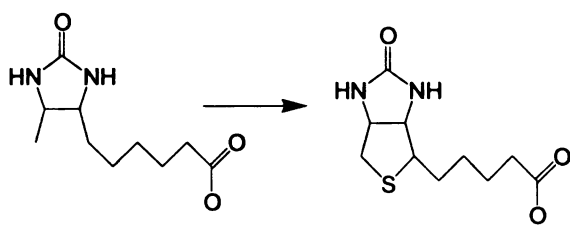
Biotin synthase
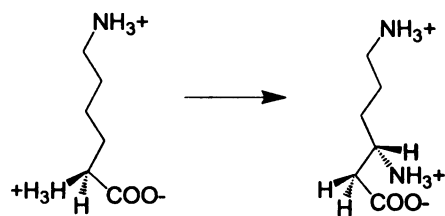
Lysine 2,3 aminomutase
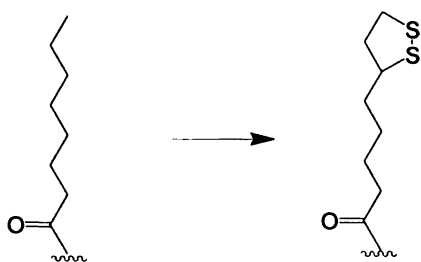
Lipoyl Synthase
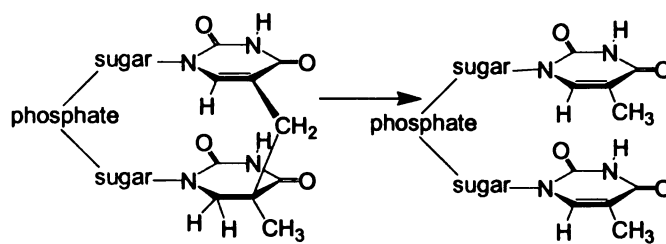
Spore photoproduct lyase
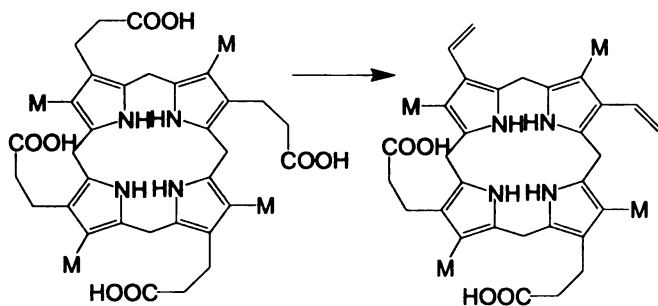
Oxygen-independent coproporphyrinogen-III oxidase
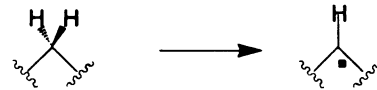
Activating Enzymes

Scheme I.3. The reactions catalyzed by six members of the radical SAM superfamily are shown above, illustrating the superfamily's diverse chemistry.

The discovery of the radical SAM superfamily started in the late 1960's and early 1970's with work carried out by Barker and coworkers on the isomerase, lysine 2,3 aminomutase, which was shown to require SAM rather then the cofactor, adenosylcobalamin (AdoCbl),used by many other isomerases(Scheme I.4).[70] AdoCbl dependent enzymes function by cleaving
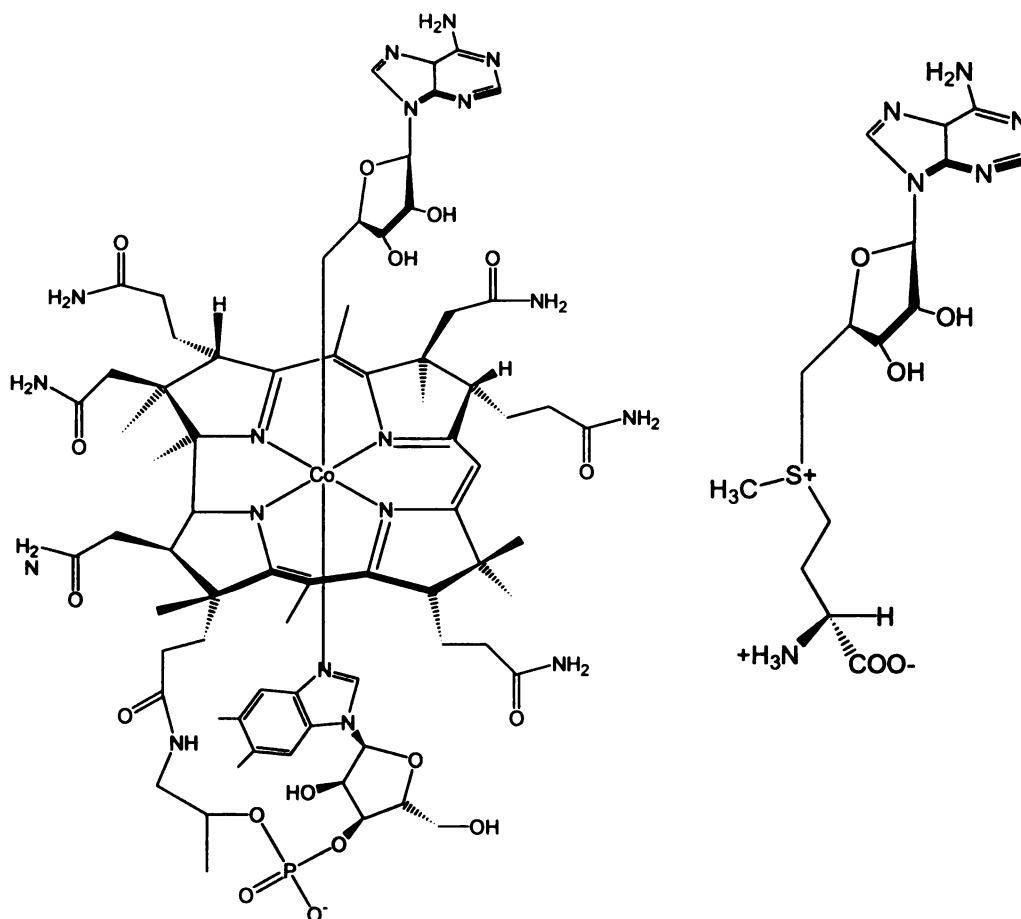
Scheme I.4. Structural comparison of adenosylcobalamin (left) and S-adenosyl-methionine (right) illustrating similarity of Co-C and C-S bond in the two molecules.

the Co-C bond to form an adenosyl radical that can initiate radical catalysis.[71]

Later work carried out by Knappe and coworkers on pyruvate formate lyase

(PFL) showed that it required a second enzyme for activity; this second enzyme

was a SAM-dependent activase which generated a glycyl radical.[72] Given the

above information, it was thought that the members of the radical SAM

superfamily cleave SAM at the C-S bond to form methionine and a

5'deoxyadenosyl radical intermediate (Scheme I.5), the latter being the same

intermediate implicated in the AdoCbl enzymes.[21-26]
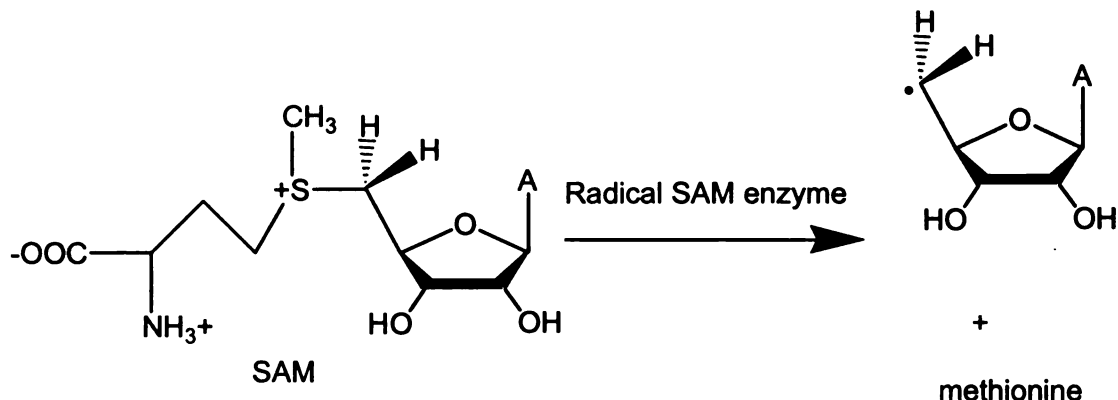
Scheme I.5 Cleavage of SAM by a radical SAM superfamily enzyme yields an adenosyl radical and methionine.

When the first members of the radical SAM superfamily were being

characterized, a review on LAM was published that called S'adenosylmethionine,

"a poor man's adenosylcobalamin,"[73] mainly because of the relatively simple

structure of AdoMet when compared to AdoCbl and because the C-S bond, with

14

an energy of 60 kCal, is double the energy of the C-Co bond at 60 kCal. However, the diversity and complexity of the chemistry carried out in the radical SAM superfamily caused a change in thinking a few years later when a new review by the same author, switched the name to "a wolf in sheep's clothing or a rich man's adenosylcobalamin."[23] While there is still no direct spectroscopic evidence for the presence of this adenosyl radical in the radical SAM reactions, work carried out on LAM allowed direct detection of an allylic analog of the putative 5'-deoxyadenosine radical intermediate.[74, 75]

As previously mentioned, with only three cysteine residues available to coordinate the iron sulfur cluster, the potential exists for multiple kinds of iron sulfur clusters to be present, along with the possibility of a non-cysteinal fourth ligand to coordinate a [4Fe-4S] cluster. Initial isolation and characterization of several enzymes including PFL-AE and BioB showed several cluster states present in the protein, including a $[3Fe-4S]^{1+}$ and $[4Fe-4S]^{2+}$ that could be reduced to a $[4Fe-4S]^{1+}$.[68, 76, 77] An elegant study by Broderick and co-workers with electron paramagnetic resonance (EPR) spectroscopy correlated the disappearance of the $[4Fe-4S]^{1+}$ signal with the appearance of an organic glycyl radical signal.[78] Other studies on LAM and anRNR had also shown the presence of a $[4Fe-4S]^{1+}$ signal in active protein.[60, 79] Taken together these results strongly suggested that the active cluster of the radical SAM superfamily was the $[4Fe-4S]^{1+}$ cluster. If the active cluster of the superfamily is the $[4Fe-4S]^{1+}$, then with

only 3 cysteinal ligands present to coordinate the cluster, the cluster is expected to be site-differentiated.

Another well studied enzyme that contains a unique iron is aconitase. Electron double nuclear resonance (ENDOR) studies on aconitase confirm coordination to the unique iron site by the substrate citrate via the carboxyl oxygens.[80-82] Model structures based on ENDOR studies in coordination with Mössbauer spectroscopy on PFL-AE confirmed the presence of the unique iron in the radical SAM superfamily.[58, 83, 84] The data provided evidence for coordination to the unique iron by the amino nitrogen and carboxyl oxygen of SAM, analogous to the coordination of citrate to aconitase (Scheme I.6).[84]
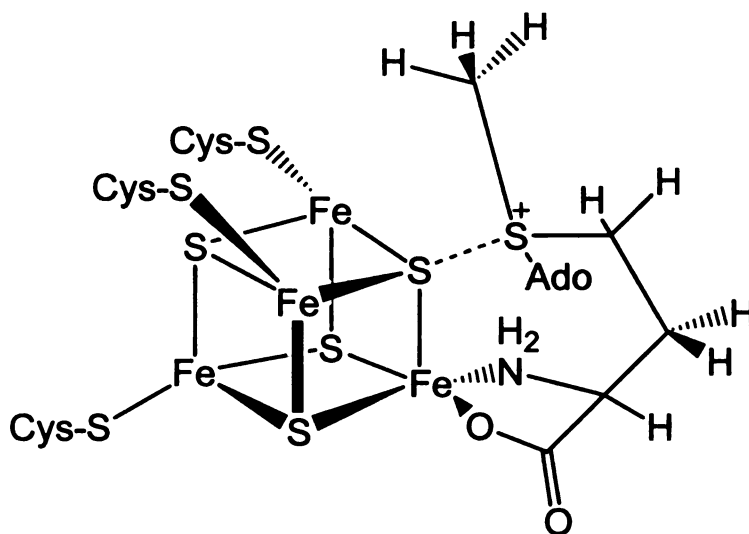
Scheme I.6. ENDOR based model of SAM binding to the [4Fe-4S] cluster of PFL-AE. The unique iron is coordinated by the amino nitrogen and carboxyl oxygen. Evidence for orbital overlap between the sulfonium sulfur and the cluster was also obtained.

16

ENDOR experiments also show an orbital overlap between the cluster and the sulfonium from SAM. Extended x-ray absorption fine structure (EXAFS) studies on the PFL-AE/Se-SAM interaction show no interaction between the selenium cation and the unique iron of the cluster, suggesting that the orbital overlap occurs via a bridging sulfide.[85] Together, the results suggest the possibility of sulfur centered rather than iron-centered, redox chemistry.[83]

ENDOR and EXAFS studies carried out on LAM, however, suggest slightly different model. While the ENDOR studies of LAM also show coordination to the unique iron as with PFL-AE, the sulfonium appears to interact with the iron of the cluster, suggesting a slightly different binding mode and possibly iron centered redox chemistry.[86, 87] Both of these results suggested an inner sphere pathway for electron transfer in the homolytic scission of the 5' C–S bond in SAM.[57, 58, 83, 86, 87] Noteworthy to this discussion, PFL-AE utilizes SAM as a substrate, while in LAM it acts as a cofactor. This is a possible rationale for the difference of sulfonium interaction in PFL-AE and LAM.

With the recent explosion of interest in the radical SAM superfamily several crystal structures have been reported including HemN, BioB, MoaA and LAM.[63, 66, 88, 89] A striking feature of these crystal structures is their similarity to each other despite the diversity of their chemistry being performed. All of the structures solved to date, share a $(\beta/\alpha)_6$ repeat motif in their structural cores. Alignment of this motif for all four structures places the iron–sulfur cluster at the same location relative to the motif. The β-sheet formed by this motif is extended

on both sides in MoaA, HemN, and LAM to form a larger crescent channel closed by an additional domain, whereas the sheet is extended by two additional β/α repeats in BioB which closes to form a TIM barrel.[89] The location of SAM relative to the iron sulfur cluster is also confirmed in these crystal structures, with the binding of the unique iron by the amino nitrogen and carboxyl oxygen.[63, 66, 88-90]

I.5   Recent Work on Spore Photoproduct Lyase

Initial work on SPL in the Nicholson lab showed conclusive evidence for SPL's ability to repair spore photoproduct *in vitro*, with specific binding to SP and not CPD.[91] In addition to this work, it was shown that SPL required SAM to carry out DNA repair and did this in the absence of light.[52] Further work on SPL confirmed the presence of an iron sulfur cluster in the protein, with the as-isolated protein containing a $[3Fe-4S]^{1+}$ that can be reduced with dithionite to a $[4Fe-4S]^{1+}$ cluster as monitored by EPR.[53] High performance liquid chromatography (HPLC) studies provided evidence for SAM cleavage by the enzyme with loss of the $[4Fe-4S]^{1+}$ EPR signal.[53] The same study proposed SPL to be a homodimer with the iron sulfur cluster serving to bind the two subunits.[53] Based on recent crystal structure of four other radical SAM superfamily members, the proposal of a homodimer with the cluster at the center seems unlikely. It is also noteworthy that the experiments in this publication did not involve protein that was shown to be active in SP repair.[53]

A mechanism for SPL was published in 1999 by Mehl and Begley in which SAM is utilized as a protein cofactor (Scheme I.7).[92] In this mechanism an electron from the cluster is transferred to SAM whereupon SAM is cleaved to methionine and the putative 5'-deoxyadnosyl radical. This radical abstracts hydrogen from the C-6 position creating a carbon radical on the thymine ring which induces a radical mediated β-scission. The subsequent carbon radical reabstracts a hydrogen atom from 5'-deoxyadenosine and reforms the initial adenosyl radical. This can then go on to further catalysis or reform SAM by the loss of an electron to the cluster.[92] This mechanism is supported by the work of Cheek and Broderick in which SP tritiated at the C-6 position is transferred to SAM, where as SP tritiated at the methyl bridge is not seen in SAM.[93] The mechanism is further confirmed by a Hartree-Fock/density functional theory calculation (DFT) with a slight modification where an additional inter-thymine hydrogen transfer step taking place before the reabstraction of hydrogen to the 5'-deoxyadenosine. The DFT calculations show the last step to be rate determining.[94]

It has been shown more recently that UV irradiation of DNA can produce both inter-strand and intra-strand spore photoproducts.[95-97] A recent study has concluded that SPL can repair the inter-strand but not the intra-strand spore photoproduct. In this study, SP was synthetically produced without incorporation into a DNA strand and repaired with SPL. Repair was tracked via HPLC and mass spectrometry.[98] This is an intriguing result but without incorporation of the synthetic SP into a DNA strand it is difficult to apply it to *in vivo* conditions.

Scheme I.7 Proposed mechanism for the repair of spore photoproduct by spore photoproduct lyase, involving the cleavage of SAM with subsequent hydrogen extraction from C-6 creating a ring based radical. This C-6 radical abstracts a hydrogen from the methyl bridge resulting in thymine separation. The resulting radical is reabstracted by 5'-deoxyadenosine to reform the adenosyl radical.
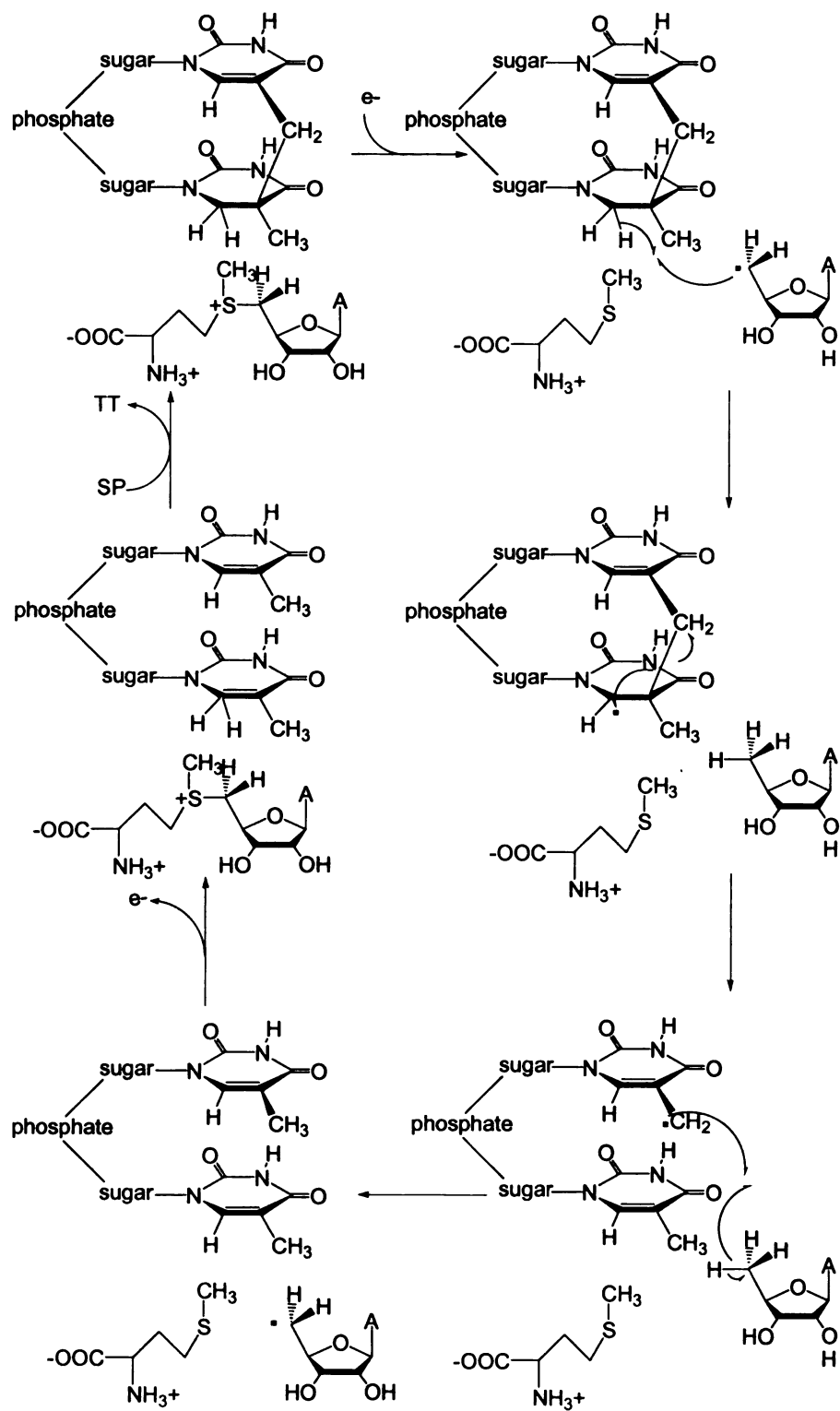
Scheme 1.7

The results reported within, further add to the knowledge base on the spore photoproduct lyase with a focus on cluster identification, SAM cluster interaction, SP repair kinetics and SPL-DNA interaction. We have purified SPL with a higher iron and sulfur content than previously reported and shown under these conditions in the absence of cluster reconstitution that it is monomeric. Our study further analyzes the cluster with an array of spectroscopic techniques and looks at the enzyme mechanism with the conclusion that unlike, PFL-AE but similar to LAM, SAM is utilized as a cofactor by SPL.

I.6 References

1. Beinert, H., Iron-sulfur proteins: ancient structures, still full of surprises. *J. Biol. Inorg. Chem.* **2000,** 5, 2-15.

2. Beinert, H.; Holm, R. H.; Munck, E., Iron-sulfur clusters: nature's modular, multipurpose structures. *Science* **1997,** 277, (5326), 653-659.

3. Peters, J., Structure and mechanism of iron-only hydrogenases. *Current Opinion in Structural Biology* **1999,** 9, (6), 670-676.

4. Drennan, C. L.; Peters, J., Suprising cofactors in metalloenzymes. *Current Opinion in Structural Biology* **2003,** 13, (2), 220-226.

5. Rouault, T. A.; Klausner, R. D., Iron-sulfur clusters as biosensors of oxidants and iron. *Trends Biochem. Sci.* **1996,** 21, 174-177.

6. Haile, D. J.; Rouault, T. A.; Harford, J. B.; Kennedy, M. C.; Blondin, G. A.; Beinert, H.; Klausner, R. D., The iron responsive element binding protein: A target for synaptic actions of nitric oxide. *Proceedings of the National Academy of Sciences of the United States of America* **1992,** 89, 11735-11739.

7. Hentze, M. W.; Kuhn, L. C., Molecular control of vertebrate iron metabolism: mRNA based regulatory circuits operated by iron, nitric oxide and oxidative stress *Proceedings of the National Academy of Sciences of the United States of America* **1996,** 93, 8175-8182.

8. Khoroshilova, N.; Beinert, H.; Kiley, P., Association of a polynuclear iron-sulfur center with a mutant FNR protein enhances DNA binding. *Proceedings of the National Academy of Sciences of the United States of America* **1995,** 92, 2499-2503.

9. Khoroshilova, N.; Popescu, C.; Munck, E.; Beinert, H.; Kiley, P. J., Iron-sulfur cluster disassembly in the FNR protein of *Escherichia coli* by O_2: [4Fe-4S] to [2Fe-2S] conversion with loss of biological activity. *Proceedings of the National Academy of Sciences of the United States of America* **1997,** 94, 6087-6092.

10. Popescu, C.; Bates, D. M.; Beinert, H.; Munck, E.; Kiley, P., Mössbauer spectroscopy as a tool for the study of activation/inactivation of the transcription regulator FNR in whole cells of *Escherichia coli. Proceedings of the National Academy of Sciences of the United States of America* **1998,** 95, 13431-13435.

11. Hildago, E.; Ding, H.; Demple, B., Direct nitric oxide signal transduction via nitrosylation of iron-sulfur centers in the SoxR transcription activator. *Trends Biochem. Sci.* **1997,** 22, 207-210.

12. Demple, B., A bridge to control. *Science* **1998**, 279, 1655-1656.

13. Ding, H.; Demple, B., *In vivo* kinetics of a redox-regulated transcriptional switch. *Proceedings of the National Academy of Sciences of the United States of America* **1997**, 94, 8445-8449.

14. Burgess, B. K.; Lowe, D. J., Mechanism of Molybdenum Nitrogenase. *Chem. Rev.* **1996**, 96, 2983-3011.

15. Drennan, C. L.; Heo, J.; Sintchak, M. D.; Schreiter, E.; Ludden, P. W., Life on carbon monoxide: X-ray structure of *Rhodospirillum rubrum* Ni-Fe-S carbon monoxide dehydrogenase. *Proceedings of the National Academy of Sciences of the United States of America* **2001**, 98, 11973-11978.

16. Vignais, P. M.; Colbeau, A., Molecular biology of microbial hydrogenases. *Curr. Issues Mol. Bio.* **2004**, 6, (2), 159-188.

17. Beinert, H.; Kennedy, M. C., Aconitase, a two-faced protein: enzyme and iron regulatory factor. *FASEB J.* **1993**, 7, 1442-1449.

18. Cunningham, R. P.; Asahara, H.; Bank, J. F.; Scholes, C. P.; Salerno, J. C.; Surerus, K.; Munck, E.; McCracken, J.; Peisach, J.; Emptage, M. H., Enodnuclease III is an iron sulfur protein. *Biochemistry* **1989**, 28, 4450-4455.

19. Porello, S. L.; Cannon, M. J.; David, S. S., Site-Directed Mutagenesis of the Cysteine Ligands to the [4Fe-4S] Cluster of *Escherichia coli* MutY. *Biochemistry* **1998**, 37, 6465-6475.

20. Sofia, H. J.; Chen, G.; Hetzler, B. G.; Reyes-Spindola, J. F.; Miller, N. E., Radical SAM, a novel protein superfamily linking unresolved steps in familiar biosynthetic pathways with radical mechanisms: functional characterization using new analysis and information visualization methods. *Nucleic Acids Research* **2001**, 29, (5), 1097-1106.

21. Cheek, J.; Broderick, J. B., Adenosylmethionine-dependent iron-sulfur enzymes: versatile clusters in a radical new role. *Journal of biological inorganic chemistry: J. Biol. Inorg. Chem.* **2001**, 6, (3), 209-26.

22. Frey, P. A., Radical mechanisms of enzymatic catalysis. *Annual Review of Biochemistry* **2001**, 70, 121-148.

23. Frey, P. A.; Magnusson, O. T., S-adenosylmethionine: A wolf in sheep's clothing, or a rich man's adenosylcobalamin? *Chemical Reviews* **2003**, 103, (6), 2129-2148.

24. Fonetcave, M.; Mulliez, E.; Ollagnier de-Choudens, S., Adenosylmethionine as a source of 5'-deoxyadenosyl radicals.*Curr. Opin. Chem. Biol.* **2001,** 5, 506-511.

25. Jarrett, J. T., *Curr. Opin. Chem. Biol.* **2003,** 7, 174-182.

26. Broderick, J. B., Iron-sulfur clusters in enzyme catalysis. *Comprehensive Coordination Chemistry II* **2004,** 8, 739-757.

27. Marsh, E. N. G.; Patwardhan, A.; Huhta, M. S., S-Adenosylmethionine radical enzymes. *Bioorganic Chemistry* **2004,** 32, (5), 326-340.

28. Friedberg, E. C.; Walker, G. C.; Siede, W., *DNA Repair and Mutagenesis.* ASM Press: Washington D.C., 1995.

29. Donnellan, J. E., Jr.; Setlow, R. B., Thymine photoproducts but not thymine dimers found in ultraviolet-irradiated bacterial spores. *Science* **1965,** 149, 308-310.

30. Smith, K. C.; Hanawalt, P. C., *Molecular Photobiology.* Academic: New York, 1969.

31. Stoy, J. H., *Biochimica et Biophysica Acta* **1956,** 22, 241-246.

32. Varghese, A. J., 5-Thyminyl-5,6-dihydrothymine from DNA irradiated with ultraviolet light. *Biochemical and Biophysical Research Communications* **1970,** 38, 484-490.

33. Setlow, P., Small, acid-soluble, spore proteins of Bacillus species: structure, synthesis, genetics, function and degradation. *Annual Review of Microbiology* **1988,** 42, 319-338.

34. Francesconi, S. C.; MacAlister, T. J.; Setlow, B.; Setlow, P., Immunoelectron microscopic localization of small, acid-soluble proteins in sporulating cells of *Bacillus subtilis. J. Bacteriol.* **1998,** 170, 5963-5967.

35. Mason, J. M.; Setlow, P., Essential role of small, acid-soluble spore proteins in resistance of *Bacillus subtilis* spores to UV light. *J. Bacteriol.* **1986,** 167, 174-178.

36. Setlow, P., Resistance of Spores of Bacillus Species to Ultraviolet Light. *Environmental and Molecular Mutagenesis* **2001,** 38, 97-104.

37. Setlow, B.; Setlow, P., Thymine-containing dimers as well as spore photoproducts are found in ultraviolet-irradiated Bacillus subtilis spores that lack small acid-soluble proteins. *Proceedings of the National Academy of Sciences of the United States of America* **1987,** 84, (2), 421-3.

38. Francesconi, S. C.; MacAlister, T. J.; Setlow, B.; Setlow, P., Immunoelectron microscopic localization of small, acid-soluble proteins in sporulating cells of *Bacillus subtilis*. *J. Bacteriol*. **1988**, 170, 5963-5967.

39. Donnellan, J. E., Jr.; Stafford, R. S., Ultraviolet photochemistry and photobiology of vegetative cells and spores of Bacillus megaterium. *Biophysical Journal* **1968**, 8, (1), 17-28.

40. Mohr, S. C.; Sokolov, N. V. H. A.; He, C.; Setlow, P., Binding of small acid-soluble spore proteins from Bacillus subtilis changes the conformation of DNA from B to A. *Proceedings of the National Academy of Sciences of the United States of America* **1991**, 88, (1), 77-81.

41. Setlow, P., DNA in dormant spores of Bacillus species is in an A-like conformation. *Molecular Microbiology* **1992**, 6, (5), 563-7.

42. Setlow, B.; Sun, D.; Setlow, P., Studies of the interaction between DNA and a/b-type small, acid-soluble spore proteins: a new class of DNA-binding proteins. *J. Bacteriol*. **1992**, 174, 2312-2322.

43. Setlow, B.; Hand, A. R.; Setlow, P., Synthesis of a Bacillus subtilis small, acid-soluble spore protein in Escherichia coli causes cell DNA to assume some characteristics of spore DNA. *Journal of Bacteriology* **1991**, 173, (5), 1642-53.

44. Munakata, N.; Rupert, C. S., Genetically controlled removal of "spore photoproduct" from deoxyribonucleic acid of ultraviolet-irradiated Bacillus subtilis spores. *Journal of Bacteriology* **1972**, 111, (1), 192-8.

45. Munakata, N.; Rupert, C. S., Dark repair of DNA containing spore photoproduct in Bacillus subtilis. *Molecular and General Genetics* **1974**, 130, (3), 239-50.

46. Sancar, A., Structure and Function of DNA Photolyase and Cryptochrome Blue-Light Photoreceptors. *Chemical Reviews* **2003**, 103, (6), 2203-2237.

47. Carell, T.; Burgdorf, L. T.; Kundu, L. M.; Cichon, M., The mechanism of action of DNA photolyases. *Current Opinion in Chemical Biology* **2001**, 5, (5), 491-498.

48. Munakata, N., Genetic analysis of a mutant of Bacillus subtilis producing ultraviolet-sensitive spores. *Mol. Gen. Genet*. **1969**, 104, 258-263.

49. Brennan, R. G.; Matthews, B. W., The helix-turn-helix DNA binding motif. *J. Biol. Chem*. **1989**, 264, 1903-1906.

50. Fajardo-Cavazos, P.; Salazar, C.; Nicholson, W. L., Molecular cloning and characterization of the Bacillus subtilis spore photoproduct lyase (spl)

gene, which is involved in repair of UV radiation-induced DNA damage during spore germination. *Journal of bacteriology* **1993**, 175, (6), 1735-44.

51. Munakata, N.; Ikeda, Y., *Biochemical and Biophysical Research Communications* **1968**, 33, 469-475.

52. Rebeil, R.; Sun, Y.; Chooback, L.; Pedraza-Reyes, M.; Kinsland, C.; Begley, T. P.; Nicholson, W. L., Spore photoproduct lyase from Bacillus subtilis spores is a novel iron-sulfur DNA repair enzyme which shares features with proteins such as class III anaerobic ribonucleotide reductases and pyruvate-formate lyases. *Journal of bacteriology* **1998**, 180, (18), 4879-85.

53. Rebeil, R.; Nicholson, W. L., The subunit structure and catalytic mechanism of the Bacillus subtilis DNA repair enzyme spore photoproduct lyase. *Proceedings of the National Academy of Sciences of the United States of America* **2001**, 98, (16), 9038-43.

54. Jarrett, J. T., The novel structure and chemistry of iron-sulfur cluster in the adenosylmethionie-dependent radical enzyme biotin synthase. *Archives of Biochemistry and Biophysics* **2003**, 433, 312-321.

55. Lotierzo, M.; Bui, B. T. S.; Florentin, D.; Escalettes, F.; Marquet, A., Biotin synthase mechanism: an overview. *Biochemical Society Transactions* **2005**, 33, (4), 820-823.

56. Ollagnier de-Choudens, S.; Fonetcave, M., The lipoate synthase from Escherichia coli is an iron-sulfur protein. *FEBS Letters* **1999**, 453, 25-28.

57. Buis, J. M.; Broderick, J. B., Pyruvate formate-lyase activating enzyme: elucidation of a novel mechanism for glycyl radical formation. *Archives of Biochemistry and Biophysics* **2005**, 433, (1), 288-296.

58. Walsby, C. J.; Ortillo, D.; Yang, J.; Nnyepi, M. R.; Broderick, W. E.; Hoffman, B. M.; Broderick, J. B., Spectroscopic Approaches to Elucidating Novel Iron-Sulfur Chemistry in the \"Radical-SAM\" Protein Superfamily. *Inorganic Chemistry* **2005**, 44, (4), 727-741.

59. Tamarit, J.; Mulliez, E.; Meier, C.; Trautwein, A.; Fontecave, M., The anaerobic ribonucleotide reductase from Escherichia coli. The small protein is an activating enzyme containing a $[4Fe-4S]^{2+}$ center. *Journal of Biological Chemistry* **1999**, 274, (44), 31291-31296.

60. Tamarit, J.; Gerez, C.; Meier, C.; Mulliez, E.; Trautwein, A.; Fontecave, M., The activating component of the anaerobic ribonucleotide reductase from Escherichia coli. An iron-sulfur center with only three cysteines. *Journal of Biological Chemistry* **2000**, 275, (21), 15669-15675.

61. Leuthner, B.; Leutwein, C.; Schulz, H.; Horth, P.; Haehnel, W.; Schiltz, E.; Schagger, H.; Heider, J., Biochemical and genetic characterization of benzylsuccinate synthase from Thauera aromatica: a new glycyl radical enzyme catalysing the first step in anaerobic toluene metabolism. *Molecular microbiology* **1998**, 28, (3), 615-28.

62. Petrovich, R. M.; Ruzicka, F. J.; Reed, G. H.; Frey, P. A., Characterization of iron-sulfur clusters in lysine 2,3-aminomutase by electron paramagnetic resonance spectroscopy. *Biochemistry* **1992**, 31, (44), 10774-81.

63. Layer, G.; Moser, J.; Heinz, D. W.; Jahn, D.; Schubert, W.-D., Crystal structure of coproporphyrinogen III oxidase reveals cofactor geometry of Radical SAM enzymes. *EMBO Journal* **2003**, 22, (23), 6214-6224.

64. Rubach, J. K.; Brazzolotto, X.; Gaillard, J.; Fontecave, M., Biochemical characterization of the HydE and HydG iron-only hydrogenase maturation enzymes from Thermatoga maritima. *FEBS Letters* **2005**, 579, (22), 5055-5060.

65. Posewitz, M. C.; King, P. W.; Smolinski, S. L.; Zhang, L.; Seibert, M.; Ghirardi, M. L., Discovery of Two Novel Radical S-Adenosylmethionine Proteins Required for the Assembly of an Active [Fe] Hydrogenase. *J. Biol. Chem.* **2004**, 279, 25711-25720.

66. Haenzelmann, P.; Schindelin, H., Crystal structure of the S-adenosylmethionine-dependent enzyme MoaA and its implications for molybdenum cofactor deficiency in humans. *Proceedings of the National Academy of Sciences of the United States of America* **2004**, 101, (35), 12870-12875.

67. Broderick, J. B.; Duderstadt, R. E.; Fernandez, D. C.; Wojtuszewski, K.; Henshaw, T. F.; Johnson, M. K., Pyruvate formate-lyase activating enzyme is an iron-sulfur protein. *Journal of the American Chemical Society* **1997**, 119, (31), 7396-7397.

68. Sanyal, I.; Cohen, G.; Flint, D. H., Biotin Synthase: Purification, Characterization as a [2Fe-2S] Cluster Protein, and *in Vitro* Activity of the *Escherichia coli bioB* Gene Product. *Biochemistry* **1994**, 3625-3631.

69. Grillo, M. A.; Colombatto, S., S-Adenosylmethionine and protein methylation. *Amino Acids* **2005**, 28, 357-362.

70. Chirpich, T. P.; Zappia, V.; Costilow, R. N.; Barker, H. A., Lysine 2,3-aminomutase. Purification and properties of a pyridoxal phosphate and S-adenosylmethionine-activated enzyme. *J. Biol. Chem.* **1970**, 245, (7), 1778-1789.

71. Banerjee, R., Radical peregrinations catalyzed by coenzyme B12-dependent enzymes. *Biochemistry* **2001**, 40, 6191-6198.

72. Knappe, J.; Schmitt, T., A novel reaction of S-adenosyl-L-methionine correlated with the activation of pyruvate formate-lyase. *Biochemical and Biophysical Research Communications* **1976**, 71, 1110-1117.

73. Frey, P. A., Lysine 2,3-aminomutase: is adenosylmethionine a poor man's adenosylcobalamin? *FASEB J.* **1993**, 7, (8), 662-670.

74. Magnusson, O. T.; Reed, G. H.; Frey, P. A., Spectroscopic Evidence for the Participation of an Allylic Analogue of the 5'-Deoxyadenosyl Radical in the Reaction of Lysine 2,3-Aminomutase. *Journal of the American Chemical Society* **1999**, 121, (41), 9764-9765.

75. Magnusson, O. T.; Reed, G. H.; Frey, P. A., Characterization of an Allylic Analogue of the 5'-Deoxyadenosyl Radical: An Intermediate in the Reaction of Lysine 2,3-Aminomutase. *Biochemistry* **2001**, 40, (26), 7773-7782.

76. Broderick, J. B.; Henshaw, T. F.; Cheek, J.; Wojtuszewski, K.; Smith, S. R.; Trojan, M. R.; McGhan, R. M.; Kopf, A.; Kibbey, M.; Broderick, W. E., Pyruvate formate-lyase-activating enzyme: Strictly anaerobic isolation yields active enzyme containing a [3Fe-4S]+ cluster. *Biochemical and Biophysical Research Communications* **2000**, 269, (2), 451-456.

77. Krebs, C.; Henshaw, T. F.; Cheek, J.; Huynh, B. H.; Broderick, J. B., Conversion of 3Fe-4S to 4Fe-4S Clusters in Native Pyruvate Formate-Lyase Activating Enzyme: Moessbauer Characterization and Implications for Mechanism. *Journal of the American Chemical Society* **2000**, 122, (50), 12497-12506.

78. Henshaw, T. F.; Cheek, J.; Broderick, J. B., The [4Fe-4S]1+ Cluster of Pyruvate Formate-Lyase Activating Enzyme Generates the Glycyl Radical on Pyruvate Formate-Lyase: EPR-Detected Single Turnover. *Journal of the American Chemical Society* **2000**, 122, (34), 8331-8332.

79. Petrovich, R. M.; Ruzicka, F. J.; Reed, G. H.; Frey, P. A., Characterization of iron-sulfur clusters in lysine 2,3-aminomutase by electron paramagnetic resonance spectroscopy. *Biochemistry* **1992**, 31, 10774-10781.

80. Telser, J.; Emptage, M. H.; Merkle, H.; Kennedy, M. C.; Beinert, H.; Hoffman, B. M., Oxygen-17 electron nuclear double resonance characterization of substrate binding to the 4-iron-4-sulfur ([4Fe-4S]1+) cluster of reduced active aconitase. *Journal of Biological Chemistry* **1986**, 261, (11), 4840-6.

81. Werst, M. M.; Kennedy, M. C.; Beinert, H.; Hoffman, B. M., Oxygen-17, proton, and deuterium electron nuclear double resonance characterization of solvent, substrate, and inhibitor binding to the iron-sulfur [4Fe-4S]$^+$ cluster of aconitase. *Biochemistry* **1990**, 29, (46), 10526-32.

82. Werst, M. M.; Kennedy, M. C.; Houseman, A. L. P.; Beinert, H.; Hoffman, B. M., Characterization of the iron-sulfur [4Fe-4S]$^+$ cluster at the active site of aconitase by iron-57, sulfur-33, and nitrogen-14 electron nuclear double resonance spectroscopy. *Biochemistry* **1990**, 29, (46), 10533-40.

83. Walsby, C. J.; Hong, W.; Broderick, W. E.; Cheek, J.; Ortillo, D.; Broderick, J. B.; Hoffman, B. M., Electron-Nuclear Double Resonance Spectroscopic Evidence That S-Adenosylmethionine Binds in Contact with the Catalytically Active [4Fe-4S]$^+$ Cluster of Pyruvate Formate-Lyase Activating Enzyme. *Journal of the American Chemical Society* **2002**, 124, (12), 3143-3151.

84. Walsby, C. J.; Ortillo, D.; Broderick, W. E.; Broderick, J. B.; Hoffman, B. M., An Anchoring Role for FeS Clusters: Chelation of the Amino Acid Moiety of S-Adenosylmethionine to the Unique Iron Site of the [4Fe-4S] Cluster of Pyruvate Formate-Lyase Activating Enzyme. *Journal of the American Chemical Society* **2002**, 124, (38), 11270-11271.

85. Cosper, M. M.; Cosper, N. J.; Hong, W.; Shokes, J. E.; Broderick, W. E.; Broderick, J. B.; Johnson, M. K.; Scott, R. A., Structural studies of the interaction of S-adenosylmethionine with the [4Fe-4S] clusters in biotin synthase and pyruvate formate-lyase activating enzyme. *Protein Science* **2003**, 12, (7), 1573-1577.

86. Chen, D.; Walsby, C.; Hoffman, B. M.; Frey, P. A., Coordination and Mechanism of Reversible Cleavage of S-Adenosylmethionine by the [4Fe-4S] Center in Lysine 2,3-Aminomutase. *Journal of the American Chemical Society* **2003**, 125, (39), 11788-11789.

87. Cosper, N. J.; Booker, S. J.; Ruzicka, F.; Frey, P. A.; Scott, R. A., Direct FeS Cluster Involvement in Generation of a Radical in Lysine 2,3-Aminomutase. *Biochemistry* **2000**, 39, (51), 15668-15673.

88. Berkovitch, F.; Nicolet, Y.; Wan, J. T.; Jarrett, J. T.; Drennan, C. L., Crystal structure of biotin synthase, an S-adenosylmethionine-dependent radical enzyme. *Science* **2004**, 303, (5654), 76-80.

89. Lepore, B. W.; Ruzicka, F. J.; Frey, P. A.; Ringe, D., The x-ray crystal structure of lysine-2,3-aminomutase from Clostridium subterminale. *Proceedings of the National Academy of Sciences of the United States of America* **2005**, 102, (39), 13819-13824.

90.   Layer, G.; Kervio, E.; Morlock, G.; Heinz, D. W.; Jahn, D.; Retey, J.; Schubert, W.-D., Structural and functional comparison of HemN to other radical SAM enzymes. *Biological Chemistry* **2005,** 386, (10), 971-980.

91.   Slieman, T. A.; Rebeil, R.; Nicholson, W. L., Spore photoproduct (SP) lyase from Bacillus subtilis specifically binds to and cleaves SP (5-thyminyl-5,6-dihydrothymine) but not cyclobutane pyrimidine dimers in UV-irradiated DNA. *J. Bacteriol.* **2000,** 182, (22), 6412-7.

92.   Mehl, R. A.; Begley, T. P., Mechanistic Studies on the Repair of a Novel DNA Photolesion: The Spore Photoproduct. *Organic Letters* **1999,** 1, (7), 1065-1066.

93.   Cheek, J.; Broderick, J. B., Direct H atom abstraction from spore photoproduct C-6 initiates DNA repair in the reaction catalyzed by spore photoproduct lyase: evidence for a reversibly generated adenosyl Radical Intermediate. *Journal of the American Chemical Society* **2002,** 124, (12), 2860-2861.

94.   Guo, J.-D.; Luo, Y.; Himo, F., DNA repair by spore photoproduct lyase: a density functional theory study. *Journal of Physical Chemistry B* **2003,** 107, (40), 11188-11192.

95.   Douki, T.; Setlow, B.; Setlow, P., Effects of the binding of a/b-type small, acid-soluble spore proteins on the photochemistry of DNA in spores of Bacillus subtilis and in vitro. *Photochemistry and Photobiology* **2005,** 81, 163-169.

96.   Douki, T.; Laporte, G.; Cadet, J., Inter-strand photoproducts are produced in high yield within A-DNA exposed to UVC radiation. *Nucleic Acids Research* **2003,** 31, (12), 3134-3142.

97.   Douki, T.; Cadet, J., Formation of the spore photoproduct and other dimeric lesions between adjacent pyrimidines in UVC-irradiated dry DNA. *Photochemical & Photobiological Sciences* **2003,** 2, (4), 433-436.

98.   Friedel, M. G.; Berteau, O.; Pieck, J. C.; Atta, M.; Ollagnier-de-Choudens, S.; Fontecave, M.; Carell, T., The spore photoproduct lyase repairs the 5S- and not the 5R-configured spore photoproduct DNA lesion. *Chemical Communications* **2006,** (4), 445-447.

CHAPTER II

GROWTH AND PURIFICATION OF SPORE PHOTOPRODUCT LYASE

II.1   Introduction

The advances in the field in molecular biology throughout the 1950's and 1960's had a major impact on the study of protein structure and function. Protein purification in the past had been both difficult and time consuming. It required a large amount of cells from the organism being studied, with the protein of interest possibly consisting of less than 1% of the total protein present in the cells. Characterization of human proteins was particularly difficult as it was hard to obtain sufficient quantities of many human organs and cells for study. With such a low percentage of protein present, purification could require well over ten steps, during which time, much of the protein was lost or degraded.[1]

The discovery and development of plasmid derived cloning vectors greatly improved *in vitro* studies of proteins. Plasmids are circular molecules of DNA that replicate autonomously in a bacterial host cell. While not essential to cellular survival, plasmids can confer selective advantages such as antibiotic resistance. This made them ideally suited for development as cloning vectors, and since the early 1970's naturally occurring plasmids have been altered to include among other things, multiple cloning sites, promoters, and *lac* operators and repressors.

With these vectors, the gene of interest can be cloned into the plasmid by use of restriction enzymes and overexpression can be controlled by the presence or absence of an inducer molecule such as isopropyl β-D-thiogalacto-pyranoside (IPTG).[2]

Despite these advances in protein overexpression and cloning, protein purification could still be difficult. Multiple separation columns were typically needed, along with dialysis and other purification techniques, to achieve a sufficiently pure protein sample. The invention of immobilized metal affinity chromatography (iMAC) in 1975 by Porath was thus a large benefit to the field of biochemistry.[3] With this purification technique, a protein is cloned with a specific multiple histidine tag sequence located at either the C-terminus or N-terminus of the protein. After cell growth, the cell lysate is purified over a column containing a resin that has a link between the beads and a nitrogen/oxygen binding claw that can coordinate a divalent metal such as nickel, cobalt, iron, manganese or magnesium. Some of the more common commercial resins used are; TALON[TM] from BD Clontech, nickel-nitrilotriacetic acid (Ni-NTA) from Qiagen, and Ni-Sepharose from GE Healthcare. The histidine tagged protein will coordinate to this metal as it is run over the column, while other proteins generally wash straight through the column. A high concentration of imidazole is then used to wash the column to elute the his-tagged protein.[4] This method yields a large quantity of protein free of other contaminants.

The iMAC approach has been employed to overexpress and purify the spore photoproduct lyase from *Bacillus subtilis* with gene insertion into a pET14b

expression vector containing an N-terminal 6 histidine tag. After insertion and transformation into *E. coli*, metal affinity chromatography is used to purify the protein for further *in vitro* characterization.

II.2   Experimental Methods

Materials

All chemicals used were commercially obtained except when noted otherwise and were of the highest purity. Tuner(DE3)pLysS competent cells were purchased from Novagen™. The Ni/Co-sepharose™ column was purchased from Amersham Biosciences now GE Healthcare and used interchangeably. SDS-PAGE gels were commercially obtained from Bio-Rad Scientific.

Growth of spore photoproduct lyase

The *splB* gene from *Bacillus subtilis* used in this work had been previously cloned into the pET14b expression vector from Novagen in our lab by Dr. Jennifer Cheek. A single colony of the overexpression strain pET14b-SPL17 transformed into *E. coli* Tuner(DE3)pLysS competent cells was used to inoculate 50 mL of Luria/Bertani (Miller's Modification)[5] medium containing 50 μg/mL of ampicillin. This culture was grown to saturation at 37 °C and used to inoculate a 10L flask of minimal media/ampicillin described elsewhere.[6] The 10 L culture was grown at 37 °C in a New Brunswick Scientific fermentor (250 rpm, 5 L/min O_2). When the culture reached an $OD_{600} = 0.6$, isopropyl β-D-thiogalacto-pyranoside (IPTG) was added to 1 mM final concentration and the medium was

supplemented with 750 mg Fe(NH$_4$)$_2$(SO$_4$)$_2$. The culture was grown for an

additional 2 hours, and then was cooled to 25 °C and placed under nitrogen (5

L/min). The culture was further cooled to 15 °C, moved to a 4 °C refrigerator and

left under nitrogen overnight for 12 hours. The cells were then harvested by

centrifugation at 4°C and stored under nitrogen at –80 °C for further use.

Purification of spore photoproduct lyase

Spore photoproduct lyase was purified from *E. coli* Tuner(DE3)pLysS

transformed with pET14b-SPL17, prepared as described above. All steps in the

purification were performed in a single day under strictly anaerobic conditions in

a Coy anaerobic chamber (Coy Laboratories, Grass Lake, MI) at 4 °C except

where noted. Solutions and buffers used in the purification were thoroughly

degassed by sparging with nitrogen or by repeated pump / purge cycles on a

Schlenk line prior to bringing them into the Coy chamber. The pelleted cells (13

to 19 grams) were brought into the anaerobic chamber and resuspended in 20-

30 mL of pH 8.0 lysis buffer containing 20 mM sodium phosphate, 500 mM NaCl,

1% Triton X-100, 5% glycerol, 10 mM MgCl$_2$, 20 mM imidazole, 1 mM PMSF, 1

mg lysozyme per gram of cells, and 0.2 mg DNAse I and RNAse A. This

suspension was agitated for one hour until homogenous and then centrifuged at

27,000 x g for 30 min at 4 °C. The resulting crude extract was loaded directly

onto a Ni/Co-Sepharose^{TM} High Performance affinity column (0.7 X 2.5 cm, 1mL)

that had been previously equilibrated with buffer A (20 mM sodium phosphate,

500 mM NaCl, 10 mM imidazole, 5% glycerol, pH 8.0). The column was washed

with 15 mL of buffer A, and then a 25 mL step gradient (5 mL steps at 10%, 20%, 50%, 70%, 100% buffer B) from buffer A to buffer B (20 mM sodium phosphate, 500 mM NaCl, 500 mM imidazole, 5% glycerol, pH 8.0) was run to elute the adsorbed proteins. SP lyase eluted as a sharp brownish band at 50% buffer B in the step gradient. The fractions were analyzed by SDS-PAGE, and those judged to be ≥95% pure were pooled and concentrated at 4 °C using an Amicon concentrator equipped with a YM-10 membrane. The protein was placed in o-ring-sealed tubes, flash-frozen, and stored at –80 °C.

Protein, iron, and sulfide assays.

Routine determinations of protein concentrations were done by the method of Bradford,[7] using a kit sold by Bio-Rad and bovine serum albumin as a standard. Iron assays were performed using the methods of Fish or Beinert.[8, 9] Sulfide assays were carried out as previously described by Broderick et al.[6] using a modification of the method developed by Beinert .[10]

Gel filtration chromatography

SPL (25 uL) was loaded onto a pre-equilibrated (20 mM sodium phosphate, 500 mM NaCl, 5% glycerol, pH 8.0) sepharose™ 12 column (1 cm x 30 cm, Pharmacia) at 0.25 mL/min and run with a isocratic flow for 100 min at 1 mL/min using the same buffer. Bio-Rad gel filtration standard was loaded and run under the above conditions to check for molecular weight. The UV absorbance was monitored at both 280 nm and 426 nm.

II.3   Results And Discussion

Purification of Spore Photoproduct Lyase

The SPL expression vector, pET14b-SPL17, was used to transform *E. coli* Tuner(DE3)pLysS for overproduction of histidine-tagged SPL (SPL-His$_6$), which migrates at approximately 43 kDa on SDS-PAGE (Figure II.1). The overexpressed cells were lysed using an enzymatic lysis procedure. The crude extract was then passed through a Co-Sepaharose™ High Performance affinity column (Figure II.2), pure fractions (>95 %) were identified by SDS-PAGE (Figure II.3), pooled, concentrated, and stored under nitrogen at –80 °C. If the SPL-His$_6$ was not sufficiently pure after a single run over the affinity column, the protein was dialyzed and re-purified over the same column. Typically approximately 25 mg of pure protein is obtained from 10 L of growth media. SPL elutes as a dark brown band from the Ni/Co-Sepaharose™ High Performance column, consistent with the presence of an iron sulfur cluster in the protein.

The anaerobically purified SPL has been found to contain iron (3.1 mol Fe per mol SP lyase and acid-labile sulfide (3.0 ± 0.3 mol S^{-2} per mol SPL). The amount of iron present in the purified SPL is dependent on the precise growth and purification conditions. The purified SPL exhibited instability at higher concentrations and precipitated above ~250 µM. Addition of a 5X excess of SAM to the protein resulted in concentration of upwards of ~750 µM and increased stability at room temperature. This could indicate a stabilizing structural role for SAM in SPL.[11]
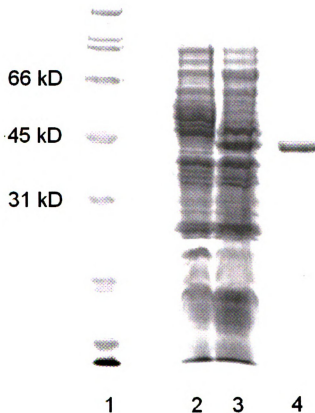
Figure II.1   SDS-PAGE of the purification of SPL from the metal affinity column chromatography, standards are shown on the left in lane 1. Lane 2 shows uninduced cells, lane 2 shows cell after addition of 1 mM IPTG to induce the cell culture. Lane 4 shows protein after purification on a Co-sepharose column.[11]
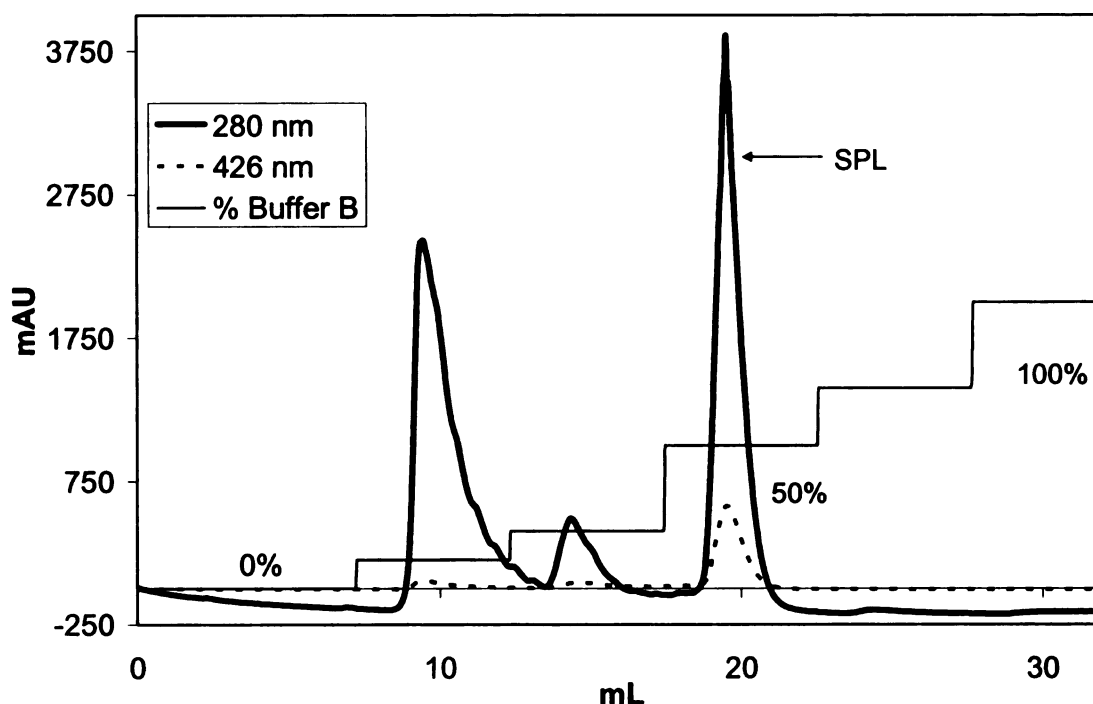
Figure II.2 FPLC chromatogram of SPL purification using cobalt metal affinity chromatography. SPL elutes ~20 min at 50% during an imidazole step gradient as a brownish-red band with a high absorbance at both 280 nm and 426 nm.

Subunit Structure of Spore Photoproduct Lyase.

SPL has been previously reported to be dimeric under conditions favoring

reconstitution of iron-sulfur clusters, and to likely contain a subunit-bridging iron

sulfur cluster.[12] As our SPL is purified with a significant proportion of iron sulfur

clusters intact, we have been able to re-investigate the question of subunit

structure using protein that has not been subjected to artificial reconstitution.

Analytical gel-filtration chromatography shows that SPL migrates

45 kDa

1   2   3   4   5
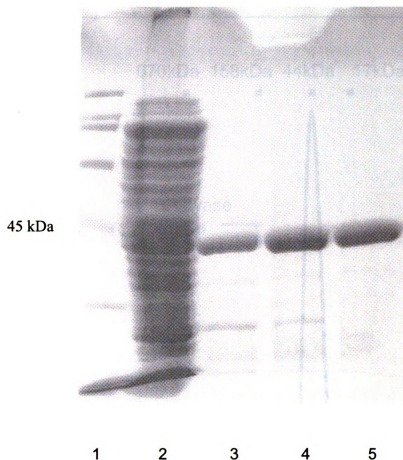
Figure II.3 SDS-PAGE gel electrophoresis of crude extract and fractions eluting from the Co-sepharose column. Lane 1: Molecular weight standard. Lane 2: Crude lysate before loading onto iMAC column. Lane 3-5: 1 mL fractions from Co-sepharose columns.

with an apparent molecular mass of 46 kDa (Figure II.4). Simultaneous detection at 426 and 280 nm shows that the visible chromophore elutes with this 46 kDa peak. A small shoulder on this peak (~85 kDa) is visible with both 280 and 426 nm detection and may represent a small amount of SP lyase dimer, which could be an artifact of the high protein concentrations used. These results together with the iron:protein ratios we obtain for purified SP lyase, provide support for SP lyase as a monomer binding a single [4Fe-4S] cluster.[11]
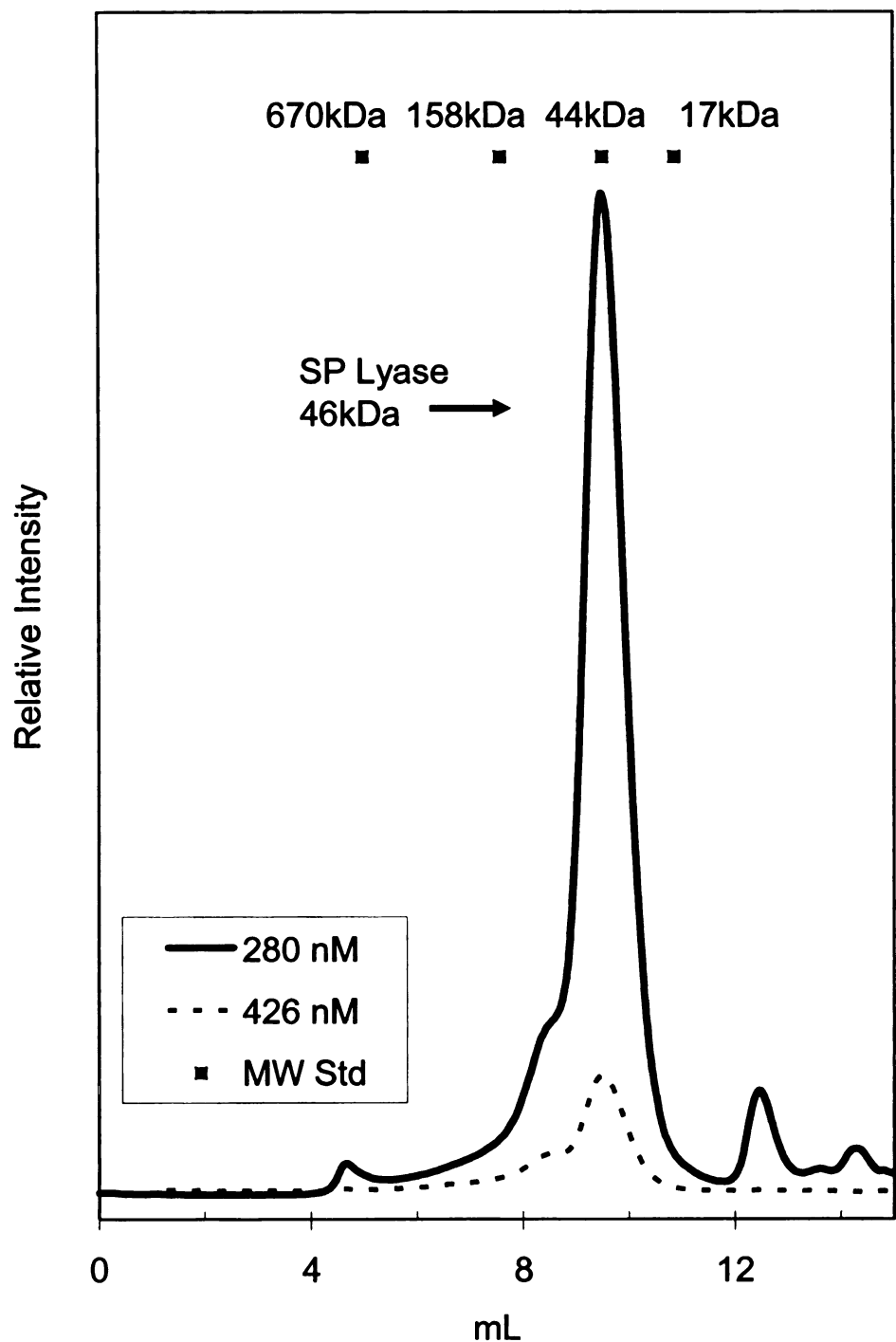
Figure II.4 Gel filtration chromatography of a SPL on a sepharose™ 12 column. SPL loaded on a gel filtration column and run with isocratic flow shows partially purified SPL elutes primarily as a single band with a molecular weight of 46 kDa. A slight shoulder at ~ 80 kDa can be assigned to a small amount of dimeric protein.

II.4   Conclusions

We have successfully overexpressed and purified SPL with immobilized metal affinity chromatography. Unlike other published reports[12] our SPL was purified with ~3 Fe and 3 S^{2-}, indicating a significantly higher cluster content than previously reported, and was not subjected to artificial reconstitution. On SDS-PAGE, SPL eluted at 43 kDa, with a purity greater than 95% as analyzed by SDS-PAGE gel electrophoresis.

Size exclusion chromatography yields a primarily monomeric protein, with an absorbance at both 280 nm and 426 nm, showing that the iron sulfur cluster is found in the monomeric SPL. A small shoulder is found at ~80 kDa and maybe the result of high protein concentrations used in these experiments. The presence of SPL as a monomeric protein coincides with many other members of the radical SAM superfamily such as PFL-AE[13] and MoaA[14] and to DNA photolyase, with which SPL shares sequence homology.[15]

Our SPL proved to be unstable at higher concentrations but the addition of SAM greatly enhanced the stability and solubility and allowed for a 3 fold increase in concentration. The enhanced stability of SPL in the presence of SAM is most likely due to the binding of SAM to SPL, possibly to the iron sulfur cluster. In previous proposals by Mehl and Begley and later by Cheek and Broderick the cluster donates an electron to SAM and causes cleavage.[16, 17]

II.5   References

1.   Voet, D.; Voet, J. G., *Biochemistry*. 2nd ed.; John Wiley & Sons: New York, 1995.

2.   Winstanley, C.; Rapley, R., Protein Derived Cloning Vectors. In *Molecular Biomethods Handbook*, Rapley, R.; Walker, J. M., Eds. Humana Press: Totowa, New Jersey, 1998; pp 165-179.

3.   Porath, J.; Carlsson, J.; Ollson, I.; Belfrage, G., Metal chelate affinity chromatography, a new approach to protein fractionation. *Nature* **1975,** 258, 598-599.

4.   Scopes, R. K., *Protein Purification: Principles and Practice*. 3rd ed.; Springer: New York, 1994.

5.   Miller, J. H., *Experiments in Molecular Genetics*. C. S. H. Press: New York, 1972.

6.   Broderick, J. B.; Henshaw, T. F.; Cheek, J.; Wojtuszewski, K.; Smith, S. R.; Trojan, M. R.; McGhan, R. M.; Kopf, A.; Kibbey, M.; Broderick, W. E., Pyruvate formate-lyase-activating enzyme: Strictly anaerobic isolation yields active enzyme containing a $[3Fe-4S]^+$ cluster. *Biochemical and Biophysical Research Communications* **2000,** 269, (2), 451-456.

7.   Bradford, M., A rapid and sensitive method for the quantitation of microgram quantities of protein utilizing the principle of protein-dye binding. *Analytical Biochemistry* **1976,** 72, 248.

8.   Fish, W. W., Rapid colorimetric micromethod for the quantitation of complexed iron in biological samples. *Methods in Enzymology* **1988,** 158, 357-364.

9.   Beinert, H., *Methods in Enzymology* **1978,** 54, (435-445).

10.   Beinert, H., Semi-micro methods for analysis of labile sulfide and of labile sulfide plus sulfane sulfur in unusually stable iron-sulfur proteins. *Analytical Biochemistry* **1983,** 131, 373-378.

11.   Buis, J. M.; Cheek, J.; Kalliri, E.; Broderick, J. B., Characterization fo an active spore photoproduct lyase, a DNA repair enzyme in the radical sam superfamily. *Journal of Biological Chemistry* **2006,** In Press.

12.   Rebeil, R.; Nicholson, W. L., The subunit structure and catalytic mechanism of the Bacillus subtilis DNA repair enzyme spore photoproduct lyase. *Proceedings of the National Academy of Sciences of the United States of America* **2001,** 98, (16), 9038-43.

13. Broderick, J. B.; Duderstadt, R. E.; Fernandez, D. C.; Wojtuszewski, K.; Henshaw, T. F.; Johnson, M. K., Pyruvate formate-lyase activating enzyme is an iron-sulfur protein. *Journal of the American Chemical Society* **1997,** 119, (31), 7396-7397.

14. Haenzelmann, P.; Schindelin, H., Crystal structure of the S-adenosylmethionine-dependent enzyme MoaA and its implications for molybdenum cofactor deficiency in humans. *Proceedings of the National Academy of Sciences of the United States of America* **2004,** 101, (35), 12870-12875.

15. Sancar, A., Structure and Function of DNA Photolyase and Cryptochrome Blue-Light Photoreceptors. *Chemical Reviews* **2003,** 103, (6), 2203-2237.

16. Mehl, R. A.; Begley, T. P., Mechanistic Studies on the Repair of a Novel DNA Photolesion: The Spore Photoproduct. *Organic Letters* **1999,** 1, (7), 1065-1066.

17. Cheek, J.; Broderick, J. B., Direct H Atom Abstraction from Spore Photoproduct C-6 Initiates DNA Repair in the Reaction Catalyzed by Spore Photoproduct Lyase: Evidence for a Reversibly Generated Adenosyl Radical Intermediate. *Journal of the American Chemical Society* **2002,** 124, (12), 2860-2861.

CHAPTER III

SOLUBILIZATION OF SPORE PHOTOPRODUCT LYASE

III.1   Introduction

Initial work on the spore photoproduct lyase protein in the Broderick lab yielded a protein that was unstable at room temperature for periods of time greater than 10 minutes and was subject to precipitation at a concentration above ~250 µM (J. Cheek and J. M. Buis unpublished work). This was problematic for a detailed study of the iron sulfur cluster of SPL, as many types of spectroscopy require a high concentration of protein.

Protein overexpression and solubility is dependent upon a number of factors, including the *E. coli* overexpression strain used, the cell lysis procedure, the buffering conditions including pH, salt concentration, glycerol and detergent content, the expression vector in which the gene is inserted, the temperature of cell growth, and the addition of co-factors and co-substrates; all these factors can all have a dramatic effect on overexpression and/or solubility.[1] For example, if a protein is in a buffer with a pH close to its isoelectric point it is far less likely to be soluble or stable in solution.[2]

Besides changing the above conditions, the protein in question can be co-expressed with other proteins such as iron-sulfur assembly proteins of the *isc*

operon as has been done with BioB.[3] In this instance the co-expressed protein aids in cluster assembly, which can be crucial to protein folding in Fe-S proteins. Other ways of increasing solubility include expressing the protein of interest with an additional peptide tag that has shown high solubility. Commercial vectors such as pET44a-c have Nus-tag located in the sequence and when a specific protein is cloned into this expression vector the resulting protein will have this highly soluble tag attached to the c-terminus of the protein, which can greatly enhance the protein solubility.

While *E. coli* are often an ideal expression system for proteins from other organisms, sometimes the protein is unable to overexpress in abundance in *E. coli* or the protein overexpresses well but is found as inclusion bodies that are located in the cell pellet after lysis.[1] There are a few possible explanations for this type of protein behavior. *E. coli* lacks the tRNA for certain so-called rare codons and is unable to transcribe the mRNA produced by the gene. This has been problematic for certain genes and organisms that are rich is GC sequences or reversely for certain AT-rich genes. Different commercial competent cells have been developed to overcome this obstacle including BL21 CodonPlus cells from Stratagene and Rosetta[TM] cells from Novagen.

Finally, the spore photoproduct lyase from *B. subtilus* has protein homologs among several other sporulating bacteria. It has been found that protein homologs in some species are more soluble *in vitro* than others.[1]

in the study of spore photoproduct lyase, many of the above schemes have been employed in an attempt to increase protein solubility; most of these approaches were unsuccessful.

III.2   Experimental Methods

Materials

All chemicals were commercially obtained except when noted otherwise, and were of the highest purity. Expression vectors pET28a, pET44a, pET42a, and pET30 EK/LIC were purchased from Novagen^{TM}. *E. Coli* strains of Novablue, Tuner(DE3)pLysS, Rosetta(DE3)pLysS, and BL21(DE3)CodonPlus were purchased from Novagen. SDS-PAGE (12% Tris-HCl) gels were commercially obtained from BioRad Scientific. FPLC experiments were carried out with an AKTA Basic FPLC from Amersham Biosciences. A BioRad GS-710 Gel imaging densitometer was used to scan SDS-PAGE gels and calculate band densities

Lysis procedures

Several types of lysis procedures were employed throughout this work and are described below:

Lysis procedure 1; whole cell lysis was carried out by removing 1 mL of a cell growth and pelleting at 27,000 g for 5 minutes. 50 µL of a 2X SDS-PAGE dye (100mM Tris-HCl, 4% SDS, 0.4% bromophenol blue, 20% glycerol) was added to cell pellet and cells were resuspended and placed in boiling water for 15 minutes.

The sample was centrifuged at 27,000 g for 10 minutes and loaded immediately onto a SDS-PAGE gel.

Lysis procedure 2; enzymatic lysis was carried out by pelleting a 50 mL cell culture at 27,000 g for 10 minutes. A lysis buffer containing 3 mL of the following buffer (50 mM Hepes, 250 mM NaCl, 5 mM β-ME,10% glycerol, 1% triton X-100, pH 7.5) was added to the cells in addition to 1 mg of lysozyme, 0.1mg of DNAse I and RNAse A. The cells were mixed at 4 °C for 30 minutes and 10 mM $MgCl_2$ was added followed by an addition 60 minutes of mixing. The cells were centrifuged at 27,000 g for 30 minutes with a 10 μL aliquot taken for SDS-PAGE.

Lysis Procedure 3; enzymatic lysis was carried out by pelleting a 50 mL cell culture at 27,000 g for 10 minutes. A lysis buffer containing 3 mL of the following buffer (20 mM sodium phosphate, 500 mM NaCl, 5% glycerol, 1% triton X-100, pH 8.0) was added to the cells in addition to 1 mg of lysozyme, 0.1mg of DNAse I and RNAse A. The cells were mixed at 4 °C for 30 minutes and 10 mM $MgCl_2$ was added followed by an addition 60 minutes of mixing. The cells were centrifuged at 27,000 g for 30 minutes with a 10 μL aliquot taken for SDS-PAGE.

Lysis Procedure 4; enzymatic lysis was carried out by pelleting a 1 L cell culture at 27,000 g for 10 minutes. A lysis buffer containing 15 mL of the following buffer (50 mM Hepes, 250 mM NaCl, 10% glycerol, 1% triton X-100, pH 7.5) was added to the cells in addition to 1 mg of lysozyme, 0.1mg of DNAse I and RNAse A. The cells were mixed at 4 °C for 30 minutes and 10 mM $MgCl_2$

was added followed by an addition 60 minutes of mixing. The cells were centrifuged at 27,000 g for 30 minutes with a 10 μL aliquot taken for SDS-PAGE.

Cloning Bacillus subtilus splB into pET28a, pET 42a and pET44a

The *splB* gene from *B. subtilus* was acquired by standard polymerase chain reaction (PCR) procedures from the previously cloned expression vector pET14b-spl17 using the DNA primers, 5'-GCCGCGAATTCATGA GAACCCATTTGTTC-3' and 5'-GATGCAGAACCCATTTGTTCCGCAGCTTGT-3' with a *EcoR1* and a *HindIII* restriction site incorporated into the respective primers. The *HindIII/EcoR1* digested PCR products were cloned into the respective overexpression vectors also digested with *HindIII/EcoR1* in pET-42a, pET44a, and pET28a using T4 DNA ligase (New England Biolabs) and NovaBlue competent cells. The PCR product was cloned in sequence with pET42a to incorporate a N-terminal GST tag and a N-terminal hexahistidine tag, the pET44a was cloned in sequence with a N-terminal Nus tag and N-terminal hexahistidine tag, and the pET28a was cloned in sequence with a N-terminal hexahistidine tag. The resulting constructs (pET-44a/spl1, pET42a/spl2, pET28a/spl1) were transformed into NovaBlue *Escherichia coli* for isolation and purification of the plasmid DNA. The constructs were then transformed into Tuner(DE3)pLysS *Escherichia coli* for protein overexpression. The fidelity of the PCR product was verified by dideoxynucleotide sequencing.

Cloning splB from Bacillus halodurans into pET30/EK/LIC

Chromosomal DNA from *Bacillus halodurans* strain (21591D) was

purchased from ATCC and used as the template DNA for standard PCR

procedures with the primers 5'GACGACGACAAGATGGAAAATATGTTTAG-3'

and 5'-GAGGAGAAGCCCGGTTTAAATTATATAG-3' which include a specific

overhang sequence that takes advantage of the 3' → 5' exonuclease activity of

T4 DNA polymerase. PCR products were treated with the T4 DNA polymerase

and annealed to a linear pET30Ek/LIC vector, followed by transformation into

NovaBlue competent cells. The *splB* gene was cloned in sequence with the

pET30EK/LIC with an N-terminal hexahistidine tag. The constructs were then

transformed into Tuner(DE3)pLysS *Escherichia coli* for protein overexpression.

The fidelity of the PCR product was verified by dideoxynucleotide sequencing.

Transformation of pET14B into various competent cell strains

The pET14B/SPL17 construct was alternatively transformed into both

Rosetta(DE3)pLysS and BL21(DE3)CodonPlus competent cell lines and grown in

1 L of MM media to OD_{600} = 0.6 followed by the addition of 0.5 mM IPTG. The

culture was grown an additional 3 hours and checked for overexpression on

SDS-PAGE gels.

Protein dialysis and concentration for varying buffer conditions

Spore photoproduct lyase was overexpressed in Tuner(DE3)pLysS *E. coli*

in a 10 L fermentor in minimal media as previously noted in Chapter 2 and

purified on a Co-Talon^{TM} metal affinity column (BD Biosciences, 10 X 1cm) with a linear gradient between 0% buffer A (50 mM Hepes, 250 mM NaCl, 5 mM β-ME,10% glycerol, pH 7.5) and 100% buffer B (50 mM Hepes, 250 mM NaCl, 250 mM imidizole,5 mM β-ME,10% glycerol, pH 7.5) run over 60 min after washing with buffer A for 20 min after loading crude lysate and prior to the linear gradient. Fractions with SPL were pooled and concentrated with a YM-10 Amicon concentrator to ~3 mg/mL and dialyzed in Spectra/Por dialysis tubing (molecular weight cutoff 12-14000 kDa, 0.32 mL / cm) with corresponding buffer in 2 X 2 L of buffer for 2 hours. Following dialysis, protein was concentrated with YM-10 Amicon ultra-concentrator.

Altered growth conditions of pET14b-spl17in Tuner(DE3)pLysS E. coli

The *splB* gene from *Bacillus subtilis* used in this work had been previously cloned into the pET14b expression vector from Novagen in our lab by Dr. Jennifer Cheek. A single colony of the overexpression strain pET14b-SPL17 transformed into *E. coli* Tuner(DE3)pLysS competent cells was used to inoculate 50 mL of Luria/Bertani (Miller's Modification)[4] medium containing 50 μg/mL of ampicillin:

Growth condition 1; this culture was grown to saturation at 37 °C and used to inoculate a 10 L flask of minimal media/ampicillin described elsewhere.[5] The 10 L culture was grown at 37 °C in a New Brunswick Scientific fermentor (250 rpm, 5 L/min O_2). When the culture reached an OD_{600} = 0.6, isopropyl β-D-thiogalacto-pyranoside (IPTG) was added to 1 mM final concentration and the

medium was supplemented with 750 mg $Fe(NH_4)_2(SO_4)_2$. The culture was grown for an additional 2 hours, and then was cooled to 25 °C and placed under nitrogen (5 L/min). The culture was further cooled to 15 °C, moved to a 4 °C refrigerator and left under nitrogen overnight for 12 hours. The cells were then harvested by centrifugation at 4°C and stored under nitrogen at −80 °C for further use.

Growth condition 2; this culture was grown to saturation and used to inoculate to inoculate a 10 L flask of Luria/Bertani (Miller's Modification)[4] medium. The 10 L culture was grown at 37 °C in a New Brunswick Scientific fermentor (250 rpm, 5 L/min O_2). When the culture reached an OD_{600} = 0.6, isopropyl β-D-thiogalacto-pyranoside (IPTG) was added to 1 mM final concentration and the medium was supplemented with 750 mg $Fe(NH_4)_2(SO_4)_2$. The culture was grown for an additional 2 hours, and then was cooled to 25 °C and placed under nitrogen (5 L/min). The culture was further cooled to 15 °C, moved to a 4 °C refrigerator and left under nitrogen overnight for 12 hours. The cells were then harvested by centrifugation at 4°C and stored under nitrogen at −80 °C for further use.

Growth condition 3; this culture was grown to saturation at 37 °C and used to inoculate a 1 L flask of minimal media/ampicillin described elsewhere.[5] The 1 L culture was grown at 37 °C in 2.5 L Bellco fermentation flasks in a New Brunswick C24 Incubator Shaker (250 rpm). When the culture reached an OD_{600} = 0.6, isopropyl β-D-thiogalacto-pyranoside (IPTG) was added to 1 mM final

concentration and the medium was supplemented with 100 mg $Fe(NH_4)_2(SO_4)_2$. The culture was grown for an additional 3 hours. The cells were then harvested by centrifugation at 4 °C and stored under nitrogen at –80 °C for further use.

Growth condition 4; this culture was grown to saturation at 37 °C and used to inoculate a 1 L flask of minimal media/ampicillin described elsewhere.[5] The 1 L culture was grown at 25 °C in 2.5 L Bellco fermentation flasks in a New Brunswick C24 Incubator Shaker (250 rpm). When the culture reached an OD_{600} = 0.6, isopropyl β-D-thiogalacto-pyranoside (IPTG) was added to 1 mM final concentration and the medium was supplemented with 100 mg $Fe(NH_4)_2(SO_4)_2$. The culture was grown for an additional 5 hours. The cells were then harvested by centrifugation at 4 °C and stored under nitrogen at –80 °C for further use.

Growth condition 5; this culture was grown to saturation at 37 °C and used to inoculate a 1 L flask of minimal media/ampicillin described elsewhere.[5] The 1 L culture was grown at 16 °C in 2.5 L Bellco fermentation flasks in a New Brunswick C24 Incubator Shaker (250 rpm). When the culture reached an OD_{600} = 0.6, isopropyl β-D-thiogalacto-pyranoside (IPTG) was added to 1 mM final concentration and the medium was supplemented with 100 mg $Fe(NH_4)_2(SO_4)_2$. The culture was grown for an additional 12 hours. The cells were then harvested by centrifugation at 4°C and stored under nitrogen at –80 °C for further use.

Growth condition 6; this culture was grown to saturation at 37 °C and used to inoculate a 10 L flask 2 X YT medium. The 10 L culture was grown at 37 °C in a New Brunswick Scientific fermentor (250 rpm, 5 L/min O_2). When the culture

53

reached an $OD_{600} = 0.6$, isopropyl β-D-thiogalacto-pyranoside (IPTG) was added

to 1 mM final concentration and the medium was supplemented with 750 mg

$Fe(NH_4)_2(SO_4)_2$. The culture was grown for an additional 2 hours, and then was

cooled to 25 °C and placed under nitrogen (5 L/min). The culture was further

cooled to 15 °C, moved to a 4 °C refrigerator and left under nitrogen overnight for

12 hours. The cells were then harvested by centrifugation at 4°C and stored

under nitrogen at –80 °C for further use.

Protein and iron assays

Routine determinations of protein concentrations were done by the

method of Bradford, using a kit sold by Bio-Rad and bovine serum albumin as a

standard.[6] Iron assays were performed using the methods of Fish or Beinert.[7, 8]

Sulfide assays were carried out as previously described by Broderick et al.[5] using

a modification of the method developed by Beinert.[9]

III.3   Results and Discussion

Cloning of Bacillus subtilus splB into pET28a, pET42a, and pET44a

The splB gene was successfully cloned into the pET28a, pET42a, and

pET44a expression vectors as monitored by dideoxynucleotide sequencing. The

plasmids pET28a-spl1 and pET42a-spl1 were transformed into

Tuner(DE3)pLysS *E. coli* and grown as described in experimental methods

section (growth condition 3). The cells were then lysed with lysis procedure 1 and

Figure III.1   SDS-PAGE of SPL from *B. subtilus* cloned into pET44a, pET42a, pET28a. A. The overexpression of pET44a-spl1, lanes 1 and 2 are uninduced cell cultures. Lanes 3 and 4 show induced cell cultures (whole cell lysis, procedure 1) to contain a large band at ~66 kDa. Lanes 5 and 6 are induced cell cultures enzymatically lysed (lysis procedure 4). Lane 7 is the BioRad broad range protein standard. Lanes 8 and 9 are cells enzymatically lysed (lysis procedure 2) B. The growth and whole cell lysis of pET28a-spl1 and pET42a-spl1 shows no significant overexpression of any band at the expected molecular weights of ~43 kDa and 55 kDa respectively; Lanes 1 is uninduced pET28a-spl1 cells and lane 2 is induced cells (growth condition 3, lysis procedure 1). Lanes 1 is uninduced pET42a-spl1 cells and lane 2 is induced cells (growth condition 3, lysis procedure 1).

A.

B.

45 kDa
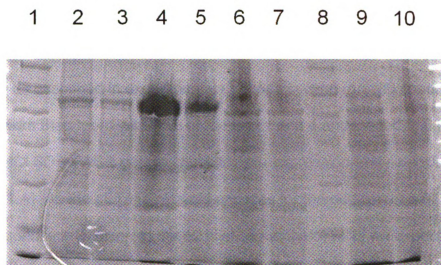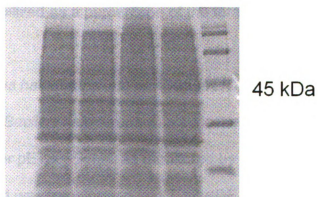
Figure III.1

loaded and run on 12% Tris-HCl SDS-PAGE gels. The SDS-PAGE gels show no expression of spore photoproduct lyase (Figure III.1.B).

The plasmid pET44a-spl1 was transformed into Tuner(DE3)pLysS *E. coli* and grown as described in experimental methods section (growth condition 3). The cells were then lysed with lysis procedure 1 and 4 and loaded and run on 12% Tris-HCl SDS-PAGE gels to check for overexpression and solubility of SPL (Figure III.1.A). As the pET44a plasmid encodes for the addition of a 54 kDa protein sequence in addition to the 42 kDa sequence of SPL, we expect a protein of ~96 kDa. However, SDS-PAGE gel with lysis procedure 1 shows a protein at ~66 kDA, which may be caused by improper transcription of the plasmid. After cell lysis with procedure 4, the 66 kDa band disappears and appears insoluble. These results are summarized in Table III.1 and shows the amount of SPL overexpressed and solubilized as a percentage of the total protein present.

Cloning splB from Bacillus halodurans into pET30/EK/LIC

The *splB* gene of *Bacillus halodurans* was successfully incorporated into the overexpression vector pET30/Ek/LIC as monitored by dideoxynucleotide sequencing. This plasmid was transformed into Tuner(DE3)pLysS and grown and overexpressed using growth condition 3. The SDS-PAGE gel of the whole cell lysis (lysis procedure 1) shows a strongly expressed band at ~43kDa as shown in Figure III.2. However, enzymatic cell lysis (lysis procedure 4) yielded no soluble protein as monitored by SDS-PAGE. Further growths (growth conditions 4 and 5) were carried out at lower temperatures at 16 °C and 25 °C to help

prevent inclusion body formation but results did not improve. Overall, while the protein was strongly overexpressed, there was no soluble protein or reddish-brown color that would indicate the presence of an abundant iron sulfur cluster containing protein.

Organism Expression Vector E. coli Strain	Overexpression: SPL as an approximate % of total cell protein	Solubility after lysis: SPL as an approximate % of total soluble protein
Bacillus subtilis pET 14B Tuner(DE3)pLysS	5%	5%
Bacillus subtilis pET 14B Rosetta(DE3)pLyS	4%	4%
Bacillus subtilis pET 14B BL21(DE3)CodonPlus	4%	4%
Bacillus subtilis pET 14B BL21(DE3)pLysS	3%	3%
Bacilllus halodurans pET 30EK/LIC Tuner(DE3)pLysS	35%	0%
Bacillus subtilis pET 28a Tuner(DE3)pLysS	0%	0%
Bacillus subtilis pET42a Tuner(DE3)pLysS	0%	0%
Bacillus subtilus pET44a Tuner(DE3)pLysS	30%	0%

Table III.1 Overexpression and solubility results from the various expression vectors, competent cells and organisms.

Figure III.2   SDS-PAGE of SPL from *B. halodurans* overexpressed and lysed.
A. The addition of IPTG, lanes 1, 3, and 5, causes significant overexpression
versus cultures (lanes 2, 4, 6) without IPTG (lysis procedure 1). Lane 7 is the
BioRad protein standard. B. After cell lysis (procedure 4) no overexpressed
protein is found in the supernatant, lanes 3 and 4. Most of the protein is found in
the cell pellet, lanes 1 and 2. Lane 5 is the BioRad protein standard.

1 2 3 4 5 6 7

A.

45 kDa

1 2 3 4 5

B.

45 kDa
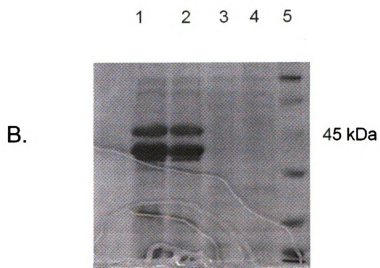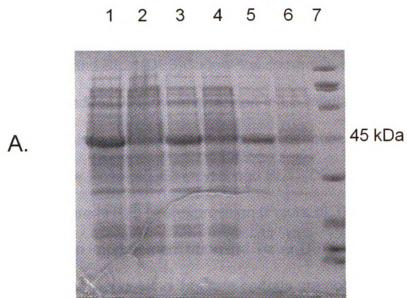
Figure III.3

Overexpression of splB in Rosetta and CodonPlus competent cells

The pET14/SPL17 construct was successfully transformed into both Rosetta(DE3)pLysS and BL21(DE3)CodonPlus compentent cells. The resulting colonies were checked for SPL overexpression in LB media via growth condition 4 and subsequent lysis by method procedure 1 as described in the experimental methods. For both the Rosetta(DE3)pLysS and BL21(DE3)CodonPlus compentent cells, there is little overexpression (Figure III.3) of the 42 kDa SPL protein and it is not an improvement upon the Tuner(DE3)pLysS cells that had been used prior to this, suggesting that rare codons are not the reason for SPL's lack of expression. These results are summarized in Table III.1

45 kDa

1   2   3   4   5
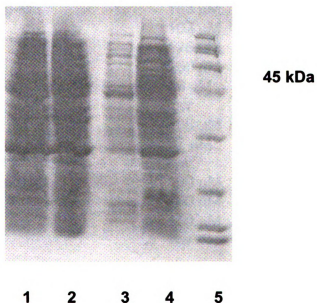
Figure III.3 SDS-PAGE gel of pET14b-spl17 transformed and overexpressed in Rosetta and CodonPlus competent cells. Lane 1 and 2, induced and uninduced SPL in Rosetta competent cells. Lane 3 and 4, induced and uninduced SPL in Codon Plus competent cells. Lane 5, BioRad broad range protein Standard.

Differing buffer conditions of the pET14b/spl17 construct

Varying the buffer conditions and their affect on the solubility of the spore

photoproduct lyase protein are summarized in Table III.2. The protein was initially

all purified in the same manner with the same buffer and then dialysis was used

to change the buffer conditions followed by protein concentration.

Most of the buffer modifications did not yield improvement in protein

solubility while other significantly hindered the stability of the protein. However,

the addition of SAM to SPL greatly enhanced the protein stability and allowed for

concentrations upwards of 750μM.

Buffer Change	[SPL] Max
0 mM imidizole	185 μM
0 mM imidizole, 0 mM β-ME	183 μM
50 mM Tris	103 μM
30% glycerol	125 μM
20% glycerol	250 μM
5% glycerol	46 μM
pH 7.0	low
200 mM NaCl	108 μM
100 mM NaCl	97 μM
1%CHAPS as detergent	low
1%Triton X-100 as detergent	100 μM
3mM SAM	750 μM
1mM EDTA	150 μM
5% Ethanol	low

Table III.2   The variance of buffering conditions and its affect on SPL. Buffer: 50mM Hepes, 300mM NaCl, 5mM β-ME, 10% glycerol, pH 7.5, ~125mM imidizole, gives a best concentration of 150 μM before precipitation. The increase in glycerol concentration was one of the few effective ways in raising the solubility of SPL. However, addition of SAM was most effective at stabilizing SPL.

Effect of altered growth conditions on overexpression of pET14b-spl17

Several proteins have been shown to have better overexpression when expressed in different medium or at different growth temperatures. Given this consideration, we have grown the pET14b-spl17 in the *E. coli* strain Tuner(DE3)pLysS and varied both the temperature and the growth media. These results are summarized in Table III.3 with growth conditions corresponding to those described in the experimental methods.

Growth Conditons	Amount of SPL as a % of total cell protein
SPL Growth 1 37 °C, MM media, 2 Hr induction O/N anaerobic incubation 10 L Fermentor	5%
SPL Growth 2 37 °C, LB Media, 2 Hr induction O/N anaerobic incubation 10 L Fermentor	2%
SPL Growth 3 25 °C, MM media, 5 Hr induction 1L Bellco Flask	5%
SPL Growth 4 16 °C, MM media, 12 Hr induction 1L Bellco Flask	4%
SPL Growth 5 37 °C, MM media, 2 Hr induction O/N anaerobic incubation 10 L Fermentor	2%

Table III.3   Amount of SPL present in whole cell lysis on SDS-PAGE gels as a percentage of the total cellular protein.

III.4 Conclusions

The cloning of *splB* from *Bacillus subtilis* into the different expression vectors pET 44a, pET 42a and pET 28a did not yield any soluble protein that was produced in sufficient quantity for purification. Whole cell SDS-PAGE lysis of the pET44a construct yield a substantial amount of protein but none of this proved to be soluble and was primarily found in the cell pellet after lysis and centrifugation. Whole cell SDS-PAGE of the pET 42a and pET28a constructs indicated no protein overexpression at the expected molecular mass.

The cloning of the *splB* gene from *Bacillus halodurans* into the expression vector pET30 EK/LIC was successful but also did not yield any soluble protein. Attempts at altering growth conditions did not improve protein overexpression. Cells grown with the constructs and the whole cell lysis wear not of a dark brownish red color that would indicate an abundance of protein with an iron sulfur cluster present.

The use of the different *E. coli* competent cell strains Rossetta(DE3)pLysS and BL21(DE3)CodonPlus did not have much of an affect on protein overexpression and were not an improvement over the previously used Tuner(DE3)pLysS cells.

Varying the buffer conditions of purified SPL from *Bacillus subtilis* did not yield substantial improvement in the solubility of SPL with the exception of addition of SAM which yielded a 3 fold increase in solubility to ~750 μM. This is

a notable result as SAM is the expected cofactor for SPL and may indicate that the presence of SAM in some way can stabilize SPL.

III.5 References

1. Scopes, R. K., *Protein Purification: Principles and Practice*. 3rd ed.; Springer: New York, 1994.

2. Voet, D.; Voet, J. G., *Biochemistry*. 2nd ed.; John Wiley & Sons: New York, 1995.

3. Cosper, M. M.; Jameson, G. N. L.; Davydov, R.; Eidsness, M. K.; Hoffman, B. M.; Huynh, B. H.; Johnson, M. K., The [4Fe-4S]2+ Cluster in Reconstituted Biotin Synthase Binds S-Adenosyl-L-methionine. *Journal of the American Chemical Society* **2002,** 124, (47), 14006-14007.

4. Miller, J. H., *Experiments in Molecular Genetics*. C. S. H. Press: New York, 1972.

5. Broderick, J. B.; Henshaw, T. F.; Cheek, J.; Wojtuszewski, K.; Smith, S. R.; Trojan, M. R.; McGhan, R. M.; Kopf, A.; Kibbey, M.; Broderick, W. E., Pyruvate formate-lyase-activating enzyme: Strictly anaerobic isolation yields active enzyme containing a [3Fe-4S]+ cluster. *Biochemical and Biophysical Research Communications* **2000,** 269, (2), 451-456.

6. Bradford, M., A rapid and sensitive method for the quantitation of microgram quantities of protein utilizing the principle of protein-dye binding. *Analytical Biochemistry* **1976,** 72, 248.

7. Beinert, H., *Methods in Enzymology* **1978,** 54, (435-445).

8. Fish, W. W., Rapid colorimetric micromethod for the quantitation of complexed iron in biological samples. *Methods in Enzymology* **1988,** 158, 357-364.

9. Beinert, H., Semi-micro methods for analysis of labile sulfide and of labile sulfide plus sulfane sulfur in unusually stable iron-sulfur proteins. *Analytical Biochemistry* **1983,** 131, 373-378.

CHAPTER IV

SPECTROSCOPIC CHARACTERIZATION OF THE IRON SULFUR CLUSTER IN SPORE PHOTOPRODUCT LYASE

IV.1 Introduction

The iron sulfur clusters of proteins have been characterized by a variety of spectroscopic techniques including ultra-violet/visible spectroscopy, electron paramagnetic resonance and Mössbauer spectroscopy.[1, 2 3] The UV/visible absorption spectroscopy of iron sulfur cluster has been well characterized over the years and is dominated by ligand to metal charge transfer (LMCT) bands between the sulfurs and the iron. The number of peaks generated by this LMCT causes the spectra to have broad absorption from 300 nm to 600 nm. Specific features are dependent upon the type and oxidation state of the cluster. It is, however, still difficult to determine precisely what type of iron sulfur cluster is present and what kind of ligands might be bound to the cluster due to the abundance of transitions present. Although UV/visible spectroscopy can provide insight as to whether a cluster is present and is redox active other techniques are needed to fully understand the electronic structure of an iron sulfur cluster.[2]

Electron paramagnetic resonance (EPR) spectroscopy is a more specific technique that probes the interaction between paramagnetic centers and an

67

applied magnetic field. It is applicable to any species containing one or more

unpaired electrons, whether this is in the form of an organic radical or the

Protein	Cluster	Oxidation State	Formal Valence	EPR g values (temp)	Mössbauer Isomer shift (mm/sec)
Rubredoxin	1Fe-0S	Oxidized	$1Fe^{3+}$	4.3, 9 (< 20 K)	0.25
		Reduced	$1Fe^{2+}$	None	0.65
2-Iron ferredoxin	2Fe-2S	Oxidized	$2Fe^{3+}$	None	0.26
		Reduced	$1Fe^{3+}$, $1Fe^{2+}$	1.89, 1.95, 2.05 (<100 K)	0.25, 0.55
3-Iron ferredoxin	3Fe-4S	Oxidized	$3Fe^{3+}$	1.97, 2.00, 2.02 (<20 K)	0.27
		Reduced	$2Fe^{3+}$, $1Fe^{2+}$	None	0.30, 0.46
4-Iron ferridoxin	4Fe-4S	Oxidized	$3Fe^{3+}$, $1Fe^{2+}$	2.04, 2.04, 2.12 (<100 K)	0.31
		Intermed.	$2Fe^{3+}$, $2Fe^{2+}$	None	0.42
		Reduced	$1Fe^{3+}$, $3Fe^{2+}$	1.88, 1.92, 2.06	0.57

Table IV.1   Typical spectroscopic properties of iron sulfur clusters.[4]

unpaired electrons of a transition metal center. An electron has a magnetic

moment. When placed in an external magnetic field of strength B_0, this magnetic

moment can align itself parallel or antiparallel to the external field. The former is

a lower energy state than the latter (this is the Zeeman effect), and the energy

separation between the two is $\Delta E = g_e \mu_B B_0$, where g_e is the gyromagnetic ratio of the electron, the ratio of its magnetic dipole moment to its angular momentum, and μ_B is the Bohr magneton. To move between the two energy levels, the electron can absorb electromagnetic radiation of the correct energy:

$$\Delta E = h\nu = g_e \mu_B B_0 \qquad (1)$$

and this is the fundamental equation of EPR spectroscopy.

The paramagnetic centre is placed in a magnetic field and the electron caused to resonate between the two states; the energy absorbed as it does so is monitored, and converted into the EPR spectrum. When an unpaired electron is in an atom, it feels not only the external magnetic field B_0 applied by the spectrometer, but also the effects of any local magnetic fields. Therefore, the effective field B_{eff} felt by the electron is:

$$B_{eff} = B_0(1 - \sigma) \qquad (2)$$

where σ allows for the effects of the local fields (it can be positive or negative), and therefore the resonance condition is

$$\Delta E = h\nu = g_e \mu_B B_{eff} = g_e \mu_B B_0(1 - \sigma) \qquad (3)$$

The quantity $g_e(1 - \sigma)$ is called the g factor, given the symbol g, so

$$\Delta E = h\nu = g \mu_B B_0 \qquad (4)$$

Given this last equation, you can measure g from the EPR experiment by measuring the field B_0 and the frequency ν at which resonance occurs. If g differs from g_e (2.0023), this implies that the ratio of the electron's magnetic moment to

its angular momentum has changed from the free electron value. Since the electron's magnetic moment is constant (it's the Bohr magneton), then the electron must have gained or lost angular momentum. It does this through spin-orbit coupling, and because the mechanisms of spin-orbit coupling are well understood, the magnitude of the change can be used to give information about the nature of the atomic or molecular orbital containing the electron.[1,2]

EPR has proven to be a highly useful technique for examining iron sulfur cluster containing proteins. Although the spin states of the iron found in the cluster is typically S = 2 or S = 5/2 for the Fe^{2+} and Fe^{3+} oxidation states, the Fe exhibits antiferromagnetic coupling between the different irons present. Thus, the spin for a typical $[4Fe-4S]^{1+}$ cluster is S =1/2 while the spin of a $[4Fe-S]^{2+}$ cluster is S = 0 (EPR silent). As such, some types of cluster are not observable by EPR spectroscopy. Despite this limitation, EPR provides powerful insight concerning the type of cluster, oxidation state of the cluster, and the cluster's surrounding environment.[1,4] Table IV.1 illustrates the different g values obtained of proteins containing different types of iron sulfur clusters.[4]

In order to get a more complete view of the cluster content of a protein such as SPL, an additional spectroscopic technique like Mössbauer spectroscopy can be utilized to complement the EPR. Mössbauer spectroscopy is one of the most useful tools in the study of iron sulfur cluster and is capable of detecting any iron center in a protein regardless of the oxidation state or magnetic properties of the iron. Thus, states such as the $[4Fe-4S]^{2+}$ cluster can be detected.[1,2] Mössbauer spectroscopy takes advantage of the recoilless

70

nuclear gamma resonance and in isotopes with a nuclear spin, such as ^{57}Fe, it

can be used to detect transitions between the nuclear ground state and nuclear

excited state which is 14.4 KeV for ^{57}Fe. The Mössbauer phenomenon rests on

the fact that in a solid most of the recoil energy is converted into lattice vibrational

energy. In a bare nucleus, one would observe only a single transition, however,

when embedded in a environment with symmetry lower than spherical,

tetrahedral or cubic, the degeneracy of the nuclear excited state is lifted by the

quadrupole moment interaction with the electric field gradient, providing the

characteristic doublet associated with a Mössbauer spectrum. The splitting of the

signal can be measured and is known as ΔE_Q. Another useful measurement is

the isomer shift (δ) which arises from the differences in s-electron density at the

nucleus created by varying environments. However, because the radial

distribution of the d and s orbitals overlap, δ is also a good indicator of the

oxidation state of the cluster.[5] Table IV.1 shows some typical values for the

isomer shifts of iron sulfur clusters in proteins. Higher isomer shifts are indicative

of a more electron rich cluster environment. Taken together, the isomer shift and

ΔE_Q can give indications to the oxidation state, spin state, degree of covalency

and coordination environment. The information from Mössbauer spectroscopy

can be enhanced by the magnetic hyperfine splitting that results from the

presence of an unpaired electron close to the nucleus and in combination with

EPR can help deduce the type of cluster present.[1, 5]

The combination of the methods above, have been employed by our lab to study both the as-isolated SPL and chemically reduced SPL. Previous studies have shown that SPL contains a redox active iron sulfur cluster that can undergo cluster transformation.[6] However, due to the difficulty of overexpressing and purifying SPL, these studies were carried out with either inactive protein or artificially reconstituted protein.[6] These studies also did not effectively account for what percentage of the enzyme's cluster was in which state. Our work herein was designed to sort out which type of clusters are present in both as purified SPL and in active SPL under reducing conditions. The protein has also been examined in the presence of the SPL's cofactor SAM.

IV.2 Experimental Methods

Materials

All chemicals used were commercially purchased and of the highest purity except where otherwise noted. ^{57}Fe was purchased from Cambridge Isotope Laboratories. S-adenosylmethionine was enzymatically synthesized as described below.

Synthesis of S-adenosyl-L-methionine

SAM was synthesized enzymatically by using the following procedure. A 10mL reaction of 100 mM Tris HCl (pH 8.0) containing 50 mM KCl, 26 mM MgCl$_2$, 13.0 mM adenosine triphosphate, 8% β-mercaptoethanol, 1mM EDTA, 10.0 mM methionine, 2.5 μL inorganic pyrophosphatase (0.25 U) and 1 mL SAM

synthetase crude lysate were stirred at room temperature for 16 hrs and quenched with 1 mL 1M HCl. The reaction was monitored by thin layer chromatography to completion and the SAM was purified by loading onto a Source 15S cationic exchange column (Pharmacia, 1 cm x 10 cm) charged with 1M HCl and equilibrated with MQ water. A linear gradient of MQ H_2O to 1 M HCl was used to elute the SAM. The fractions containing SAM were lyophilized and redissolved in 50 mM HEPES, 200 mM NaCl (pH 8.0).

Growth and purification of ^{57}Fe spore photoproduct lyase

Growth and purification of ^{57}Fe SPL was carried out as previously stated in Chapter II.2 with the modification of removing all iron from the minimal media and supplementing with ^{57}Fe. The ^{57}Fe stock solution was made by dissolving ^{57}Fe metal in 3:1 MQ H_2O to H_2SO_4. The final concentration of ^{57}Fe in the growth media was 20 μM.

UV/Visible spectroscopy

UV-Visible spectra were recorded on a HP-8453 diode-array spectrophotometer. All samples were prepared anaerobically in a mBraun box and transferred to the spectrophotometer with a rubber septum on top of the cuvette. A 1 mL sample of SPL was prepared at a concentration of 65 μM and measured in a quartz cuvette with a 1 cm path length. The SPL sample was titrated with increasing amounts of sodium dithionite and DTT and checked for cluster reduction.

Electron paramagnetic spectroscopy

EPR measurements were obtained at X-band on a Bruker ESP300E spectrometer equipped with a liquid He cryostat and a temperature controller from Oxford Instruments. Spectra were recorded at 12 K for the $[4Fe-4S]^{1+}$ and the $[3Fe-4S]^{1+}$ clusters. The double integrals of the EPR signals were evaluated by using a computer on-line with the spectrometer. Spin concentration in the protein samples was determined by calibrating double integrals of the EPR recorded under non-saturating conditions with a standard sample of 0.1 mM Cu (II) and 1 mM EDTA.

EPR samples were prepared using 0.35 mM SPL. Samples were reduced with 10 mM sodium dithionite and 10 mM DTT. SAM (3mM) was added to some samples. All samples contained 300 μL of protein solution and were transferred to a 4 mm quartz EPR tube (Wilmad).

Mössbauer spectroscopy

Samples for Mössbauer spectroscopy were prepared with ^{57}Fe SPL at a concentration of ~0.7 mM in 500 μL Delran cups with 450 μL of protein solution. Reduced samples were made by adding 10 mM sodium dithionite and 10 mM DTT and incubating for 10 minutes on ice. SAM (3 mM) was added to some samples.

Mössbauer spectra were recorded at Emory University in either a weak-field spectrometer equipped with a Janis 8DT variable-temperature cryostat or a strong-field spectrometer furnished with a Janis CNDT/SC SuperVaritemp

cryostat encasing an 8-T superconducting magnet. Both spectrometers operate in a constant acceleration mode in a transmission geometry. Mössbauer data analysis was performed by Ricardo Garcia and Vincent Huynh at Emory University.

IV.3   Results and Discussion

Synthesis of S-adenosyl-L-methionine

The SAM synthesis reaction and purification (Scheme IV.1) is currently carried out as described in the Experimental Methods. SAM elutes as a broad band from the cation exchange column between 0.4 and 0.6 M HCl (Figure IV.1). The isolated SAM was lyophilized to yield a crystalline colorless solid, presumably in the chloride salt form. A total of 35 mg was obtained corresponding to 70% reaction yield.

Methionine + ATP $\xrightarrow{\text{SAM Synthetase}}$
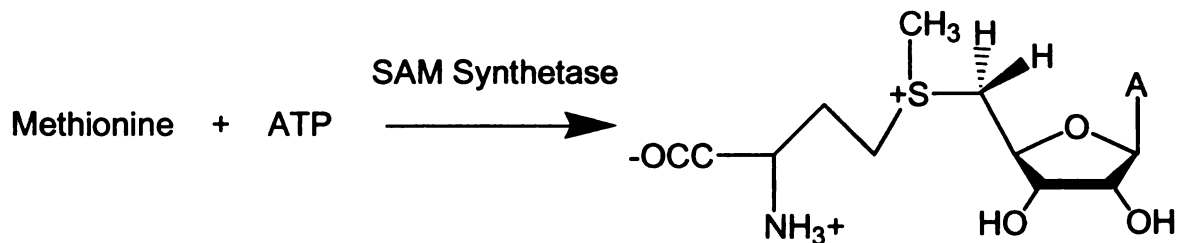
Scheme IV.1 Generalized reaction scheme for the enzymatic synthesis of AdoMet.
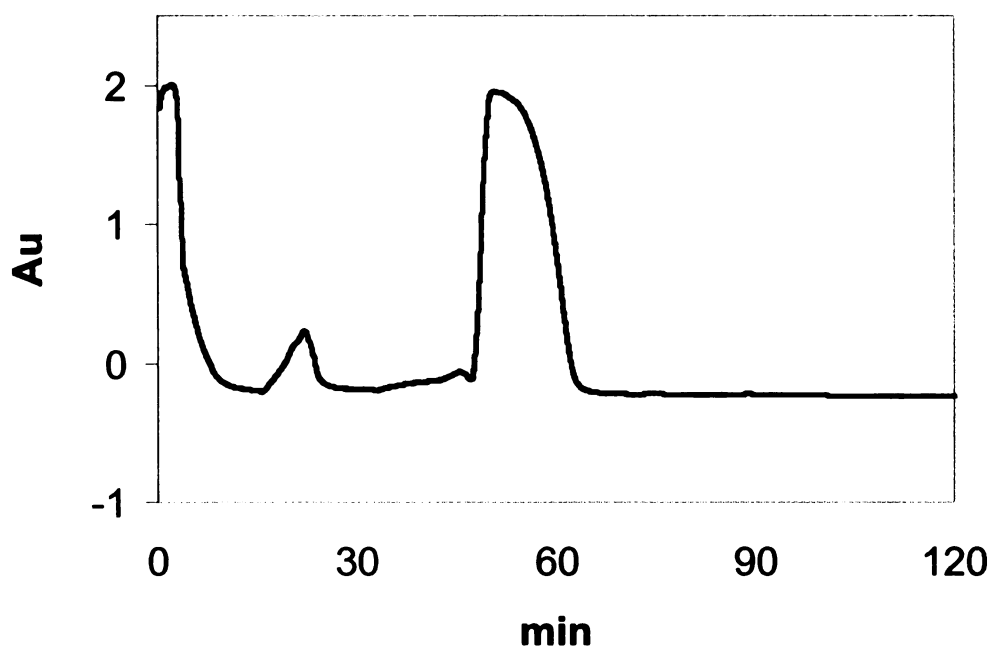
Figure IV.1 Purification of SAM by cation exchange chromatography. SAM elutes as a large broad peak (A_{260}) between approximately 0.4 and 0.6 M HCl on a source 15s cationic exchange column with a linear gradient between MQ H_2O and 1M HCl.

UV/visible spectroscopy

The UV-visible spectrum of the purified enzyme (Figure IV.2) is characteristic of the presence of an iron-sulfur cluster, although it is not particularly definitive of a specific cluster type. The spectrum exhibits a broad shoulder with maxima at 410 nm (11.9 $mM^{-1}cm^{-1}$) and 450 nm (10.5 $mM^{-1}cm^{-1}$), similar to what has been observed for anaerobically purified pyruvate formate-lyase activating enzyme[7] and lipoyl synthase.[8] This signal can be reduced by the addition of dithionite as seen in Figure IV.2 with the loss of the shoulder peaks

76

typical of a reduction to a $[4Fe-4S]^{1+}$ cluster. The UV/Vis thus confirms the

presence of an iron sulfur cluster and that the iron sulfur cluster is redox active.
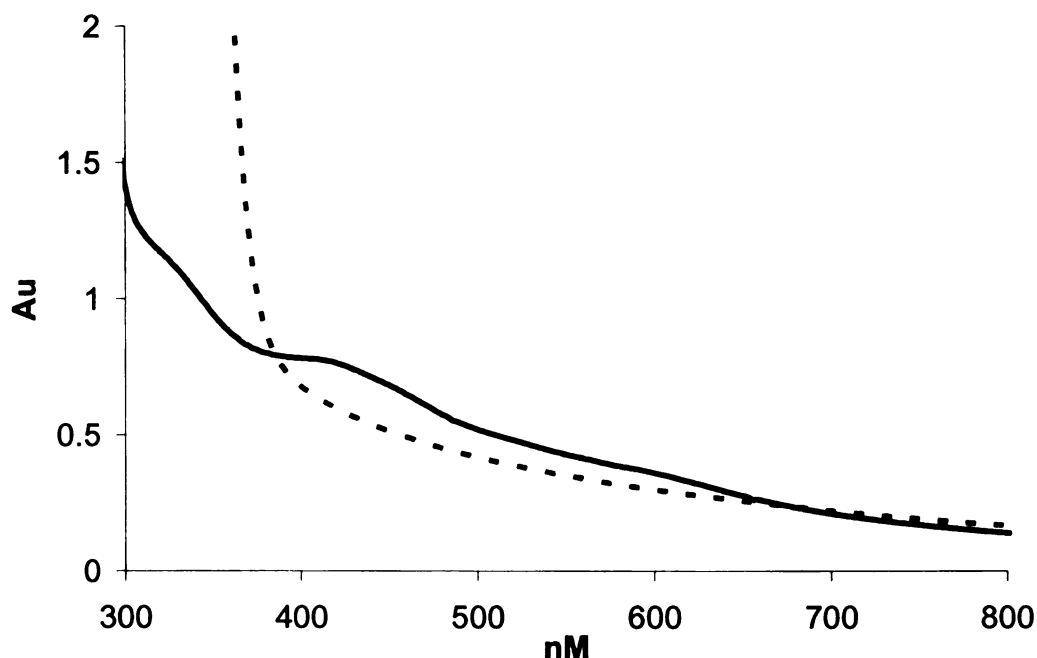
Figure IV.2 UV-visible absorption spectra of SPL as isolated (solid line) and reduced with dithionite (dashed line). For both spectra, the protein was 65 μM in 20 mM sodium phosphate/500 mM NaCl/5 mM dithiothreitol/5% glycerol, pH 8.0. The reduced protein also contained 5 mM dithionite. The spectra were recorded in a 1 cm pathlength cuvette under anaerobic conditions at room temperature.[9]

Electron paramagnetic spectroscopy

SP lyase exhibits a strong, nearly isotropic electron paramagnetic

resonance (EPR) signal which is centered at g = 2.02 and observable only below

35 K (Figure IV.3). The g value, the low anisotropy, and the temperature

dependence are consistent with the assignment to a $[3Fe-4S]^{1+}$ cluster being

present in the as isolated form of the enzyme. Spin quantification of the [3Fe-

4S]$^{1+}$ show that it accounts for up to 35% of the total iron. SP lyase can be

reduced under anaerobic conditions by titration with sodium dithionite (Figure

IV.2). The work presented in this section on the UV/Visible spectroscopy of SPL

was published in the Journal of Biological Chemistry.[9]
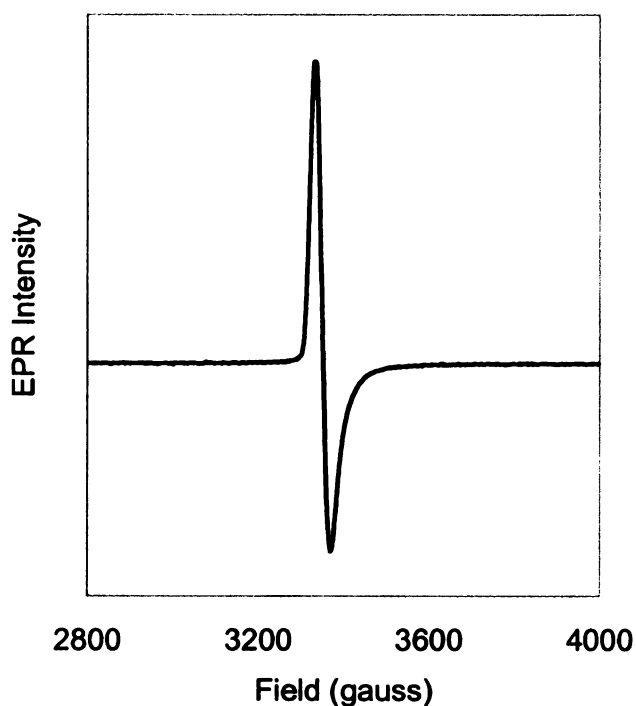
Figure IV.3 X-band EPR spectrum of anaerobically isolated SPL. The protein was 350 μM in 20 mM sodium phosphate/500 mM NaCl/10 mM dithiothreitol/5% glycerol, pH 8.0. Conditions of measurement, T=12 K microwave power, 2 mW; microwave frequency, 9.4841 GHz; modulation amplitude, 10.084; and receiver gain, 2 x 10^4, 1 scan accumulated.[9]

This reduction results in a dramatic change in the EPR spectral properties

(Figure IV.4). Rather than the fairly intense, nearly isotropic signal observed for

the as-isolated enzyme, the reduced enzyme has a weaker, nearly axial signal

that is characteristic of a $[4Fe-4S]^{1+}$ cluster, with g_z = 2.025, g_y = 1.928, and g_x = 1.890 (based on simulations, data not shown). The relaxation properties of this signal are also consistent with its assignment as a $[4Fe-4S]^{1+}$ cluster, as the signal broadens above 20 K and is unobservable above 40 K. Spin quantification of the $[4Fe-4S]^{1+}$ cluster shows that it accounts for up to 54% of the total iron present in the protein Dithionite reduction of SP lyase in the presence of its cofactor S-adenosylmethionine results in a $[4Fe-4S]^{1+}$ EPR signal essentially
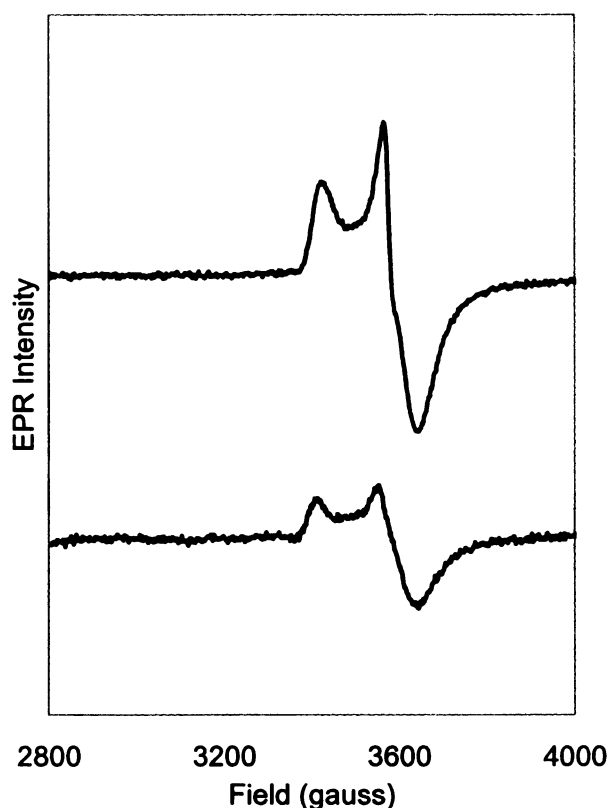
Figure IV.4 X-band EPR spectrum of reduced SP lyase with and without AdoMet. The protein was 350 μM in 20 mM sodium phosphate/500 mM NaCl/10 mM dithiothreitol/5% glycerol, pH 8.0. Dithionite was added to 5 mM (both spectra) and AdoMet to 2 mM (lower spectrum only). Conditions of measurement, T = 12 K microwave power, 2 mW; microwave frequency, 9.4841 GHz; modulation amplitude, 10.084; and receiver gain, 2 x 10^4, 1 scan accumulated.

identical to that seen in the absence of SAM, albeit with a lower signal intensity.

The EPR spectra of SPL are similar to those observed in previous studies of reconstituted SPL,[6] with a $[3Fe-4S]^{1+}$ cluster being observed prior to reduction. After reduction, the $[3Fe-4S]^{1+}$ cluster is transformed to a $[4Fe-4S]^{1+}$. The $[3Fe-4S]^{1+}$ however only accounts for one third of the total iron in the as-isolated sample, with the remaining being present in an EPR silent form. The EPR silent iron is also likely in an iron sulfur cluster as the Fe:S ratio is 1:1. SPL gains both catalytic activity (Chapter V) and a $[4Fe-4S]^{1+}$ cluster upon reduction, consistent with previous work demonstrating the presence of a catalytically relevant $[4Fe-4S]^{1+}$ cluster in the radical SAM enzymes PFL-AE[10] and LAM.[11] Our data suggests that this $[4Fe-4S]^{1+}$ cluster is generated by reductive cluster conversion of our $[3Fe-4S]^{1+}$ cluster because of the loss of this signal after reduction and the appearance of a $[4Fe-4S]^{1+}$ cluster signal.

In contrast to other members of the radical SAM superfamily, addition of SAM to the reduced SPL does not alter the line shape or g values of the $[4Fe-4S]^{1+}$ EPR signal; however, it does result in a decrease in the intensity of the signal (Figure IV.4). This reduction in intensity in the presence of SAM has previously been observed for SPL;[6] one interpretation of this observation could be that there is nonproductive reductive cleavage of SAM (and corresponding oxidation of the cluster). We have, however found no evidence for SAM cleavage in the presence of SPL (Chapter VI), indicating that other explanations such as a change in spin state of some population of the cluster, must be considered. Both

Q-band EPR (Chapter VIII) and Mössbauer spectroscopy provide some early

evidence for this possibility.

The work presented in this section on the EPR spectroscopy of SPL was

published in the Journal of Biological Chemistry.[9]

Mössbauer spectroscopy

Mössbauer spectroscopy of the as-isolated SPL demonstrates the

presence of multiple types of iron sulfur cluster (Figure IV.5.A). Simulations of the

iron sulfur content show it to contain 53% $[2Fe-2S]^{2+}$ cluster with δ = 0.28 mm/s;

ΔE_Q = 0.62mm/s; Γ = 0.43mm/s. The rest of the iron is a paramagnetic species

as noted by the splitting of the quadrupole doublet; this is most likely a $[3Fe-4S]^{1+}$

cluster, with maybe some admixture of $[4Fe-4S]^{1+}$.

Mössbauer spectroscopy of chemically reduced SPL also demonstrated a

mixture of cluster states (Figure IV.5.B). This spectrum can be simulated and

contains 10% $[4Fe-4S]^{2+}$ cluster with δ=0.49mm/s, ΔE_Q=1.11mm/s, and

Γ=0.43mm/s. The other 90% of the iron is a $[4Fe-4S]^{1+}$ cluster. The spectrum is

simulated using two equal intensity S = 1/2 centers, with δ = 0.60 mm/s, ΔE_Q =

1.29 mm/s, and A = (-30, -22, -11)kG, and δ = 0.55mm/s ΔE_Q=0.66mm/s A=(2,

15, 18)kG. Note that the isomer shift (δ) of both clusters are unusually high,

which is indicative of an electron-rich environment. As shown in Table IV.1,

typically for a $[4Fe-4S]^{2+}$ cluster, δ = 0.42 and δ = 0.57 for a $[4Fe-4S]^{1+}$

81
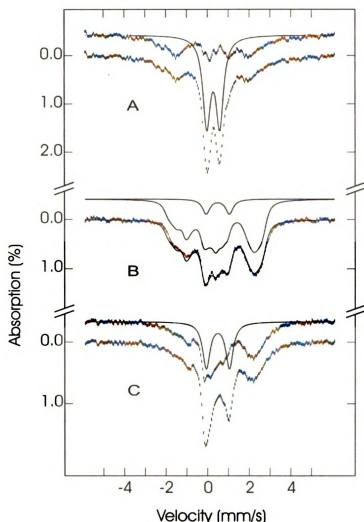
Figure IV.5 Mössbauer spectra of SPL. A. Native state SPL. The dashed black line is the actual experimental spectrum. The smoothed line is a simulated spectrum of a $[4Fe-4S]^{2+}$ cluster, weighted to 53% of the iron and the black line is the subtraction of the dashed black line and the simulation. The remaining is indicative of a $[3Fe-4S]^{1+}$ cluster. B. Reduced SPL. The dashed black line is the experimental spectrum, overlaid on this spectra (black line) is the addition of two simulated clusters, the upper line being a $[4Fe-4S]^{2+}$ cluster and the lower being a $[4Fe-4S]^{1+}$ cluster weighted to 10% and 90% of the total iron. C. Reduced SPL with SAM (dashed black line) and a simulation for a $[4Fe-4S]^{2+}$ cluster (smoothed line) weighted to 33% of the iron. The black line is the subtraction of the two above spectra, and is indicative of a $[4Fe-4S]^{1+}$ cluster.

Mössbauer spectroscopy of the chemically reduced SPL with SAM, as

with the above spectra, shows a mixture of cluster states (Figure IV.5.C).

Simulations of the spectra indicate that 33% of the iron is in a $[4Fe4S]^{2+}$ cluster, with the same parameters as in B, δ = 0.49mm/s, ΔE_Q = 1.11mm/s, and Γ = 0.43mm/s. The rest is most likely a $[4Fe-4S]^{1+}$ cluster, the spectrum of which is different from the ones in Figure IV.5.A and B. This may indicate that the SAM is bound to the cluster. If the bound state is confirmed, the question remains as to why some $[4Fe-4S]^{1+}$ clusters stay bound to SAM while others are oxidized to the $[4Fe-4S]^{2+}$ state.

IV.4   Conclusions

Through the use of several spectroscopic techniques it has been demonstrated that our purified SPL contains an iron sulfur cluster without having to artificially reconstitute the site as has been previously described.[6] UV/visible spectroscopy indicates the presence of an iron sulfur cluster with a broad absorption band between 300 nm and 600 nm but does not give any indication as to the type of cluster present. As with other members of the radical SAM superfamily and with previous work on SPL[6], the cluster can be reduced, showing it to be a redox active iron sulfur cluster.[12]

EPR of the as-isolated SPL yielded a spectrum consistent with that of a typical $[3Fe-4S]^{1+}$ cluster. However, the spin quantification showed that it accounted for only ~25-35% of the total iron present in the protein, meaning that the rest of the iron must be present in some sort of EPR silent state. EPR of the reduced cluster yields a spectrum characteristic of a $[4Fe-4S]^{1+}$ cluster but again

only up to 54% of the cluster is present in this state indicating the presence of another form of cluster.

Mössbauer spectroscopy of SPL grown in ^{57}Fe enriched media gives further insight into the cluster state of the SPL. This indicates that the native state protein is a mixture of a $[2Fe-2S]^{2+}$ cluster and a $[3Fe-4S]^{1+}$ cluster. This is somewhat in line with the EPR data that indicates a $[3Fe-4S]^{1+}$ and a EPR silent state. Upon reduction the majority of the cluster is changed to a $[4Fe-4S]^{1+}$ cluster with a high isomer shift. A summary of the different cluster states observed by both EPR and Mössbauer spectroscopy is provided in Table IV.2.

	As-isolated SPL	Reduced SPL	Reduced SPL + SAM
EPR	35% $[3Fe-4S]^{1+}$ 65% EPR silent	54% $[4Fe-4S]^{1+}$ 46% EPR silent	11% $[4Fe-4S]^{1+}$ 89% EPR silent
Mössbauer	53% $[2Fe-2S]^{1+}$ 47% $[3Fe-4S]^{1+}$	10% $[4Fe-4S]^{2+}$ 90% $[4Fe-4S]^{1+}$	33% $[4Fe-4S]^{2+}$ 67% $[4Fe-4S]^{1+}$

Table IV.2 Percentage of total iron present in the iron sulfur cluster of SPL as monitored by EPR and Mössbauer spectroscopy.

The high isomer shift is indicative of an electron rich cluster environment which may facilitate the transfer of an electron from the cluster of SPL to SAM and cause cleavage to methionine and the putative 5'-deoxyadenosyl radical during enzymatic turnover.

The facile cluster rearrangement that is observed in SPL by both EPR and Mössbauer spectroscopies has been seen in other radical SAM superfamily members including PFL-AE[7] and BioB[13] and may be a characteristic of the superfamily as a whole. This type of cluster conversion has also been seen in the well studied aconitase enzyme.[14] The presence of multiple cluster states is likely the result of cluster oxidation during purification and growth because of the non-cysteinal iron site that is found in the superfamily.

Finally the spectrum of reduced SPL and SAM indicates some cluster oxidation to a $[4Fe-4S]^{2+}$ cluster as well as an iron sulfur cluster with different parameters from the spectrum of the reduced SPL. This is likely the result of a interaction between the cluster and SAM, although it is still unknown as to what type of interaction is occurring. Another possibility is that the presence of AdoMet may cause some population of the cluster to change to a higher spin state, which would be consistent with the reduction in signal observed by EPR of $[4Fe-4S]^{1+}$ cluster in the presence of SAM.

IV.5 References

1. Que, L., *Physical Methods in Bioinorganic Chemistry*. University Science Books: Sausilito, CA, 2000.

2. Solomon, E. I.; Lever, A. B. P., *Inorganic Electronic Structure and Spectroscopy*. Wiley-Interscience: New York, 1999; Vol. I and II.

3. Rao, P. V.; Holm, R. H., Synthetic Analogues of the Active Sites of Iron-Sulfur Proteins. *Chem. Rev.* **2004,** 104, (2), 527-560.

4. Lippard, S. J.; Berg, J. M., *Principles of Bioinorganic Chemistry*. University Science Books: Mill Valley, CA, 1994.

5. Gutlich, P.; Link, R.; Trautwein, A., *Mossbauer Spectrscopy and Transition Metal Chemistry*. Springer - Verlag: Berlin, 1979.

6. Rebeil, R.; Nicholson, W. L., The subunit structure and catalytic mechanism of the Bacillus subtilis DNA repair enzyme spore photoproduct lyase. *Proceedings of the National Academy of Sciences of the United States of America* **2001,** 98, (16), 9038-43.

7. Broderick, J. B.; Henshaw, T. F.; Cheek, J.; Wojtuszewski, K.; Smith, S. R.; Trojan, M. R.; McGhan, R. M.; Kopf, A.; Kibbey, M.; Broderick, W. E., Pyruvate formate-lyase-activating enzyme: Strictly anaerobic isolation yields active enzyme containing a [3Fe-4S]$^+$ cluster. *Biochemical and Biophysical Research Communications* **2000,** 269, (2), 451-456.

8. Ollagnier de-Choudens, S.; Fonetcave, M., The lipoate synthase from Escherichia coli is an iron-sulfur protein. *FEBS Letters* **1999,** 453, 25-28.

9. Buis, J. M.; Cheek, J.; Kalliri, E.; Broderick, J. B., Characterization fo an active spore photoproduct lyase, a DNA repair enzyme in the radical sam superfamily. *Journal of Biological Chemistry* **2006,** In Press.

10. Henshaw, T. F.; Cheek, J.; Broderick, J. B., The [4Fe-4S]$^{1+}$ Cluster of Pyruvate Formate-Lyase Activating Enzyme Generates the Glycyl Radical on Pyruvate Formate-Lyase: EPR-Detected Single Turnover. *Journal of the American Chemical Society* **2000,** 122, (34), 8331-8332.

11. Lieder, K. W.; Booker, S.; Ruzicka, F. J.; Beinert, H.; Reed, G. H.; Frey, P. A., S-Adenosylmethionine-Dependent Reduction of Lysine 2,3-Aminomutase and Observation of the Catalytically Functional Iron-Sulfur Centers by Electron Paramagnetic Resonance. *Biochemistry* **1998,** 37, (8), 2578-2585.

12. Cheek, J.; Broderick, J. B., Adenosylmethionine-dependent iron-sulfur enzymes: versatile clusters in a radical new role. *J. Biol. Inorg. Chem.* **2001,** 6, (3), 209-26.

13. Jarrett, J. T., The novel structure and chemistry of iron-sulfur cluster in the adenosylmethionie-dependent radical enzyme biotin synthase. *Archives of Biochemistry and Biophysics* **2003,** 433, 312-321.

14. Broderick, J. B., Iron-sulfur clusters in enzyme catalysis. *Comprehensive Coordination Chemistry II* **2004,** 8, 739-757.

CHAPTER V

ENZYMATIC ACTIVITY OF SPORE PHOTOPRODUCT LYASE

V.1   Introduction

In the late 19th century it was discovered that a number of bacterial species spend part of their lives in a dormant cellular structure known as endospores.[1] These endospores are some of the hardiest forms of life on the planet. Endospores exhibit extreme resistance to desiccation, harsh chemicals, heat, UV radiation and γ radiation. Much effort has been expended investigating the molecular mechanism responsible for this high resistance to harsh environments. Some of the factors affecting resistance include the spore coat, the core water content, mineral content, the presence of SASPs and an ability to repair macromolecules such as DNA. The latter is the focus of this work. UV irradiation of spores has been shown to induce a specific type of DNA damage, known as the spore photoproduct.[2, 3]

Spore photoproduct lyase is known to repair the DNA lesion spore photoproduct.[4] Most likely this occurs immediately after the onset of spore germination since little metabolic activity occurs in the dormant spore phase.[5, 6] Although it has been shown that spore photoproduct lyase can repair DNA

damage both *in vivo* and *in vitro*, there had been no published specific activity of the spore photoproduct lyase nor has repair been correlated to the amount and type of iron sulfur cluster present in the protein.

Spore photoproduct has been generated *in vivo* upon exposure of sporulating bacteria such as *B. subtilis* or non-sporulating bacteria overexpressing SASP proteins to UV light.[7] Spore photoproduct has also been produced *in vitro* by the addition of SASP to DNA followed by UV irradiation.[8] SP has also been synthesized in the laboratory,[9, 10] although not incorporated into a DNA oligomer. In all cases, the structure of SP has been determined/verified by NMR techniques.[3, 7, 8, 10, 11] Repair by spore photoproduct lyase has been seen in all of the above circumstances.

Due to difficulty in working with bacterial spores and difficulties in synthesizing SP, in this work we have produced SP by the irradiation of the radiolabeled (at thymine) pUC18 plasmid DNA under SP forming conditions. Upwards of 5% of the thymine is converted to SP using the methods described herein. Repair of SP can be monitored by HPLC separation of thymine and SP followed by liquid scintillation counting. Using these methods, we have examined SP repair by SPL as a function of time to acquire a specific activity for SPL. Repair of SP can be monitored by HPLC separation of thymine and SP and liquid scintillation counting. We have also examined the effect of the cluster redox state on SP repair activity.

V.2 Experimental methods

Materials

Except where noted otherwise, all chemicals were purchased commercially and were of high purity. Radiolabeled [*methyl* - ^3H] thymidine was purchased from Amersham Biosciences.

^3H labeling and synthesis of the spore photoproduct

Labeling of pUC18 DNA was carried out as follows. NovaBlue *E. coli* (Novagen) carrying pUC18 was grown overnight at 37 °C in 50 mL of 2 x YT medium (per liter: 16 g tryptone, 10 g yeast extract, 5 g NaCl) containing 50 μg/mL ampicillin, 0.45 mM 2'-deoxyadenosine, and 10 μM [*methyl*-^3H]-thymidine (0.74 MBq/mL) (Amersham-Pharmacia). Labeled DNA was extracted from the overnight culture using a Promega Wizard Mini-Prep Kit. The specific activity of the purified DNA was typically 1.5 x 10^7 cpm/μmol. To form a complex between the ^3H-DNA and the SASP-C, the two were mixed in a 5:1, SASP-C: DNA ratio in 70 μL of 25 mM Tris-acetate, 125 mM NaCl, pH 6.5 and incubated at 37 °C for 2 hours in a custom made quartz vacuum hydrolysis tube. This complex was irradiated with 30 kJ/m^2 UV light at 254 nm in order to form spore photoproduct on the ^3H-DNA. This ^3H-DNA was then used in the assay. The amount of spore photoproduct generated was quantified by hydrolyzing the irradiated ^3H-DNA and separating SP from thymine on a Waters Spherisorb S5P 4.0 X 250 mm analytical column, run with MQ H$_2$O at a flowrate of 1.8 mL/min in degassed MQ

H$_2$O for 25 min with fractions collected every 0.5 or 1 min. Liquid scintillation counting was performed on each fraction using a Wallac 1414-001 Liquid Scintillation Counter. Labeled thymine elutes at ~ 3 min and the spore photoproduct elutes at 10-11 min. Dividing the CPM eluting of the SP peak by the total CPM eluting from the column gives the percentage of thymine in the spore photoproduct form. The total amount of SP present is calculated as follows:

$$Amount\ of\ SP = \frac{\lfloor A260 \quad DNA * 50\mu g/mL \rfloor}{1700\ kDa} * 1325 \frac{T}{pUC18} * \frac{SP\ CPM}{Total\ T\ CPM}$$

(1)

Time course repair assay of spore photoproduct

SP lyase activity was determined using a slightly modified version of the assay developed by Nicholson and coworkers. All solutions except DNA and protein solutions were prepared anaerobically in an mBraun glove box just prior to use. Protein and DNA solutions were made anaerobic by repeated vacuum-purge cycles prior to bringing them into the glove box. Assay experiments with and without SP lyase (1 µM) were set up in parallel in custom-made vacuum hydrolysis tubes in the glove box. Reaction mixtures (1 mL total volume) contained 1 nmol SP lyase, 2 mM AdoMet, 25000-50000 cpm of ^{3}H-pUC18 DNA (^{3}H at the thymine methyl and containing 200-435 nmol SP), 4 mM dithiothreitol, 3 mM dithionite, and 30 mM KCl, all in 20 mM sodium phosphate, 500 mM NaCl, 5% glycerol, pH 7.0. All reaction mixtures were incubated under anaerobic conditions at 37 °C for 60 minutes with aliquots taken every 10 minutes and

terminated with the addition of 0.5 mL trifluoroacetic acid. The hydrolysis tubes were sealed under vacuum and heated to 165 °C for 2 hours. The trifluoroacetic acid was evaporated and the dried residue was resuspended in 100 µL of MQ H_2O. A portion of the solution (15µL) was loaded onto a Waters Spherisorb S5P 4.0 X 250mm analytical column and run at a flow rate of 1.8mL/min in degassed MQ H_2O for 25 min with fractions collected every 0.5 or 1min. Liquid scintillation counting was performed on each fraction using a either a Wallac 1414-001 Liquid Scintillation Counter or a Beckman LS 6500 Liquid Scintillation Counter with the addition of 15 mL of Safety Solve liquid scintillation cocktail.

Repair assay with pre-reduced SPL

Time course repair assays were carried out as above except that SPL used had previously been reduced under anaerobic conditions by the addition of 10 mM sodium dithionite and 10 mM DTT. EPR spectroscopy was conducted on a 300 µL sample of SPL that was 550 µM in concentration on an X-band Bruker ESP300E spectrometer equipped with a liquid He cryostat and a temperature controller from Oxford Instruments. Spectra were recorded at 12 K. Spin quantifications were carried out as previously described. The double integrals of the EPR signals were evaluated by using a computer on-line with the spectrometer. Spin concentration in the protein samples was determined by calibrating double integrals of the EPR recorded under non-saturating conditions with a standard sample of 0.1 mM Cu (II) and 1 mM EDTA.

V.3   Results and discussion

After purification and irradiation of pUC18 methyl ^{3}H thymidine DNA, the amount of spore photoproduct produced as a total percentage of thymine was between 4 and 7% (Figure V.1).
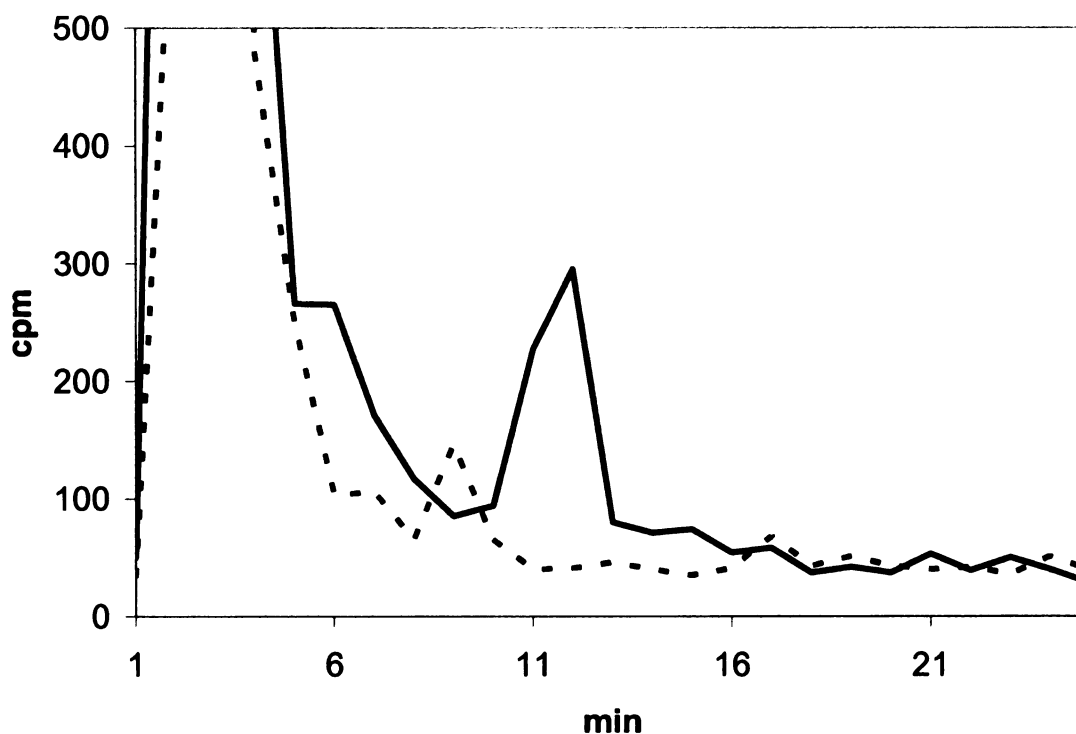
Figure V.1   The separation of thymine and SP after HPLC is illustrated above. The solid line is UV-irradiated and hydrolyzed DNA without the addition of SPL. The dashed line is UV-irradiated and hydrolyzed DNA after the addition of SPL and incubated for 60 min. Both samples were acid hydrolyzed and loaded onto a Waters Spherisorb S5P column and run with an isocratic flow of degassed MQ water for 25 minutes at 1.8 mL/min. Fractions were collected every minute and run on a liquid scintillation counter.

This DNA proved to be stable under repair conditions in the absence of SPL, after 1 hour incubation at 37°C, no change in the amount of SP was seen. Time course experiments show the addition of SPL to SP under reducing conditions

causes a reduction in the amount of spore photoproduct present. This repair is

linear over the course of 1 hour (Figures V.2 and V.3) with 70% of the SP

repaired after 1 hour. Prior to our work, repair of SP by SPL has been reported in
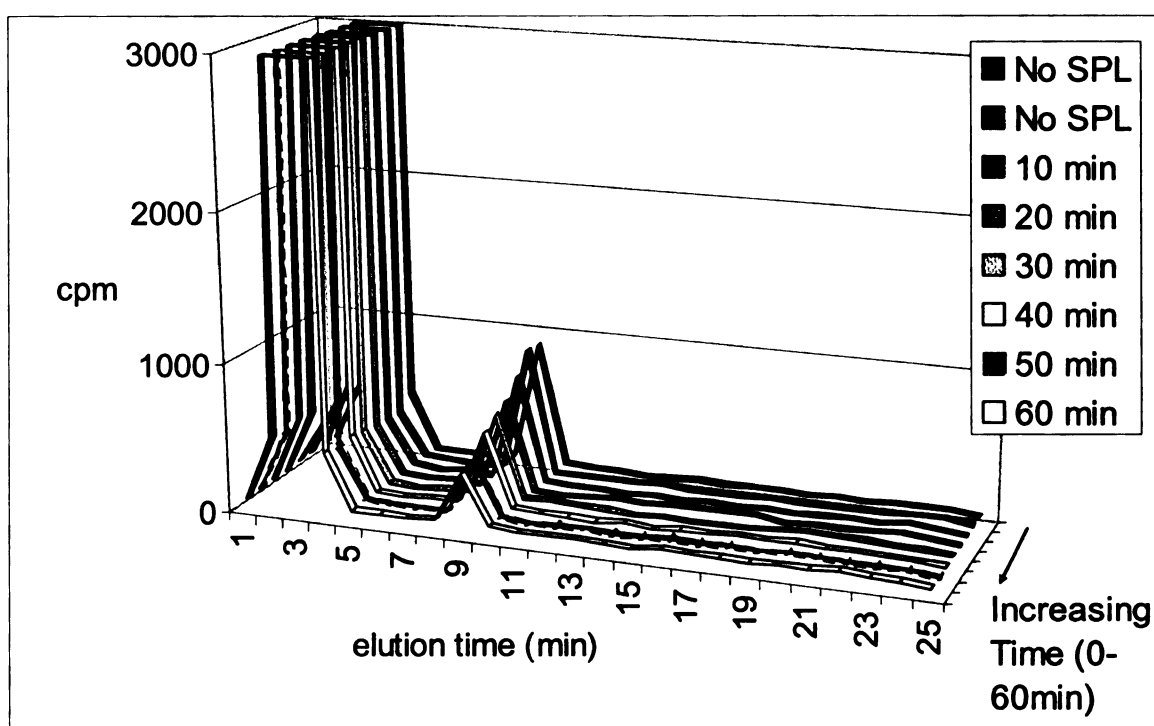
Figure V.2   A representation of SP repair over a time of 60 min. Thymine elutes at ~ 3 min, and SP elutes at ~10 min. Over the course of 60 minutes the amount of SP decreases 70%.

terms of the percentage of SP repaired. While useful in illustrating the presence

of SP repair activity, numbers in terms of % SP repaired are not standard activity

rates do not allow for any sophisticated enzyme kinetics. By plotting of nmols of

SP repaired versus time, in contrast a standard specific activity can be calculated

(Figure V.3). The specific activity of SPL based on our work to date is 0.33 μmols

SP repaired/min/mg SPL.[12]
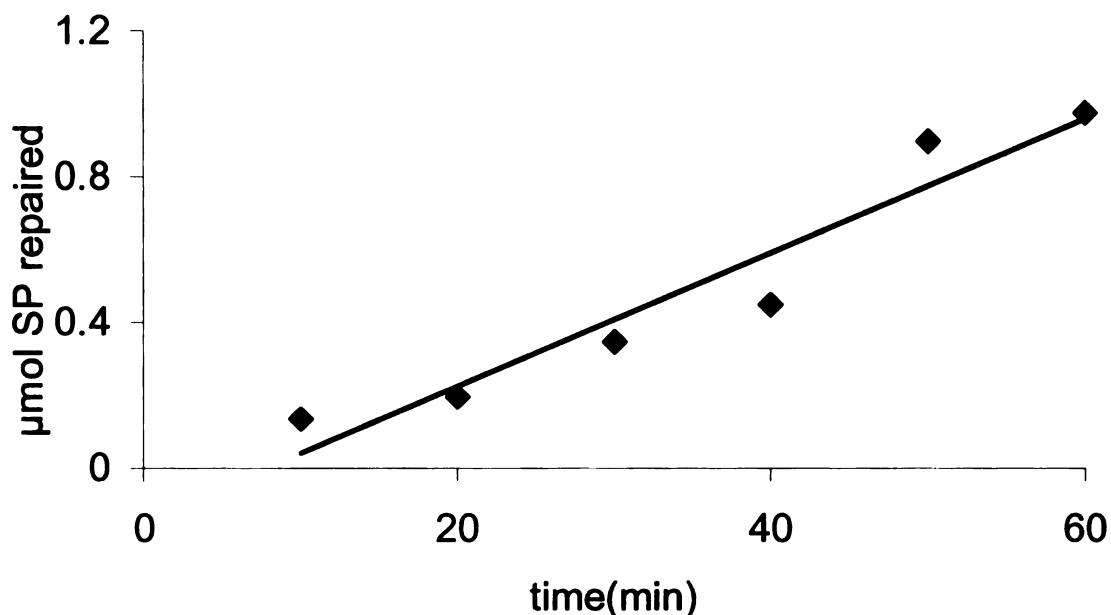
Figure V.3   SP lyase is active in SP repair. Representative time course of SP repair by reduced SP lyase. Repair of pUC18 DNA was monitored at 10 min intervals by removal of 100 μL aliquots, which were quenched hydrolyzed, and monitored by HPLC for SP repair. Linear repair is observed up to 60 minutes with a specific activity of 0.33 μg SP repaired/min/mg SPL. The apparent lag time may result from a need for reduction of SP lyase prior to the initiation of SP repair.[12]

While the time course repair assay shows that a specific activity can be

calculated for SPL, the calculation did not take into account the degree to which

SPL was in the [4Fe-4S]$^{1+}$ state. It is has been shown in other members of the

radical SAM superfamily such as PFL-AE and LAM that the [4Fe-4S]$^{1+}$ is the

active cluster form. It is therefore important to determine a specific activity based

on the amount of [4Fe-4S]$^{1+}$ cluster present in reduced SPL. To this end, SPL

that had been previously reduced with sodium dithionite and whose cluster

content had been measured by EPR spin quantification (Figure V.4) was used in

a repair assay.
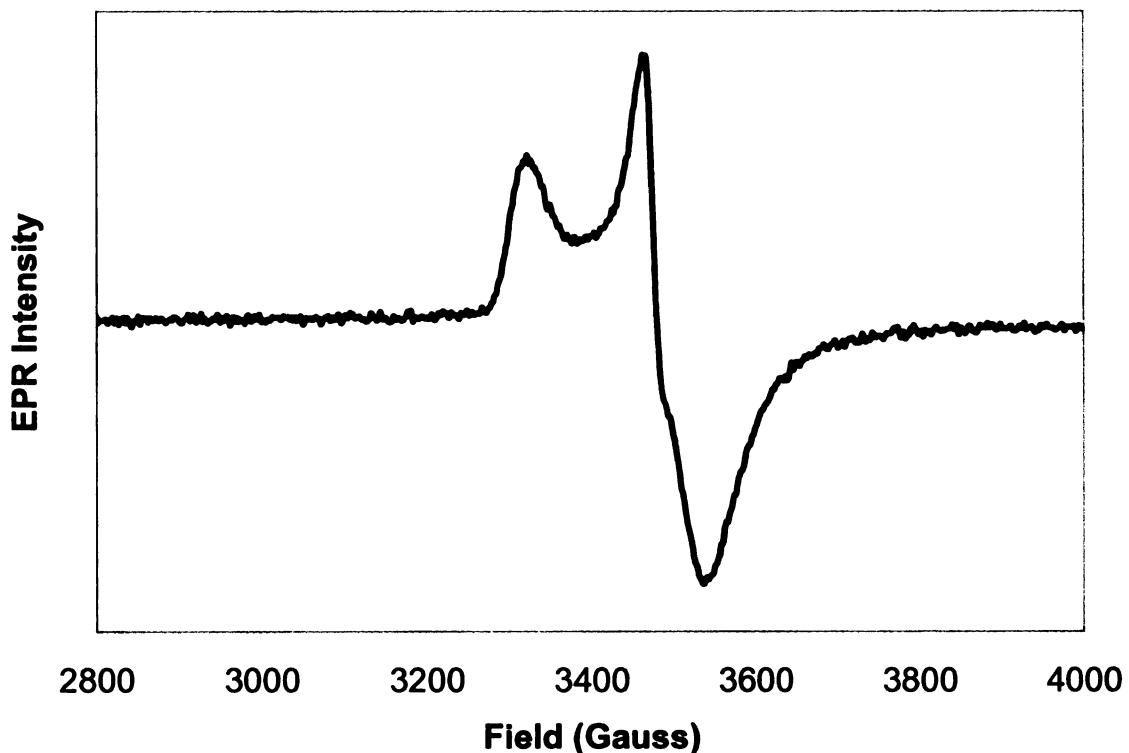
Figure V.4   EPR of SPL used in repair of SP dimers shows that 54% of the protein is in the $[4Fe-4S]^{1+}$ state, as measured by spin quantification versus a Cu-EDTA standard, prior to its assay for DNA repair activity.

The SPL contained 54% $[4Fe-4S]^{1+}$ (297 μM) and repair assays run with this

protein show linear repair up to 50 minutes (Figure V.5). A specific activity of 1.33

μmols SP repaired/min/μg SPL was calculated, which if calculated by content of

$[4Fe-4S]^{1+}$ present is 2.4 μmols SP repaired/min/mg SPL with $[4Fe-4S]^{1+}$. This is

over a 4 fold increase in activity compared with protein that was not reduced prior

A.

B.
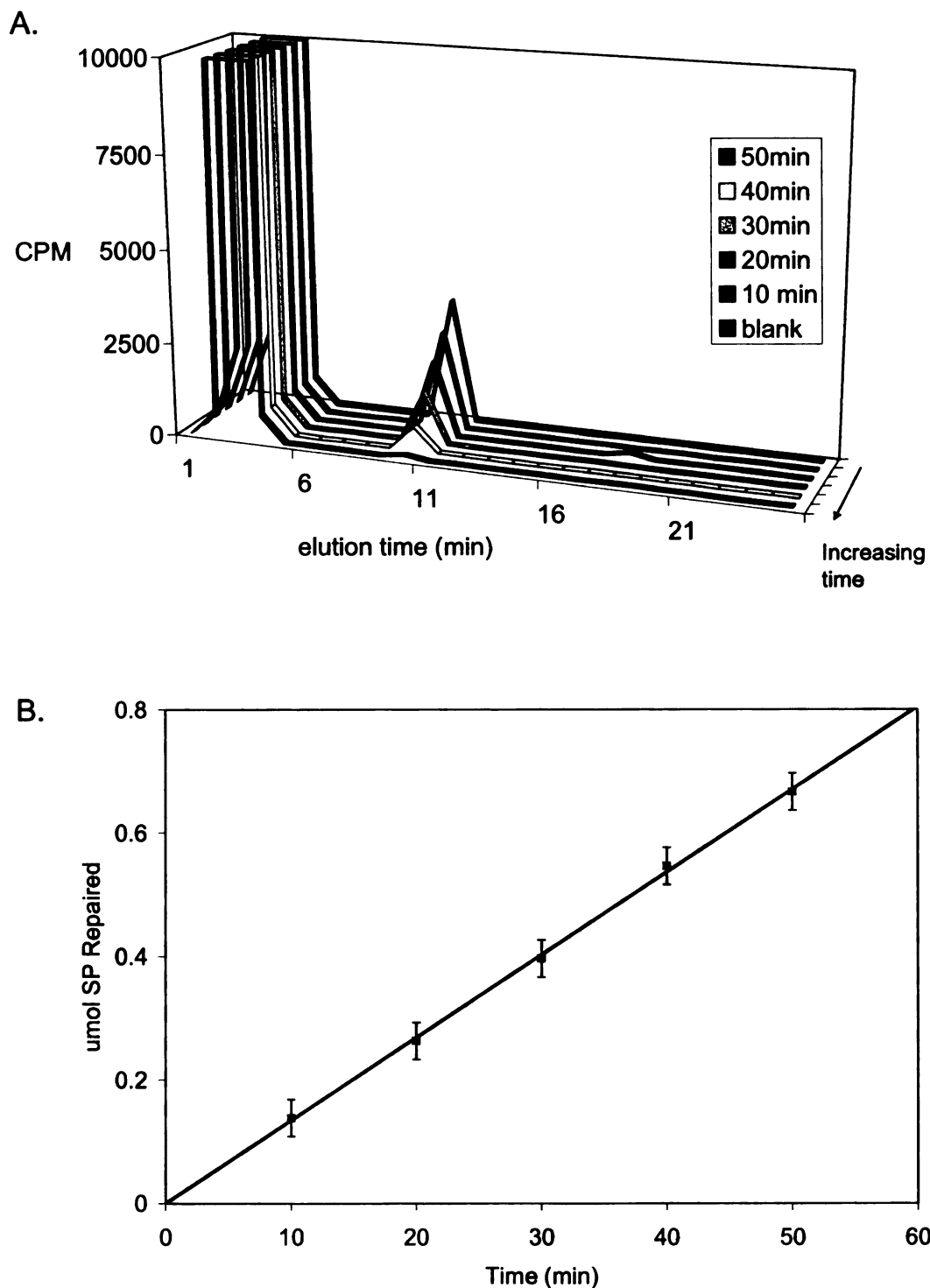
Figure V.5   Time course of SP repair by reduced SPL. A. Representative HPLC chromatograms show loss of the SP peak as a function of time. B. Linear repair is observed up to 50 minutes with a specific activity of 1.33 μmol SP repaired/min/mg SPL.

to use in SP repair assays, suggesting that in previous assays the rate was being limited by the amount of $[4Fe-4S]^{1+}$ cluster present. The amount of reductant in those assays may have been insufficient for complete cluster reduction. By reducing prior to DNA repair, a greater percentage of the protein is active.

V.4   Conclusions

Prior reports as to the DNA repair capabilities of SPL have provided activity in terms of % DNA repaired and have not mentioned a specific activity of the enzyme.[13, 14] We were however able to calculate a specific activity of 0.0002 μmol SP repaired/min/mg SPL based on the information in the literature, nearly 1000 fold lower than our activity reported here.[14] The determination of an accurate specific activity is important to future studies involving the kinetics and mechanism of SPL. In addition, our results indicate that SPL is much faster at SP repair than initially thought, which may be important as SPL is thought to be active only during cell germination. That is, it is crucial for cellular function that SPL repairs the damaged DNA expediently in order for other proteins to be produced correctly.

We have also shown that the activity of SPL can be enhanced by reducing the protein prior to use in repair assays. In the "standard" assay described in this chapter, as-isolated SPL is added immediately to a SP repair reaction with 3 mM sodium dithionite present. We then start timing the SP repair and remove samples every 10 minutes. This method leads to a specific activity of 0.33 μmol SP repaired/min/mg SPL, however, plots of SP repaired versus time show a an

amount of lag time present in SP repair and are not fully linear. This may be the result of the protein not being reduced to a $[4Fe-4S]^{1+}$ cluster at the beginning of the reaction, thus inhibiting SPL's repair rate. By chemically pre-reducing the SPL, our activity increased 4 fold to ~1.33 μmol SP repaired/min/mg SPL. By correlating this activity to the amount of protein that contains a $[4Fe-4S]^{1+}$ cluster based on EPR we obtain an activity of 2.4 μmol SP repaired/min/mg SPL with $[4Fe-4S]^{1+}$. Based on this evidence of enhanced activity with pre-reduced SPL, we conclude that similar to other members of the radical SAM superfamily [15, 16], SPL utilizes a $[4Fe-4S]^{1+}$ as the active cluster. Confirmation of this conclusion will require a more detailed study examining the correlation between the amount of $[4Fe-4S]^{1+}$ cluster present in the protein and the rate of SP repair.

V.5 References

1. Cohn, F., Untersuchungen uber Bakterien IV. Beitrage zur Biologie der Bacillen. *Beitre. Biol. Pflanz* **1876**, 2, 249-276.

2. Donnellan, J. E., Jr.; Setlow, R. B., Thymine photoproducts but not thymine dimers found in ultraviolet-irradiated bacterial spores. *Science* **1965**, 149, 308-310.

3. Donnellan, J. E., Jr.; Stafford, R. S., Ultraviolet photochemistry and photobiology of vegetative cells and spores of Bacillus megaterium. *Biophysical Journal* **1968**, 8, (1), 17-28.

4. Munakata, N.; Rupert, C. S., Dark repair of DNA containing spore photoproduct in Bacillus subtilis. *Molecular and General Genetics* **1974**, 130, (3), 239-50.

5. Setlow, P., I will survive: protecting and repairing spore DNA. *J. Bacteriol.* **1992**, 174, 2737-2741.

6. Setlow, P., Resistance of Spores of Bacillus Species to Ultraviolet Light. *Environmental and Molecular Mutagenesis* **2001**, 38, 97-104.

7. Setlow, B.; Hand, A. R.; Setlow, P., Synthesis of a Bacillus subtilis small, acid-soluble spore protein in Escherichia coli causes cell DNA to assume some characteristics of spore DNA. *Journal of Bacteriology* **1991**, 173, (5), 1642-53.

8. Nicholson, W. L.; Setlow, B.; Setlow, P., Ultraviolet irradiation of DNA complexed with alpha/beta-type small, acid-soluble proteins from spores of Bacillus or Clostridium species makes spore photoproduct but not thymine dimers. *Proceedings of the National Academy of Sciences of the United States of America* **1991**, 88, (19), 8288-92.

9. Nicewonger, R.; Begley, T. P., Synthesis of the spore photoproduct. *Tetrahedron Letters* **1997**, 38, (6), 935-936.

10. Friedel, M. G.; Berteau, O.; Pieck, J. C.; Atta, M.; Ollagnier-de-Choudens, S.; Fontecave, M.; Carell, T., The spore photoproduct lyase repairs the 5S- and not the 5R-configured spore photoproduct DNA lesion. *Chemical Communications (Cambridge, United Kingdom)* **2006**, (4), 445-447.

11. Chandor, A.; Berteau, O.; Douki, T.; Gasparutto, D.; Sanakis, Y.; Ollagnier-de-Choudens, S.; Atta, M.; Fontecave, M., Dinucleotide spore photoproduct: A minimal substrate of the DNA repair spore photoproduct lyase enzyme from bacillus subtilis. *J. Biol. Chem.* **2006**, In Press.

12. Buis, J. M.; Cheek, J.; Kalliri, E.; Broderick, J. B., Characterization fo an active spore photoproduct lyase, a DNA repair enzyme in the radical sam superfamily. *Journal of Biological Chemistry* **2006**, In Press.

13. Rebeil, R.; Sun, Y.; Chooback, L.; Pedraza-Reyes, M.; Kinsland, C.; Begley, T. P.; Nicholson, W. L., Spore photoproduct lyase from Bacillus subtilis spores is a novel iron-sulfur DNA repair enzyme which shares features with proteins such as class III anaerobic ribonucleotide reductases and pyruvate-formate lyases. *Journal of Bacteriology* **1998**, 180, (18), 4879-85.

14. Slieman, T. A.; Rebeil, R.; Nicholson, W. L., Spore photoproduct (SP) lyase from Bacillus subtilis specifically binds to and cleaves SP (5-thyminyl-5,6-dihydrothymine) but not cyclobutane pyrimidine dimers in UV-irradiated DNA. *Journal of Bacteriology* **2000**, 182, (22), 6412-7.

15. Henshaw, T. F.; Cheek, J.; Broderick, J. B., The [4Fe-4S]1+ Cluster of Pyruvate Formate-Lyase Activating Enzyme Generates the Glycyl Radical on Pyruvate Formate-Lyase: EPR-Detected Single Turnover. *Journal of the American Chemical Society* **2000**, 122, (34), 8331-8332.

16. Gambarelli, S.; Luttringer, F.; Padovani, D.; Mulliez, E.; Fontecave, M., Activation of the anaerobic ribonucleotide reductase by S-adenosylmethionine. *ChemBioChem* **2005**, 6, (11), 1960-1962.

CHAPTER VI

MECHANISTIC CONSIDERATIONS FOR SPORE PHOTOPRODUCT LYASE

VI.1   Introduction

S-adenosylmethionine has been shown to act as both a co-factor and a co-substrate among members of the radical SAM superfamily.[1] For example, in PFL-AE and anRNR-AE a single SAM is used to activate a single PFL or anRNR by generation of a glycyl radical.[1,2] In LAM, however, one SAM molecule can lead to multiple enzyme turnovers.[3] Whether the subtle difference observed between PFL-AE and LAM by ENDOR and EXAFS reflect this difference in utilization of SAM remains to be determined.[4-7]

There is still debate as to whether SAM acts as either a cofactor or as a cosubstrate with SPL. A mechanism originally proposed by Mehl and Begley (Scheme VI.1) gives SAM the role as an enzyme cofactor.[8] In this mechanism, an electron from presumably the $[4Fe-4S]^{1+}$ cluster of SPL is transferred to SAM causing reductive cleavage to form the putative 5'-deoxyadenosyl radical and methionine. The 5'-deoxyadenosyl radical initiates radical catalysis by abstracting a H atom from the C-6 position of the thymine ring. This initial H atom abstraction
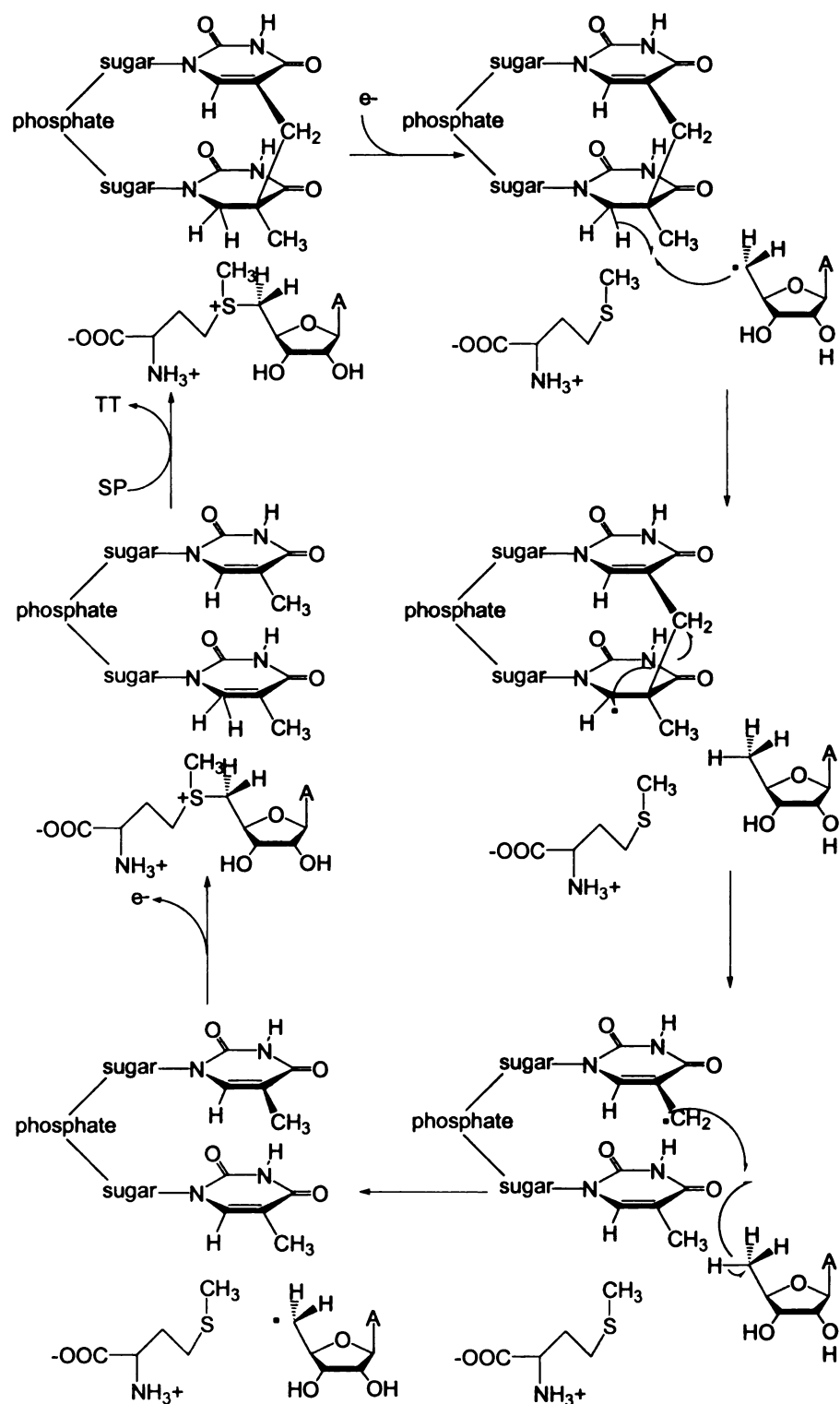
Scheme VI.1 Proposed mechanism for SP repair by SPL in which SAM is homolytically cleaved by an electron from the iron sulfur cluster of SPL. A putative 5'-deoxyadenosyl radical is formed which abstracts a hydrogen from the C-6 on the thymine ring and initiates radical catalysis.[8]

has been supported by the work of Cheek and Broderick.[9] After H atom

abstraction by 5'-deoxyadenosine, a radical mediated β-scission cleaves the

methylene bridge and separates the thymine bases, leaving a methyl radical on

one of the thymine bases. This methyl radical then abstracts a H atom from 5'-

deoxyadenosine to reform the putative 5'-deoxyadenosyl radical. This radical is

then free to interact with methionine and reform SAM donating its electron back

to the FeS cluster. However, work in the Nicholoson lab and the Fontecave lab

show cleavage of SAM into 5'-deoxyadenosine and methionine by SPL both non-

productively[10] and during repair of model substrates.[11, 12] As mentioned above

though, work carried out in the Broderick group confirmed part of Mehl and

Begley's mechanism by showing ^{3}H label transfer from the C-6 of the thymine

ring to SAM during repair.[9] This helped to substantiate the proposed mechanism

in Scheme VI.1 involving SAM as a co-factor in SPL catalysis. A recent DFT

study also provided evidence that the proposed mechanism involving SAM as a

cofactor was energetically plausible.[13] This study concluded the abstraction of a

hydrogen atom from 5'-deoxyadenosine should be the limiting step in this

reaction with an energy barrier of 23.1 kcal/mol.

The goal of the work described in this chapter was to further investigate

the mechanism of SP repair by SPL with a particular focus on the role of SAM. If

SAM acts as a cofactor, then no 5'-deoxyadenosine should be formed during

repair. We have therefore conducted experiments in which we monitor the

production of 5'-deoxyadenosine and the loss of SAM during repair of SP. Based

on the mechanism proposed in Scheme VI.1 if SAM is labeled at the 5-C position

with ^{3}H (Scheme VI.2), a portion of this should be transferred to thymine during enzymatic turnover. This would occur when the methyl radical abstract a hydogren from 5'-deoxyadenosine to reform the putative 5'-deoxyadenosyl radical. The transfer of this label from SAM to thymine should be subject to a selective isotope effect, as the hydrogen on the methyl group of 5'-dAdo would be energetically favored for abstraction versus tritium.
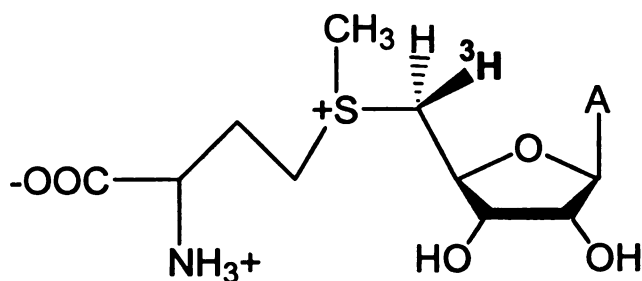
Scheme VI.2 S-adenosylmethionine with a tritium label at the 5'-C.
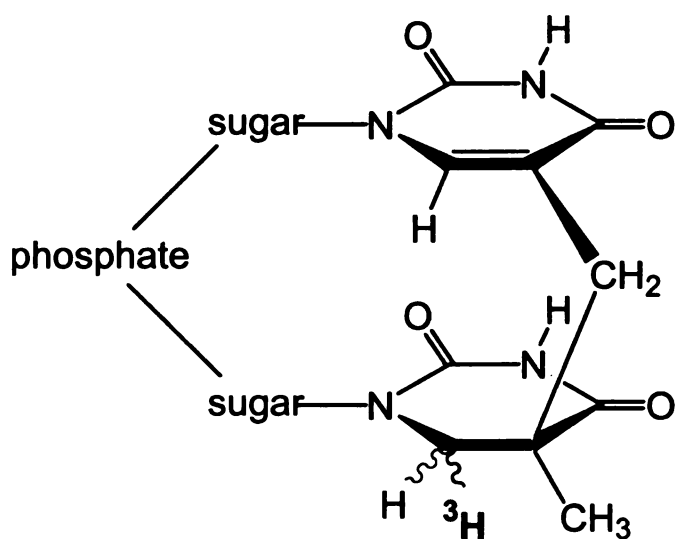
Scheme VI.3 Spore photoproduct label with tritium at C-6.

105

Work by Cheek and Broderick used labeled [C-6 – ^3H] thymidine to produce SP (Scheme VI.3) and examined initial H atom abstraction of the reaction catalyzed by SPL.[9] We have designed experiments to expand upon this work by using labeled [C-6 – ^3H] thymidine to produce labeled SP. We then used this SP to probe the presence of an isotope effect in the initial H-atom abstraction step of the SP repair mechanism. The presence of an isotope effect would provide insight into the relative heights of energetic barriers in an enzyme catalyzed reaction.[14] Isotope effects have been observed in several members of the adenosylcobalamin-dependent isomerase group of enzymes, specifically glutamate mutase.[15] Together these experiments should provide further insight into the mechanism of spore photoproduct lyase.

VI.2   Experimental Methods

Materials

All chemicals used in this work were purchased commercially and were of a high quality. [2, $5'$, 8 - ^3H] - ATP and [C-6 - ^3H] - thymidine were purchased from Amersham Biosciences.

Synthesis of [2, $5'$, 8 - ^3H] SAM

SAM was labeled with ^3H by using the following procedure. A 5 mL reaction of 100 mM Tris HCl (pH 8.0), 50 mM KCl, 26 mM $MgCl_2$, 5.2 mM adenosine triphosphate (ATP), 8% β-mercaptoethanol, 1mM EDTA, 6.8 mM

106

methionine, 2.5μL inorganic pyrophosphatase, 500 μL SAM synthetase crude lysate, and 1 mCi [2, 5′, 8 - ^3H] - ATP was stirred at room temperature for 16 hrs and quenched with 500 μL 1 M HCl. The reaction was monitored by TLC to completion and purified by loading onto a Source 15s.6 cationic exchange column (Pharmacia). A linear gradient from MQ H_2O to 1M HCl was used to elute the SAM. The fractions containing SAM (elutes between 0.4 M and 0.6 M HCl) were lyophilized and redissolved in 50 mM HEPES, 200 mM NaCl (pH 7.5).

Production of unlabeled spore photoproduct

NovaBlue *E. coli* (Novagen) carrying pUC18 was grown overnight at 37 °C in 50 mL of 2 x YT medium (per liter: 16 g tryptone, 10 g yeast extract, 5 g NaCl) containing 50 μg/mL ampicillin. Unlabeled DNA was extracted from the overnight culture using a Promega Wizard Mini-Prep Kit. To form a complex between the DNA and the SASP-C, the two were mixed in a 5:1, SASP-C: DNA ratio in 70 μL of 25 mM Tris-acetate, 125 mM NaCl, pH 6.5 and incubated at 37 °C for 2 hours in a custom made quartz vacuum hydrolysis tube. The solution was placed over a saturated ZnCl solution and equilibrated for 5 days. This complex was irradiated with 30 kJ/m^2 UV light at 254 nm in order to form spore photoproduct on the pUC18 DNA. The DNA was then redissolved in a buffer containing 20 mM sodium phosphate/500 mM NaCl/5% glycerol pH 8.0. This DNA was then used in the assay.

Production of [C-6 - ^{3}H] thymine labeled spore photoproduct

Labeling of pUC18 DNA was carried out as follows. NovaBlue *E. coli* (Novagen) carrying pUC18 was grown overnight at 37 °C in 50 mL of 2 x YT medium (per liter: 16 g tryptone, 10 g yeast extract, 5 g NaCl) containing 50 µg/mL ampicillin, 0.45 mM 2'-deoxyadenosine, and 10 µM [C-6 - ^{3}H]-thymidine (0.74 MBq/mL) (Amersham Biosciences). Labeled DNA was extracted from the overnight culture using a Promega Wizard Mini-Prep Kit. The specific activity of the purified DNA was typically 1.5 x 10^7 cpm/µmol. To form a complex between the ^{3}H-DNA and the SASP-C, the two were mixed in a 5:1, SASP-C: DNA ratio in 70 µL of 25 mM Tris-acetate, 125 mM NaCl, pH 6.5 and incubated at 37 °C for 2 hours in a custom made quartz vacuum hydrolysis tube. The solution was dried and place over a saturated ZnCl solution to equilibrate for 5 days. This complex was irradiated with 30 kJ/m^2 UV light at 254 nm in order to form spore photoproduct. This [C-6 - ^{3}H] thymine labeled spore photoproduct was then used in the assay.

Tritium transfer from SAM to thymine

SP lyase activity for detection of ^{3}H transfer from SAM to repaired thymine was determined using a slightly modified version of the assay developed by Nicholson and coworkers.[16, 17] All solutions except DNA and protein solutions were prepared anaerobically in an mBraun glove box just prior to use. Protein and DNA solutions were made anaerobic by repeated vacuum-purge cycles prior

to bringing them into the glove box. All experiments were prepared in o-ring

sealed 1.5 mL centrifuge tubes with the following reaction conditions: 4 mM DTT,

3 mM sodium dithionite, 150 µM [*2, 5', 8 - ^{3}H*]-SAM (0.67 µCi/µmol), 30 mM KCl,

0.5 mg/mL pUC18 irradiated DNA in 20 mM sodium phosphate, 500 mM NaCl,

5% glycerol, in a total volume of 400 uL. Samples were prepared in duplicate

both in the presence and absence of SPL. Samples were incubated for 60 min at

37 °C and DNA was purified using a wizard mini-prep DNA kit in order to

separate DNA from SAM. A control was carried out in the absence of DNA to

make sure SAM was removed by the purification procedure. Triflouroacetic acid

(500 µL) was added to the purified DNA which, was then placed in a customized

vacuum hydrolysis tube then sealed under vacuum. The solution was heated at

165° C for 3 hours and lyophilized on a Shlenk line until dry, then redissolved in

100 µL MQ H$_2$O. A portion of the solution (15 µL) was loaded onto a Waters

Spherisorb S5P 4.0 X 250 mm analytical column and run at a flowrate of 1.8

mL/min in degassed MQ H$_2$O for 25 min with fractions collected at 1 min

intervals. Liquid scintillation counting was performed on each fraction using a

Beckman-Coulter 6500 Liquid Scintillation Counter after the addition of 15 mL of

Safety Solve liquid scintillation cocktail.

Tritium transfer from thymine to SAM

A typical SP repair reaction was run as described in chapter 5 except that

311 nmols of SP and 0.1 mg of SPL was used per reaction. Instead of [*methyl-

^{3}H*] thymidine, [*C-6-^{3}H*] thymidine was used to produce labeled DNA. The SAM

concentration was increased to 4 mM SAM. was used. In addition, Samples were incubated for time intervals of 0, 2.5, 5 and 10 minutes. After reaction, the samples were purified through a YM-3 membrane to remove protein and then lyophilized and redissolved in 20 μL MQ H_2O. Each sample was loaded onto a C18 Waters Spherisorb 5μM ODS2 4.6 mm X 150 mm column at 1 mL/min with a step gradient.(4 mL MQ H_2O 0.1% triflouroacetic acid (TFA) , 13 mL 82% MQ H_2O 0.1% triflouroacetic acid, 18% acetonitrile with 0.1% TFA, 14 mL 100% acetonitrile with 0.1% TFA) used to elute. Fractions were collected every minute, and 15 mL scintillation fluid was added, and samples were counted using a LSC.

SAM cleavage by spore photoproduct lyase

Standards of SAM and 5'deoxyadenosine were run over a C18 Waters Spherisorb 5μM ODS2 4.6 mm X 150 mm column at 1 mL/min with a step gradient.(4 mL MQ H_2O 0.1% triflouroacetic acid (TFA) , 13 mL 82% MQ H_2O 0.1% triflouroacetic acid, 18% acetonitrile with 0.1% TFA, 14 mL 100% acetonitrile with 0.1% TFA) used to elute. Samples of 200 μL were prepared in anaerobic glovebox containing 3 mM dithiothreitol, 4 mM sodium dithionite, 36 μM SAM, 30 mM KCl and 10μg SP lyase in 25 mM Tris-acetate pH 7.0 buffer and incubated at 37°C for time periods between 1 min, 40 min, 90 min, 130 min and 24 hrs. Samples were divided in half, one part was used as above to test for repair activity, the other half was ultra-centrifuged through a YM-10 to remove protein and DNA and a 15μL aliquot was loaded onto the C-18 column and run with the above step gradient. Control samples were prepared without SP lyase to

determine SAM stability over time and without SAM to check for background signals.

VI.3   Results and discussion

SAM is not cleaved to 5'-deoxyadenosine during SP repair

In the generally accepted mechanism for the radical SAM enzymes, AdoMet is reductively cleaved to generate a 5'-deoxyadenosyl radical intermediate, which then abstracts a hydrogen atom from substrate. If AdoMet is being used as a substrate, then 5'deoxyadenosine should be present as a stoichimetric product of the reaction. In contrast, if SAM is being used as a catalytic cofactor, then the 5'-deoxyadenosine is an intermediate, not a product, of the reaction. It has previously been reported that 5'-deoxyadenosine is generated during repair of of SP by SPL[10, 11], however such an observation is not consistent with data from the Broderick lab supporting a catalytic role for SAM in SP repair.[9, 18]

We have therefore reinvestigated AdoMet cleavage by SP lyase. SP repair reactions containing a 1:1 mixture of AdoMet to SP lyase, in addition to SP and other reaction components were carried out and divided in half. One half of the reaction was quenched and checked for SP repair by the methods described in chapter 5. The other half of each sample was filtered through a YM-10 membrane to remove protein and DNA; the filtrate was then run of a C18 ODS2 column. The resulting chromatograms (Figure VI.1) show that essentially no
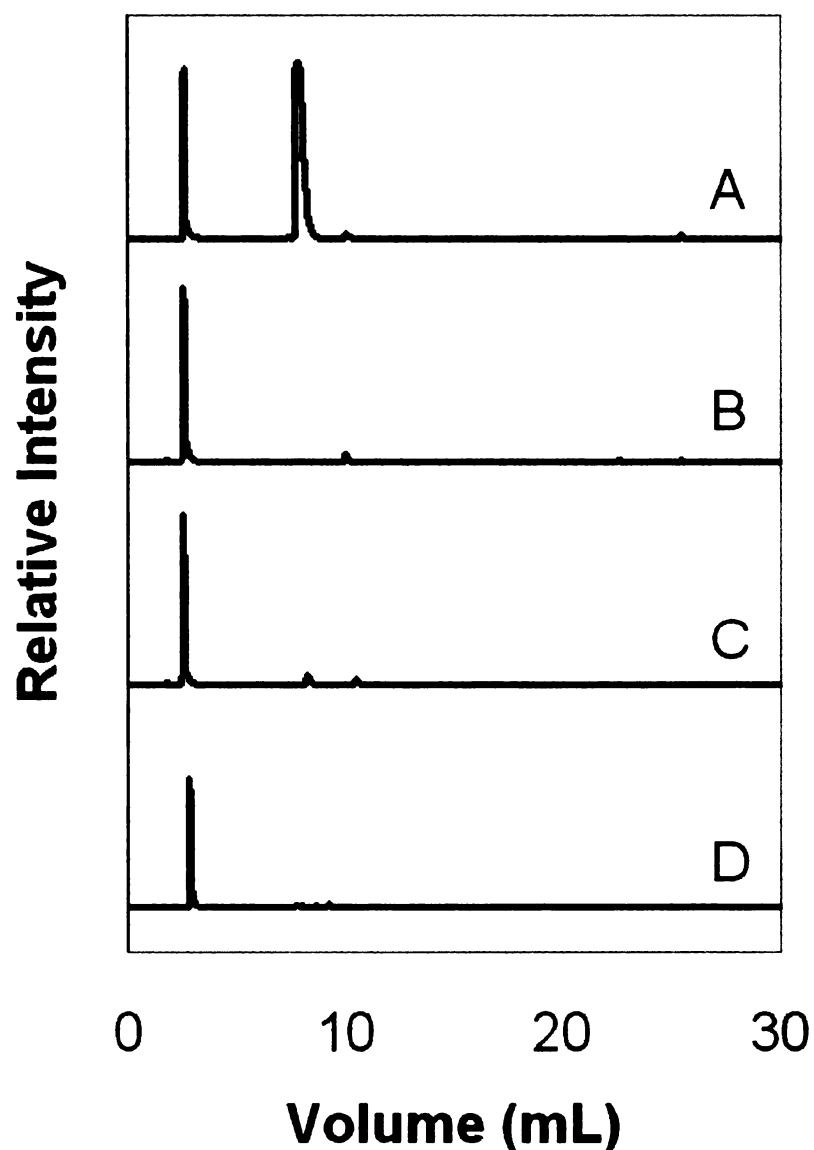
Figure VI.1 HPLC analysis of SAM cleavage to 5'-deoxyadenosine by SPL. HPLC chromatograms of (A) standard sample containing SAM (2.5 min) and 5'-deoxyadenosine (8 min); (B) control sample containing SAM under assay conditions with no SPL; and assay mixes containing SPL after 90 min (C) and overnight (D). Samples B-D contained 3 mM sodium dithionite, 4 mM DTT, 30 mM KCl and 25 mM Tris-acetate pH 7.0. Samples C and D also contained 200 µg SP containing pUC18 DNA, 36 µM SAM and 36 µM SPL.[18]

5'-deoxyadenosine is produced under the conditions employed. In the reaction

run for 90 minutes (Figure VI.1.C), our standard repair assay revealed that 146

nmol of SP had been repaired and yet the HPLC chromatogram shows that less

than 0.1nmol of 5'-deoxyadenosine is present; >95% of the 7 nmols of AdoMet

present in the reaction remains as AdoMet. Similar results are obtained after

overnight incubation (Figure VI.1D). The data obtained from these

chromatograms indicating the amount of 5'-dAdo produced and the amount of SP

repaired is summarized in Table VI.1. The results clearly indicate that AdoMet is

Sample	Time of incubation (Hours)	SP repaired (nmol)	5'-dAdo produced (nmol)	Specific Activity of SPL (μmol SP repaired/min/mg)
B	24	0	0	N/A
C	1.5	146	0.1	0.16
D	24	150	0.03	0.0104

Table VI.1 Summary of SAM cleavage during SP repair reaction.

not cleaved stoichiometrically to methionine and 5'-deoxyadenosine during SP

repair. The lack of AdoMet cleavage observed here differentiates our results from

two previously published reports, which show 5' deoxyadenosine production by

SPL;[10, 11] the reasons for these differences remains unclear although they could

be an artifact of cluster reconstitution in the other studies. The results above

have been published in the Journal of Biological Chemistry.[18]

113

Direct H atom transfer from [2, 5', 8 – ^{3}H]-SAM to repaired thymine

SAM, labeled with ^{3}H at the 5' position (Scheme VI.2) was successfully synthesized and purified via cation exchange chromatography to yield of 34%. We have previously shown that SP repair is initiated by direct H-atom abstraction from the C-6 position of SP by an AdoMet-derived 5'deoxyadenosyl radical intermediate.[9] These results support a mechanism (Scheme VI.1) in which the resulting substrate radical undergoes a radical mediated β-scission to generate the product thymine radical. The product thymine radical is then proposed to re-abstract a H atom from the 5'-deoxyadenosine formed in the first step, thereby re-generating the 5'-deoxyadenosyl radical intermediate. The 5'-deoxyadenosyl radical could then recombine with methionine to reform AdoMet as shown in Scheme VI.1.

In order to further investigate this mechanism, we have carried out repair assays in which the AdoMet is labeled at the 5'-position with tritium. The mechanism shown in Scheme VI.1 would predict a label transfer from this position into the repaired thymine. Repair assays were carried out using the labeled AdoMet and unlabeled irradiated DNA. Control experiments were conducted in the absence of SPL to check for erroneous label transfer or other experimental problems. In all cases, repaired DNA was isolated from the other reaction components, hydrolyzed and then subjected to chromatography on a Waters Spherisorb S5P column. Analysis of the fractions by scintillation counting reveals a peak at 3 minutes (Figure VI.2), the elution time of thymine under these

114

conditions. This peak is observed reproducibly in experimental samples

containing SPL and is absent in samples containing no SPL. Furthermore, the

amount of label appearing in the thymine peak is consistent with what we would

predict (115 CPM) based on the specific activity of the starting AdoMet and using

15.8 as an estimate of the tritium
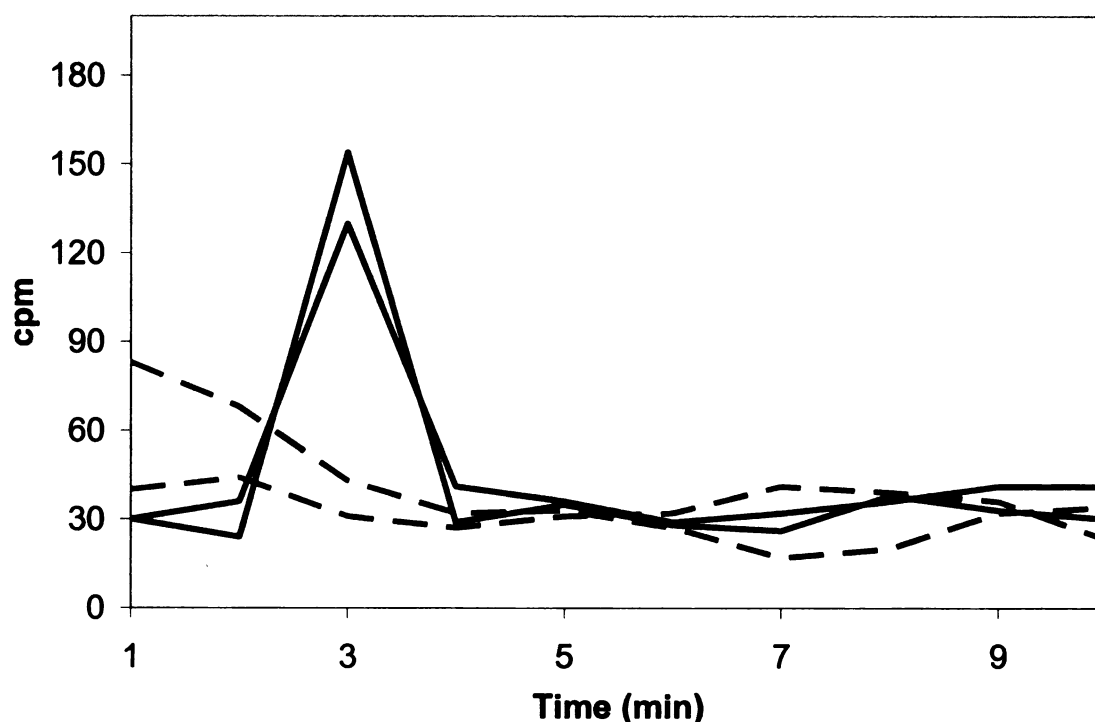
Figure VI.2 ^{3}H transfer from labeled [2, 5', 8 – ^{3}H]-SAM to repaired thymine. DNA repaired by SP lyase in the presence of [2, 5', 8 – ^{3}H]-SAM (solid lines are duplicate experiments) shows ^{3}H incorporation into thymine (elution time of 3 min.). Samples prepared in the absence of SPL shows no such incorporation (dashed lines).[18]

isotope effect.[14] This calculation was done as follows: theoretically, 7.3 nmol of

SP was repaired in this reaction, as SAM (70 nmol) was added in excess, we

thus assume that 7.3 nmol of SAM reacted during the course of SP repair. The

115

activity of the *[2, 5', 8 – ^{3}H]-SAM* used was 1,500,000 DPM/ μmol SAM or

750,000 CPM/μmol SAM, however only 1/3 of this activity is present at the 5'

position giving 250,000 CPM/μmol 5' ^{3}H. In our reaction if 7.3 nmol of SAM was

used, then the theoretical value for the CPM expected after label transfer would

be 1875 CPM. However, there should be an isotope effect as to which of the

three H atoms from the methyl group of 5'-dAdo will be abstracted. We have

used the estimate of 15.8 for the isotope effect, which gives us a theoretical

value of 115 CPM. After subtracting the background CPM from our results in

Figure VI.2, the CPM observed in the thymine peaks are 124 and 100. This is

close to our theoretical value and well within experimental error. The transfer of

the expected amount of tritium from AdoMet to thymine during repair by SPL

provides further support for a mechanism in which AdoMet is a catalytic cofactor,

and in which there is direct H atom transfer between AdoMet-derived

deoxyadenosyl radicals and substrate product. The results reported above have

been published in the Journal of Biological Chemistry.[18]

A potential isotope effect for H atom abstraction

As mentioned above, previous studies of SPL had shown evidence for

direct H atom abstraction from the C-6 position of SP by the putative 5'-

deoxyadenosyl radical.[9] In these studies, SP was produced in which the C-6

position of thymine was labeled with tritium and transfer to AdoMet was

observed, however this study did not attempt to quantify the tritium transfer or

examine its rate. By quantifying tritium transfer at various extents of reaction, we

can determine the tritium isotope effect on the overall reaction from the initial H atom abstraction. Further, by comparing the theoretical amount of tritium transferred after complete reaction to our experimental value, we can determine whether the initial H-atom abstraction is stereospecific. For example if SP is created non-stereospecifically and if SPL stereospecifically abstracts a H atom from C-6, then the CPM observed should be equal to 1/2 the theoretical amount of label transfer possible given the amount of SP used. On the other hand if SPL is non-stereospecific, then the amount of label transfer would be less because of the preference for abstracting an H atom over a tritium atom. Other possibilities include the case of SP production being stereospecific, if it is stereospecific and SP is stereospecific, then we would observe either no label transfer or 100% label transfer depending upon the stereospecificity involved.

In order to address these questions, we used a defined amount of SP (311 nmol) tritiated at C-6. The amount of time the assays were incubated was determined by use of the previously determined specific activity for SPL (0.33μmol/min/mg SPL). In order to repair 311 nmol of SP with ~0.1mg of SPL, 10 minutes is required to repair 100% of the SP lesions. The calculated activity of the SP is ~1,000 CPM/ 1 nmols SP, thus after 100% repair of ~311 nmol of SP, 7500 CPM should be transferred to SAM if the SPL repair reaction is stereospecific and creation of SP is non-stereospecific; for 50% SP repair, ~3770 CPM should be present in SAM and at 25% SP repair ~1880 CPM. However, if there is a tritium isotope effect of 15.8, the 50% and 25% SP repair samples should only have 238 and 119 CPM.

Our results closely match these values above as shown in Figure VI.3 and summarized in Table VI.2. At full reaction 5928 CPM is observed (78% of the theoretical value) and the DNA is fully repaired. Due to the complex experimental techniques involved, it is likely that certain % of the label is lost during the experiment. As such we have used the 100% SP repair reaction as our standard
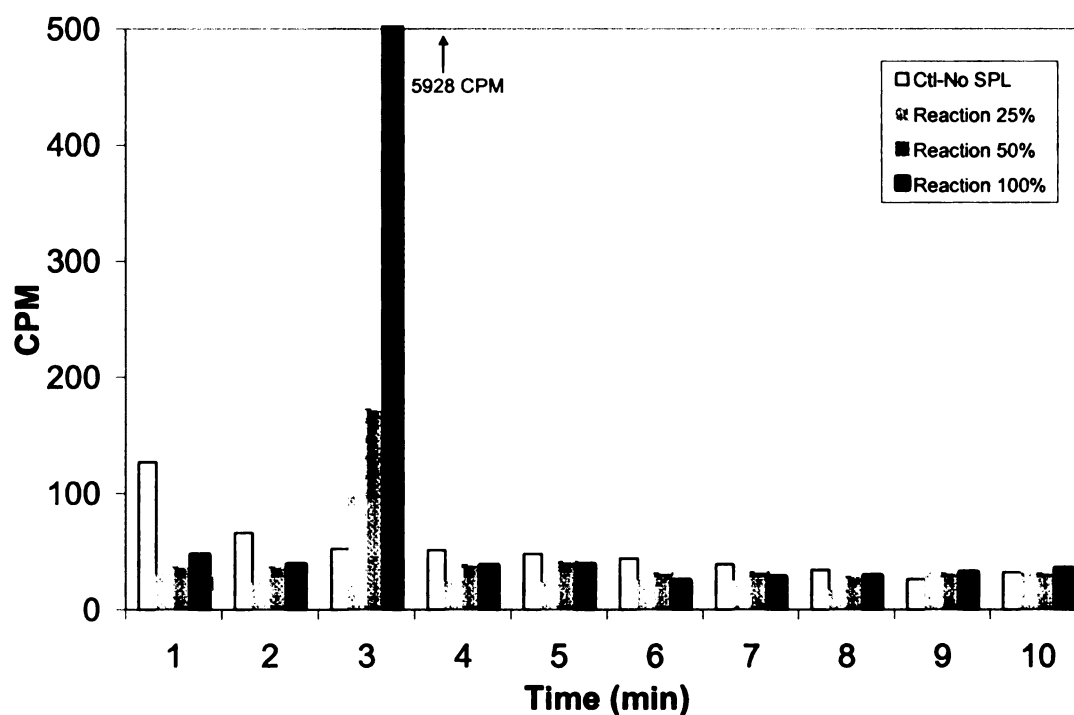
Figure VI.3 Tritium isotope effect for H atom abstraction. The bar graph above shows the number of counts present in purified SAM after use in a SP repair reaction with [C-6 - ^3H]-thymine SP. Reaction times shown are for 0, 2.5, 5 and 10 minutes. An isotope affect between 15.1 and 17.2 can be calculated for tritium during SP repair and H atom abstraction.

to determine what % of CPM (22%) is lost during the procedure. At 50% repair

we observe the CPM to be 172, by using the 100% reaction as a correction factor

we would obtain 172CPM/0.78 = 220 CPM. An isotope effect can then be

calculated by dividing the theoretical amount of CPM given no isotope effect by

the experimentally determined CPM (220CPM) to give a value of 17.2. The same

can be done at 25% reaction, giving a value of 15.1.

Sample	% of SP repaired	Theoretical Label transfer with no isotope effect (CPM)	Theoretical Label transfer with and isotope effect of 15.8 (CPM)	Experimental Label transfer (CPM)	Calculated isotope effect
1	0	0	0		N/A
2	25	1890	119	99	15.1
3	50	3770	238	172	17.2
4	100	7540	7535	5928	N/A

Table VI.2 Summary of label transfer from C-6 to SAM at increasing SPL repair reaction times and the corresponding isotope effect.

The results above give us insight into the reaction of SPL. First, these

results indicate that SP formation is non-stereospecific while, SP repair by SPL is

stereospecific, though the result in no way indicate which C-6 H atom is

abstracted, only that it is abstracted stereospecifically. Also these results

indicated the presence of a tritium isotope effect for initial H atom abstraction,

suggesting that H atom abstraction from the C-6 is rate determining.

119

VI.4   Conclusions

Our observation of ^{3}H Label transfer from SAM to repaired thymine is

supports Mehl and Begley's suggested mechanism for SP repair (Scheme VI.1).[8]

This mechanism involves initial SAM cleavage by electron donation from the iron

sulfur cluster to form the putative 5'-deoxyadenosyl radical. This radical species

has been shown abstract a hydrogen from the C-6 position of the thymine ring,

resulting in label transfer SAM. The mechanism proposes that the C-6 hydrogen

is abstracted leaving an organic radical at C-6. The SP then undergoes a radical-

mediated β-scission resulting in the separation of the adjacent thymine bases.

The resulting methyl radical abstracts hydrogen from 5'-deoxyadenosine to

reform the putative adenosyl radical, which can reform SAM by electron donation

to the iron sulfur cluster and go on to repair further spore photoproducts.

In the last step of the step of SP repair, a hydrogen from

5'deoxyadenosine is abstracted and transferred to repaired thymine. If this

mechanism is accurate, then labeling the 5'C of SAM with tritium should result in

label transfer to SAM. Our work confirms that indeed this 5' label is transferred

from SAM to repaired thymine. This evidence together with other evidence that

show that a single SAM can be used to repair over 400 SP lesions and that the

production of 5'-deoxyadenosine is not observed during repair provides strong

evidence for SAM's role as a cofactor in the repair of SP by SPL. It also strongly

supports the mechanism proposed in Scheme VI.1.

The observation of a tritium isotope effect of ~15-17 observed during initial H atom abstraction suggests that this step is energetically high and may be the rate limiting step of the reaction. This would be in conflict with DFT calculations that predict an energy barrier of 14.1 kcal/mol, far from the highest energy barrier calculated during the reaction.[13] Rather, DFT predicts that the production of the 5'-dAdo radical by the methyl radical is far more energetically unfavorable with a barrier of 23.1 kcal/mol as the 5'-dAdo radical is predicted to be less stable then the thymine radical.[13] These calculations, however, do not take into account the surrounding protein environment which can have a large effect on energy barriers.

VI.5 References

1.   Henshaw, T. F.; Cheek, J.; Broderick, J. B., The [4Fe-4S]1+ Cluster of
     Pyruvate Formate-Lyase Activating Enzyme Generates the Glycyl Radical
     on Pyruvate Formate-Lyase: EPR-Detected Single Turnover. *Journal of
     the American Chemical Society* **2000**, 122, (34), 8331-8332.

2.   Harder, J.; Eliasson, R.; Pontis, E.; Ballinger, M. D.; Reichard, P.,
     Activation of the anaerobic ribonucleotide reductase from Escherichia coli
     by S-adenosylmethionine. *Journal of Biological Chemistry* **1992**, 267, (35),
     25548-52.

3.   Moss, M.; Frey, P. A., The role of S-adenosylmethionine in the lysine 2,3-
     aminomutase reaction. *Journal of Biological Chemistry* **1987**, 262, (31),
     14859-62.

4.   Chen, D.; Walsby, C.; Hoffman, B. M.; Frey, P. A., Coordination and
     Mechanism of Reversible Cleavage of S-Adenosylmethionine by the [4Fe-
     4S] Center in Lysine 2,3-Aminomutase. *Journal of the American Chemical
     Society* **2003**, 125, (39), 11788-11789.

5.   Walsby, C. J.; Ortillo, D.; Broderick, W. E.; Broderick, J. B.; Hoffman, B.
     M., An Anchoring Role for FeS Clusters: Chelation of the Amino Acid
     Moiety of S-Adenosylmethionine to the Unique Iron Site of the [4Fe-4S]
     Cluster of Pyruvate Formate-Lyase Activating Enzyme. *Journal of the
     American Chemical Society* **2002**, 124, (38), 11270-11271.

6.   Walsby, C. J.; Hong, W.; Broderick, W. E.; Cheek, J.; Ortillo, D.; Broderick,
     J. B.; Hoffman, B. M., Electron-Nuclear Double Resonance Spectroscopic
     Evidence That S-Adenosylmethionine Binds in Contact with the
     Catalytically Active [4Fe-4S]$^+$ Cluster of Pyruvate Formate-Lyase
     Activating Enzyme. *Journal of the American Chemical Society* **2002**, 124,
     (12), 3143-3151.

7.   Walsby, C. J.; Ortillo, D.; Yang, J.; Nnyepi, M. R.; Broderick, W. E.;
     Hoffman, B. M.; Broderick, J. B., Spectroscopic Approaches to Elucidating
     Novel Iron-Sulfur Chemistry in the \"Radical-SAM\" Protein Superfamily.
     Inorganic Chemistry **2005**, 44, (4), 727-741.

8.   Mehl, R. A.; Begley, T. P., Mechanistic Studies on the Repair of a Novel
     DNA Photolesion: The Spore Photoproduct. *Organic Letters* **1999**, 1, (7),
     1065-1066.

9.   Cheek, J.; Broderick, J. B., Direct H Atom Abstraction from Spore
     Photoproduct C-6 Initiates DNA Repair in the Reaction Catalyzed by
     Spore Photoproduct Lyase: Evidence for a Reversibly Generated
     Adenosyl Radical Intermediate. *Journal of the American Chemical Society*
     2002, 124, (12), 2860-2861.

10.   Rebeil, R.; Nicholson, W. L., The subunit structure and catalytic mechanism of the Bacillus subtilis DNA repair enzyme spore photoproduct lyase. *Proceedings of the National Academy of Sciences of the United States of America* **2001,** 98, (16), 9038-43.

11.   Friedel, M. G.; Berteau, O.; Pieck, J. C.; Atta, M.; Ollagnier-de-Choudens, S.; Fontecave, M.; Carell, T., The spore photoproduct lyase repairs the 5S- and not the 5R-configured spore photoproduct DNA lesion. *Chemical Communications* **2006,** (4), 445-447.

12.   Chandor, A.; Berteau, O.; Douki, T.; Gasparutto, D.; Sanakis, Y.; Ollagnier-de-Choudens, S.; Atta, M.; Fontecave, M., Dinucleotide spore photoproduct: A minimal substrate of the DNA repair spore photoproduct lyase enzyme from bacillus subtilis. *J. Biol. Chem.* **2006,** In Press.

13.   Guo, J.-D.; Luo, Y.; Himo, F., DNA repair by spore photoproduct lyase: a density functional theory study. *Journal of Physical Chemistry B* **2003,** 107, (40), 11188-11192.

14.   O'Leary, M. H., Multiple isotope effects on enzyme-catalyzed reactions. *Annual Review of Biochemistry* **1989,** 58, 377-401.

15.   Chih, H. W.; Marsh, E. N. G., Tritium partioning and isotope effects in adenosylcobalamin-dependent glutamate mutase. *Biochemistry* **2001,** 40, (13060-13067).

16.   Sun, Y.; Palasingam, K.; Nicholson, W. L., High-pressure liquid chromatography assay for quantitatively monitoring spore photoproduct repair mediated by spore photoproduct lyase during germination of uv-irradiated Bacillus subtilis spores. *Analytical biochemistry* **1994,** 221, (1), 61-5.

17.   Rebeil, R.; Sun, Y.; Chooback, L.; Pedraza-Reyes, M.; Kinsland, C.; Begley, T. P.; Nicholson, W. L., Spore photoproduct lyase from Bacillus subtilis spores is a novel iron-sulfur DNA repair enzyme which shares features with proteins such as class III anaerobic ribonucleotide reductases and pyruvate-formate lyases. *Journal of bacteriology* **1998,** 180, (18), 4879-85.

18.   Buis, J. M.; Cheek, J.; Kalliri, E.; Broderick, J. B., Characterization fo an active spore photoproduct lyase, a DNA repair enzyme in the radical sam superfamily. *Journal of Biological Chemistry* **2006,** In Press.

CHAPTER VII

DNA BINDING PROPERTIES OF SPORE PHOTOPRODUCT LYASE

VII.1   Introduction

A variety of proteins have been shown to interact and bind to DNA. Some of the more well studied DNA binding proteins include DNA photolyase,[1] DNase I,[2] EcoR1 endonuclease[3] and topoisomerase I[4] among a variety of others. The various DNA binding proteins have different methods of binding to the DNA and can be categorized into several families including helix-turn-helix,[5] zinc binding, leucine zipper and beta hairpin/ribbon.[6]

As mentioned in the introduction, spore photoproduct lyase shares sequence homology with DNA photolyases towards its C-terminal end.[7] DNA photolyase is known to be a helix-turn-helix DNA binding protein and the region of sequence homology to SPL is in the vicinity of this binding motif.[8] It is therefore reasonable to hypothesize that SPL utilizes a helix-turn-helix binding motif similar to that of DNA photolyase.

There are many different ways to check for DNA-protein interactions, including DNA fingerprinting and gel-shift assays.[6] The studies described herein

utilized the latter, to examine some of the DNA binding properties of SPL. The gel shift assay utilizes (usually) a ^{32}P end-labeled DNA oligonucleotide, which can be electrophoresed in either the presence or absence of the target protein. If protein binds to the DNA, the oligonucleotide will be retarded on the gel and travel a shorter distance. By carrying out the experiment at a range of protein concentrations, a binding constant can be determined. We have used this technique to determine whether the presence or absence of an iron sulfur cluster or SAM affects the binding affinity of SPL to DNA.

Previous studies in the Nicholson lab had demonstrated that SPL bound specifically to SP and repaired the DNA but did not bind to cyclobutane dimers or 6'4'- photoproducts.[9] These studies, however, were not quantitative and thus did not provide dissociation constants. The previous studies also did not provide any insight as to what region of the protein bound to the DNA or if this binding was dependent upon the iron sulfur cluster of SPL or the co-factor SAM. For this reason we have used gel shift assays to look at the dissociation constant of SPL with DNA oligomers under varying conditions.

VII.2   Experimental Methods

^{32}P End labeling of 94mer oligonucleotide

Two complementary nucleotides were synthesized (Integrated DNA Technologies) based upon the B. subtilis sequence (322456-322550). These oligonucleotides are shown below:

5'-CGG GAT CAA CCA GAG CAT CAT GCT TGC GTT ATC AAT GGT TGT TAT

CGC CGC AAT GGT CGG TGC ACC GGG ACT TGG TTC TGA AGT ATA CAG

TGC C-3' (TK4-72a)

with the complementary strand being:

5'-GGC ACT GTA TAC TTC AGA ACC AAG TCC CGG TGC ACC GAC CAT

TGC GGC GAT AAC AAC CAT TGA TAA CGC AAG CAT GAT GCT CTG GTT

GAT CCC G – 3' (TK4-72b).

The TK4-72a oligonucleotide (1 µL, 5.8 pmoles) was added to a 5 X

Exchange reaction buffer (Invitrogen) with 5 µL [γ-^{32}P] ATP (10 µCi/µL, 3000

Ci/mmol), 0.05 µL T4 polynucleotide kinase (Invitrogen), and 13.5 µL autoclaved

MQ water to final volume of 25 µL. The reaction mixture was incubated at 37 °C

for 10 minutes, followed by heat inactivation at 65 °C for 10 minutes. The

oligonucleotide was purified by standard ethanol precipitation procedures in

which 250 µL of 4.67 M ammonium acetate and 100% ethanol (ice cold) were

added. The oligomers were kept on ice for 30 minutes and centrifuged at 12,000

RPM for 20 minutes. The supernatant was removed and 500 µL of 80% ethanol

was added followed by centrifugation at 12,000 RPM for 20 minutes. The

supernatant was again removed and the oligomer was dried under nitrogen and

resuspended in 50 µL TAE buffer. The labeled strand was annealed to the

unlabeled complementary strand by adding 5.8 pmoles of the complementary

strand and heating at 90 °C for 3 minutes then slowly cooling to room

temperature over the course of 1 hour. The double stranded DNA oligo was

further purified using a Mini Spin Quick Oligo column (Roche Applied Science) and stored at -80 °C.

Gel-shift DNA binding assay

An 8% polyacrylamide gel was prepared using 10mL 40% acrylamide stock solution, 1 mL of 50 X TAE buffer (1L contains 242 g Tris base, 57.1 mL glacial acetic acid, and 100 mL of 0.5 M EDTA pH 8.0), 0.35mL ammonium persulfate (0.1 g/mL) and 17.5 μL TEMED. The mixture was prepared and poured between glass plates to a final size of 20 cm x 20 cm x 1 mm. The gel was pre-electrophoresed at 100 V for 30 minutes before loading sample.

Lane	1	2	3	4	5	6	7	8	9	10	11
Binding Buffer (μL)	2	2	2	2	2	2	2	2	2	2	2
50% Glycerol (μL)	4	4	4	4	4	4	4	4	4	4	4
94mer oligo (pmol)	0.46	0.46	0.46	0.46	0.46	0.46	0.46	0.46	0.46	0.46	0.46
NP-40 (μL)	1	1	1	1	1	1	1	1	1	1	1
MQ H$_2$O (μL)	11	10	9	8	7	6	5	4	3	2	1
SPL (pmol)	0	2.3	4.6	6.9	9.2	11.5	13.8	16.1	18.4	23	46
SPL (nM)	0	115	230	345	460	575	690	805	920	1150	2300
Protein to DNA Ratio	0	5	10	15	20	25	30	35	40	50	100

Table VII.1   Reaction conditions for the gel shift assay of SPL and DNA under anaerobic conditions

127

Lane	1	2	3	4	5	6	7	8	9	10	11
Binding Buffer (μL)	2	2	2	2	2	2	2	2	2	2	2
50% Gyl (μL)	4	4	4	4	4	4	4	4	4	4	4
94mer oligo (pmol)	0.46	0.46	0.46	0.46	0.46	0.46	0.46	0.46	0.46	0.46	0.46
NP-40 (μL)	1	1	1	1	1	1	1	1	1	1	1
MQ H_2O (μL)	11	10	9	8	7	6	5	4	3	2	1
SPL (pmol)	0	4.6	9.2	13.8	18.4	23	27.6	32.2	36.8	46	92
SPL (nM)	0	115	230	345	460	575	805	1035	920	1380	2300
Protein to DNA Ratio	0	5	10	15	20	25	35	45	60	100	200

Table VII.2   Reaction conditions for the gel shift assay of SPL and DNA under aerobic conditions.

Lane	1	2	3	4	5	6	7	8	9	10	11
Binding Buffer (μL)	2	2	2	2	2	2	2	2	2	2	2
50% Gly (μL)	4	4	4	4	4	4	4	4	4	4	4
94mer oligo (pmol)	0.11	0.11	0.11	0.11	0.11	0.1	0.11	0.11	0.11	0.11	0.11
NP-40 (μL)	1	1	1	1	1	1	1	1	1	1	1
MQ H_2O (μL)	11	10	9	8	7	6	5	4	3	2	1
SPL (pmol)	0	22	44	66	88	110	220	550	1100	1375	1650
SPL (μM)	0	1.1	2.2	3.3	4.4	5.5	11	27	54	67.5	81
Protein to DNA Ratio	0	20	40	60	80	100	200	400	2000	2500	3000

Table VII.3 Reaction conditions for the gel shift assay of SPL and DNA under anaerobic conditions with Apo-SPL.

Lane	1	2	3	4	5	6	7	8	9	10	11
Binding Buffer (μL)	2	2	2	2	2	2	2	2	2	2	2
50% Gylcerol (μL)	4	4	4	4	4	4	4	4	4	4	4
94mer oligo (pmol)	0.46	0.46	0.46	0.46	0.46	0.46	0.46	0.46	0.46	0.46	0.46
NP-40 (μL)	1	1	1	1	1	1	1	1	1	1	1
MQ H_2O (μL)	11	10	9	8	7	6	5	4	3	2	1
SPL (pmol)	0	2.3	4.6	7.9	9.2	11.5	13.8	16.1	18.4	23	27.6
SPL (nM)	0	115	230	345	460	575	690	805	920	1150	1380
Protein to DNA Ratio	0	5	10	15	20	25	30	35	40	50	60
AdoMet (nmol)	1	1	1	1	1	1	1	1	1	1	1

Table VII.4   Reaction conditions for the gel shift assay of SPL and DNA under anaerobic conditions with AdoMet.

Samples (Table VII.1 – 4) were prepared in an anaerobic Coy chamber at 4°C except were otherwise noted. Samples were incubated for 2 hours followed by the addition of 2 µL of loading dye. The entire sample was loaded and the gel was run at 200 V for 3 hours. The gel was fixed in 7% acetic acid and then dried between two sheets of cellophane in a drying rack overnight. The gel was cut from the drying racks and visualized by audioradiography (X-OMAT AR-5 film from Kodak).

Preparation of Apo-SPL

Purified SPL (1 mL, 100 µM) was dialyzed against 2 X 500 mL Buffer A (20 mM sodium phosphate, 500 mM NaCl, 10 mM imidazole, 5% glycerol, pH 8.0) containing 10 mM EDTA for 2 hours at 4 °C followed by dialysis in 2 X 500 mL Buffer A at 4 °C for an additional 1 hour. The protein was removed from the dialysis tubing and concentrated with a Amicon Ultra concentrator with a YM - 10 membrane

VII.3 Results and Discussion

DNA binding of as isolated protein

A 94mer DNA oligomer was prepared based on a sequence from the *B. subtilis* chromosomal DNA in hopes of simulating the type of DNA sequences located in endospores. The 94 DNA base sequence was chosen because it is short enough to be easily observed on the polyacrylamide gel after protein binding but long enough to allow multiple proteins to bind one oligo. The protein

used in these experiments was isolated as normal and contained ~ 1.9 Fe/SPL; no chemical reductant was added to the protein.

The addition of increasing amounts of SPL to the synthesized 94 base pair oligonucleotide shows increasing amounts of the ^{32}P end labeled DNA being retarded in the gel (Figure VII.1). The dissociation constant was measured by scanning the gel with a GS-900 gel scanner from BioRad and calculating the band density (Table VII.5) of the retarded gel and plotting a linear graph of the [SPL-total] versus v ([SPL-DNA]/[DNA])(Figure VII.2). One can then calculate the K_d from the point at which v = 0.5 (50% of DNA is bound to protein). The resulting dissociation constant is K_d = 450±100 nM.

| Lane | 1 | 2 | 3 | 4 | 5 | 6 | 7 | 8 | 9 | 10 | 11 |

Figure VII.1 Anaerobically isolated SPL binding to a 94 base pair DNA oligomer. An increasing amount of SPL was added ranging from 0 pmol (lane 1) to 46 pmol (lane 11), as detailed in Table VII.1. As more SPL is added to the DNA oligomer, the DNA band is retarded an increasing amount. A dissociation constant of 450 ± 100 nM can be calculated by measuring the band densities.

The binding constant calculated for SPL falls within a typical range for DNA

binding proteins binding non-specifically to DNA.[10] For example, DNA photolyase

has a K_D = 1 μM for non specific DNA binding.[1]
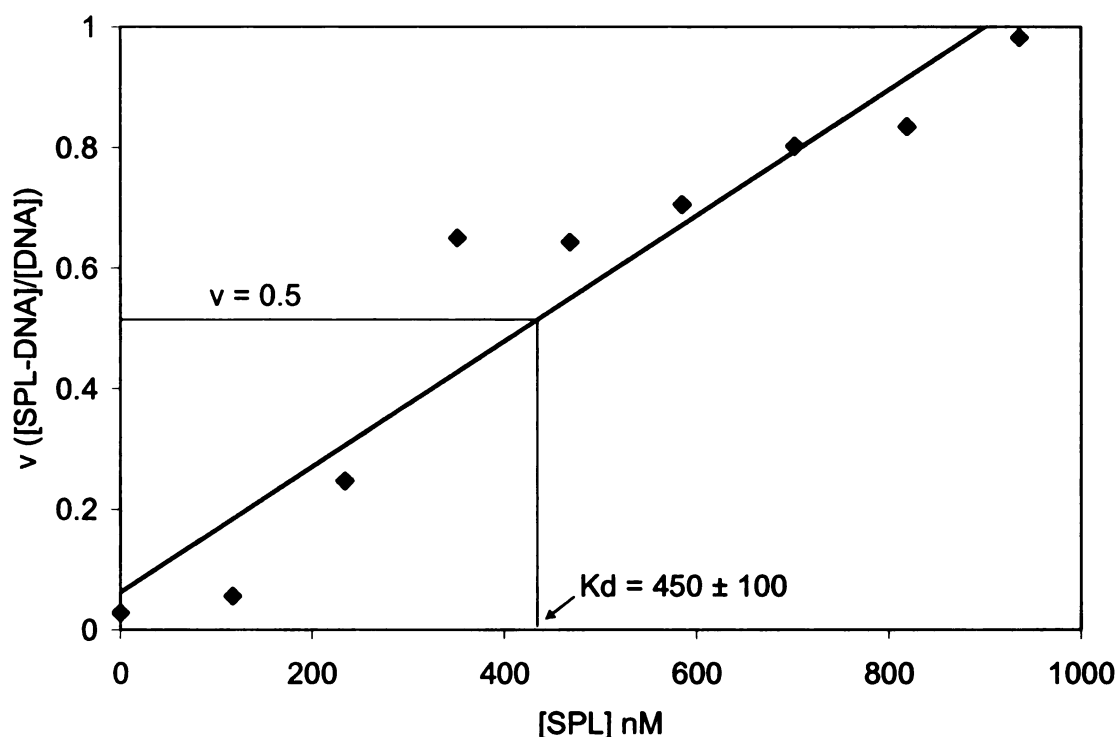
Figure VII.2 Plot of [SPL-total] versus v ([SPL-DNA]/[DNA]) for the anaerobically as isolated SPL binding to a 94 base pair DNA oligomer.

DNA binding of SPL under aerobic conditions

The binding of SPL to our synthesized oligo was measured under aerobic

conditions in an attempt to see if the oxidation state or amount of iron affected

the DNA binding properties of SPL. It has been noted in SPL that exposure to

oxygen results in a loss of protein color and reduced UV spectrum, most likely

the result of cluster oxidation and loss of iron from the cluster.

The addition of increasing amounts of SPL to the synthesized 94 base pair

oligonucleotide shows increasing amounts of the ^{32}P end labeled DNA being

retarded (Figure VII.3). The dissociation constant was measured by scanning the

gel with a GS-900 gel scanner from BioRad and calculating the band density

(Table VII.5) of the retarded gel and plotting a linear graph of the [SPL-total]

versus v ([SPL-DNA]/[DNA])(Figure VII.4). One can then calculate the K_d from

the point at which v = 0.5 (50% of DNA is bound to protein). The resulting

dissocitation constant is K_d= 700 ± 100 nM.

| Lane | 1 | 2 | 3 | 4 | 5 | 6 | 7 | 8 | 9 | 10 | 11 |

Figure VII.3 Anaerobically isolated SPL exposed to oxygen binding to a 94 base pair DNA oligomer. An increasing amount of SPL was added ranging from 0 pmol (lane 1) to 92 pmol (lane 11), as detailed in Table VII.2. As more SPL is added to the DNA oligomer, the DNA band is retarded an increasing amount. A dissociation constant of 700 ± 100 nM can be calculated by measuring the band densities.

It is therefore observed that the affect of cluster oxidation on the non-specific DNA binding properties of SPL is minimal at best as the increase in K_d is almost within experimental error. This gives an early indication that the iron sulfur cluster of SPL has little effect on the DNA binding properties.
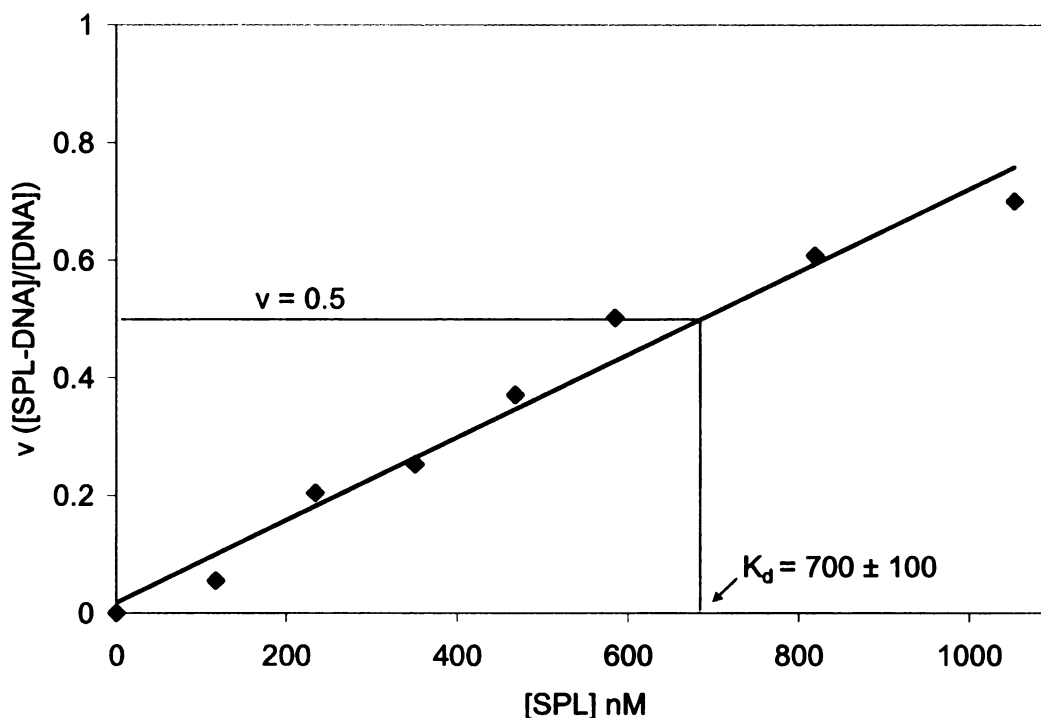
Figure VII.4 Plot of [SPL-total] versus v ([SPL-DNA]/[DNA]) for the apo-SPL binding to a 94 base pair DNA oligomer.

DNA binding of apo-SPL

The iron sulfur cluster of SPL was successfully removed by EDTA dialysis and only 0.1 Fe per SPL was found after dialysis. Similar to the above experiment carried out in aerobic conditions, this experiment was designed to determine whether the DNA binding of SPL is affected by the iron sulfur cluster. If

the cluster is aiding DNA binding, then we should see a significant affect on the gel by removal of the cluster.

Similar to the as-isolated protein, non-specific DNA binding was seen on the gel-shift assay with an increase in oligo retardation with increasing amounts of SPL (Figure VII.5); the dissociation constant was measured to be 550±100 nM

Lane   1   2   3   4   5   6   7   8   9   10   11
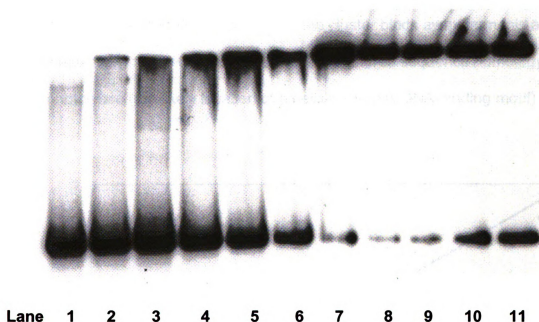
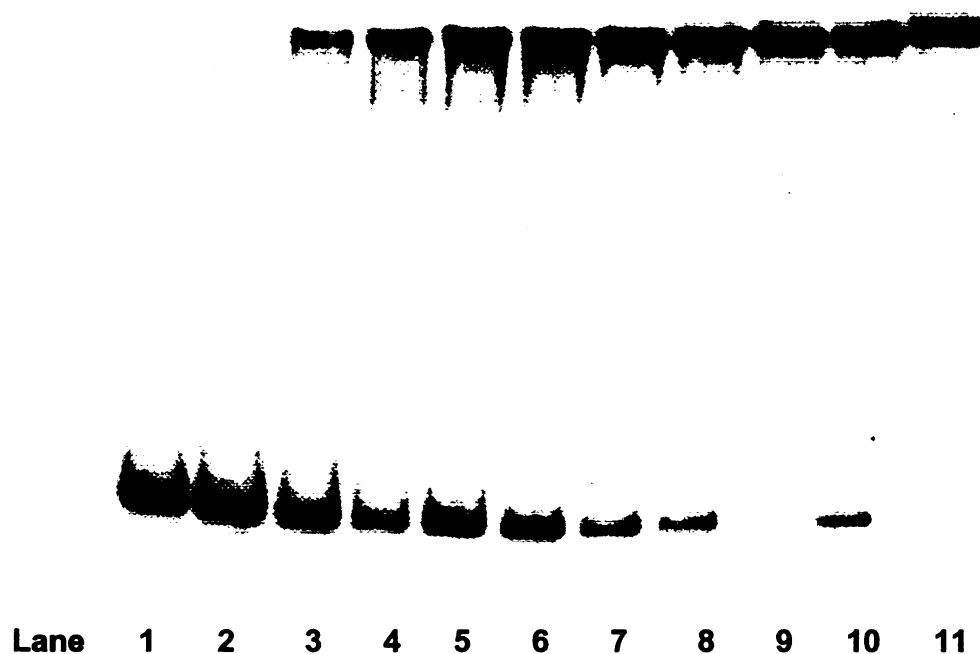**Figure VII.5** Apo-SPL binding to a 94 base pair DNA oligomer. An increasing amount of SPL was added ranging from 0 nmol (lane 1) to 1.65 nmol (lane 11), as detailed in Table VII.3. As more SPL is added to the DNA oligomer, the DNA band is retarded an increasing amount. A dissociation constant of 550 ± 100 nM can be calculated by measuring the band densities.

The dissociation constant was measured by scanning the gel with a GS-900 gel scanner from Bio-Rad and calculating the band density (Table VII.5) of the retarded gel and plotting a linear graph of the [SPL-total] versus v ([SPL-

136

DNA]/[DNA])(Figure VII.6). One can then calculate the K_d from the point at which

v = 0.5 (50% of DNA is bound to protein).

As in the experiment carried out under aerobic conditions, there is very little affect on the dissociation constant of SPL and DNA. Removal of the iron sulfur cluster increases the dissociation constant but not by a large amount and is within experimental error. It is, therefore, likely that the iron sulfur cluster is not significantly involved in DNA binding and the cluster binds away from this area of the protein, likely at the C – terminus were SPL shares sequence homology with DNA photolyase (the likely location of a helix-turn-helix DNA binding motif).
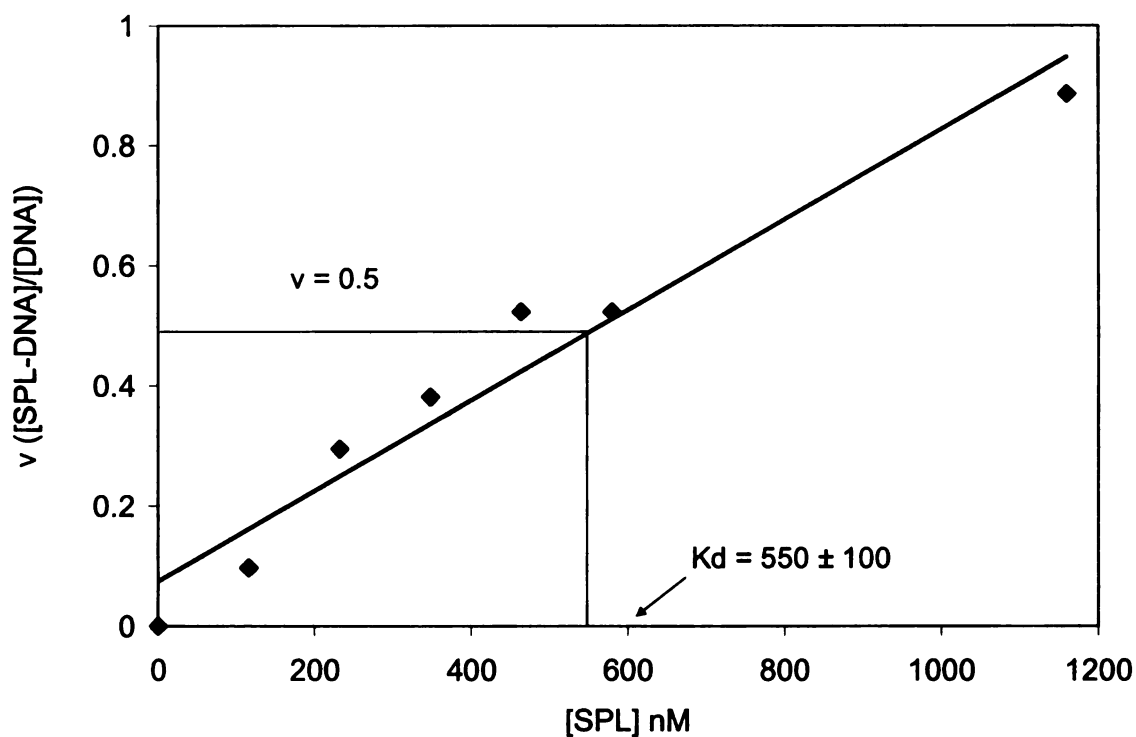
Figure VII.6 Plot of [SPL-total] versus v ([SPL-DNA]/[DNA]) for the apo-SPL binding to a 94 base pair DNA oligomer.

Based on crystal structures of the other radical SAM superfamily members,[11-15] the iron sulfur cluster is likely located at the C terminus of an TIM barrel nearer to the N-terminus of the protein.

DNA binding of as isolated protein with SAM

The addition of the co-factor AdoMet to SPL has been shown to increase the proteins stability. Since AdoMet is used in the reaction catalyzed by SPL, it is possible that it affects the binding affinity of SPL for DNA. However, since DNA binding likely occurs away from the site of SAM binding at the cluster, it is also possible that non-specific DNA binding may not be affected.

SAM was added to the as-isolated SPL to see if this affects its DNA binding properties. (Figure VII.7) As with the samples without SAM, the more SPL that was added, the more the DNA was retarded on the gel. Calculating the dissociation constant for SPL/SAM binding to DNA gives $K_d = 550 \pm 100$ nM (Figure VII.8). The dissociation constant was measured by scanning the gel with a GS-900 gel scanner from BioRad and calculating the band density (Table VII.5) of the retarded gel and plotting a linear graph of the [SPL-total] versus v ([SPL-DNA]/[DNA])(Figure VII.8). One can then calculate the K_d from the point at which v = 0.5 (50% of DNA is bound to protein).

The addition of SAM therefore does not have an effect on the non-specific binding between SPL and DNA, as the dissociation constants are almost identical in the presence and absence of SAM.

Lane   1   2   3   4   5   6   7   8   9   10   11

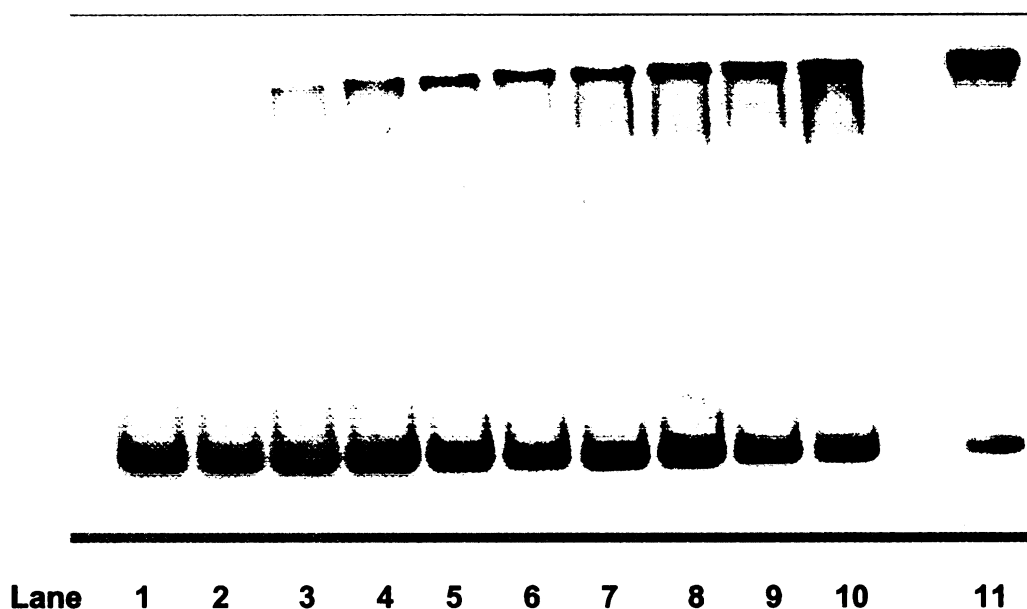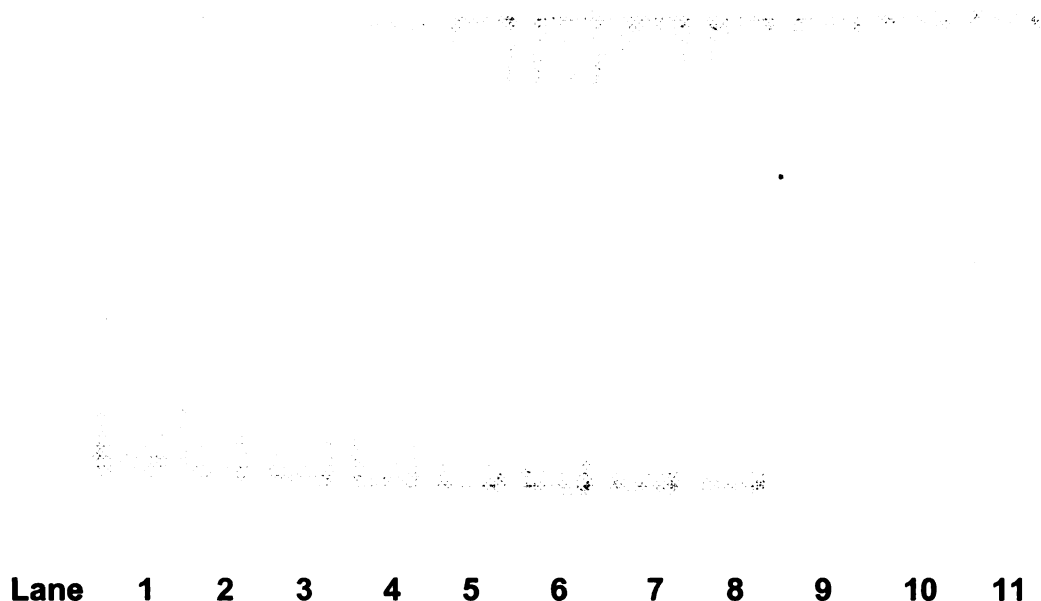**Figure VII.7** Anaerobically isolated SPL with SAM binding to a 94 base pair DNA oligomer. An increasing amount of SPL was added ranging from 0 pmol (lane 1) to 27.6 pmol (lane 11), as detailed in Table VII.4. As more SPL is added to the DNA oligomer, the DNA band is retarded an increasing amount. A dissociation constant of 550 ± 100 nM can be calculated by measuring the band densities.

VII.4 Conclusions

Based on the gel-shift assays carried out throughout this work, SPL can bind non-specifically to DNA oligomers in the absence of the SP photolesion. It appears that SPL can bind to the DNA in both the presence and absence of the iron sulfur cluster and that the presence of oxygen or SAM makes little difference in the binding capability. This leads one to draw the conclusion that the SPL binds to DNA away from the iron sulfur cluster site.

Chart axis labels: y-axis: v ([SPL-DNA]/[DNA]); x-axis: [SPL] nM

v = 0.5

$K_d = 550 \pm 100$
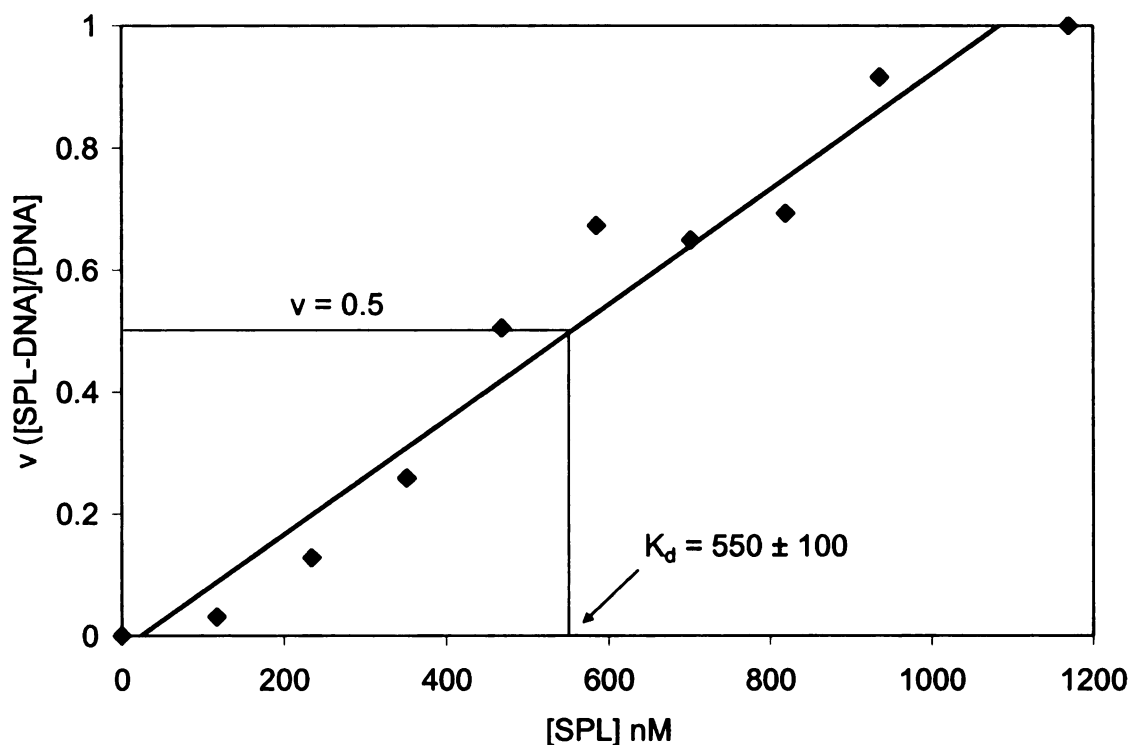
VII.8 Plot of [SPL-total] versus v ([SPL-DNA]/[DNA]) for the anaerobically as isolated SPL with SAM binding to 94 base pair DNA oligomer.

Lanes	1	2	3	4	5	6	7	8	9	10	11
Anaerobic Figure VII.1	2.8	5.6	24.7	65	64.3	70.5	80.2	83.4	98.2	83	98
Aerobic Figure VII.2	0	5.5	20.4	25.3	37.1	50.2	60.8	70	74.2	80.2	90.4
Apo-SPL Figure VII.3	0	9.7	29.5	38.1	52.3	52.3	88.6	96.9	92.6	73.4	66.1
SPL w/SAM Figure VII.4	0	3.1	12.8	25.9	50.5	67.3	64.9	69.3	91.6	100	100

Table VII.5 Percentage of bound protein as calculated from the band density of the gel shift assay.

Non-specific DNA binding has been implicated recently as the reason for quick recognition of specific sequences and specific damaged bases by enzymes that interact with DNA.[10] The proposed mechanism for an increase in enzymatic activity involves enzyme binding DNA and then sliding along the DNA helix until it recognizes the specific damage or sequence upon which the enzyme will act.[3, 10] This binding enhances an enzyme's activity by allowing it to more rapidly recognize substrates along the DNA helix.

In recent crystal structures of DNA photolyase, a DNA oligo with a cyclobutane dimer incorporated in the middle was bound to the protein. In this structure, the dimer was observed to flip out of the DNA double helix and into the active site of DNA photolyase.[8] This is likely the same method that SPL uses to recognize photoproducts. After the onset of germination, the pH of the cell changes and allows SASP to dissociate from the DNA and get destroyed.[16] SPL may then bind loosely to the DNA via a C – terminal helix-turn-helix motif and move up and down the double helix searching for photoproducts that have flipped out of the double helix. Upon recognition of SP, the flipped out bases pair would be centered in the middle of the beta barrel, that is likely the N – terminal structure of SPL similar to other radical SAM superfamily proteins.[12-14] The cluster would than transfer the electron to SAM and cleave the C-S bound to create the 5'-deoxyadenosyl radical that would abstract a hydrogen from the C-6 thymine ring and begin repair. Upon repair, the base pairs would return to their normal configuration in the double helix and SPL would search for other photoproducts to repair.

VII.5 References

1. Sancar, A., Structure and Function of DNA Photolyase and Cryptochrome Blue-Light Photoreceptors. *Chemical Reviews* **2003**, 103, (6), 2203-2237.

2. Suck, D., DNA recognition by DNase I. *Journal of Molecular Recognition* **1994**, 7, (2), 65-70.

3. Woodhead, J. L.; Malcolm, A. D. B., Non-specific binding of restriction endonudease EcoR1 to DNA. *Nucleic Acids Research* **1980**, 8, (2), 389-402.

4. Lanza, A.; Tornaletti, S.; Rodolfo, C.; Scanavini, M. C.; M., P. A., Human DNA Topoisomerase I-mediated Cleavages Stimulated by Ultraviolet Light-induced DNA Damage. *Journal of Biological Chemistry* **1996**, 271, (12), 6978-6986.

5. Aravind, L.; Anantharaman, V.; Balaji, S.; Babu, M. M.; Iyer, L. M., The many faces of the helix-turn-helix domain: transcription regulation and beyond. *FEMS Microbiology Reviews* **2005**, 29, (2), 231-262.

6. Voet, D.; Voet, J. G., *Biochemistry*. 2nd ed.; John Wiley & Sons: New York, 1995.

7. Fajardo-Cavazos, P.; Salazar, C.; Nicholson, W. L., Molecular cloning and characterization of the Bacillus subtilis spore photoproduct lyase (spl) gene, which is involved in repair of UV radiation-induced DNA damage during spore germination. *Journal of bacteriology* **1993**, 175, (6), 1735-44.

8. Mees, A.; Klar, T.; Gnau, P.; Hennecke, U.; Eker, A. P. M.; Carell, T.; Essen, L.-O., Crystal structure of a photolyase bound to a CPD-like DNA lesion after in situ repair. *Science* **2004**, 306, (5702), 1789-1793.

9. Slieman, T. A.; Rebeil, R.; Nicholson, W. L., Spore photoproduct (SP) lyase from Bacillus subtilis specifically binds to and cleaves SP (5-thyminyl-5,6-dihydrothymine) but not cyclobutane pyrimidine dimers in UV-irradiated DNA. *Journal of Bacteriology* **2000**, 182, (22), 6412-7.

10. Halford, S. E.; Marko, J. F., How do site-specific DNA-binding proteins find their targets? *Nucleic Acids Research* **2004**, 32, (10), 3040-3052.

11. Lepore, B. W.; Ruzicka, F. J.; Frey, P. A.; Ringe, D., The x-ray crystal structure of lysine-2,3-aminomutase from Clostridium subterminale. *Proceedings of the National Academy of Sciences of the United States of America* **2005**, 102, (39), 13819-13824.

142

12. Berkovitch, F.; Nicolet, Y.; Wan, J. T.; Jarrett, J. T.; Drennan, C. L., Crystal structure of biotin synthase, an S-adenosylmethionine-dependent radical enzyme. *Science* **2004**, 303, (5654), 76-80.

13. Layer, G.; Kervio, E.; Morlock, G.; Heinz, D. W.; Jahn, D.; Retey, J.; Schubert, W.-D., Structural and functional comparison of HemN to other radical SAM enzymes. *Biological Chemistry* **2005**, 386, (10), 971-980.

14. Layer, G.; Moser, J.; Heinz, D. W.; Jahn, D.; Schubert, W.-D., Crystal structure of coproporphyrinogen III oxidase reveals cofactor geometry of Radical SAM enzymes. *EMBO Journal* **2003**, 22, (23), 6214-6224.

15. Haenzelmann, P.; Schindelin, H., Crystal structure of the S-adenosylmethionine-dependent enzyme MoaA and its implications for molybdenum cofactor deficiency in humans. *Proceedings of the National Academy of Sciences of the United States of America* **2004**, 101, (35), 12870-12875.

16. Kosman, J.; Setlow, P., Effects of carboxy-terminal modifications and pH on binding of a Bacillus subtilis small, acid-soluble spore protein to DNA. *Journal of Bacteriology* **2003**, 185, (20), 6095-6103.

CHAPTER VIII

INTERACTION OF S-ADENOSYLMETHIONINE WITH THE IRON SULFUR CLUSTER OF SPORE PHOTOPRODUCT LYASE

VIII.1 Introduction

A characteristic feature of the radical SAM superfamily is the use of an iron sulfur cluster and AdoMet in activity.[1] It has been of significant interest over the years to characterize the interaction between AdoMet and the cluster, with work on PFL-AE, LAM, and BioB giving some of the most detailed results for this interaction and the corresponding adenosyl radical that results.

Work on PFL-AE has provided great detail for the interaction between SAM and the iron sulfur cluster. ENDOR and Mössbauer studies have been able to model this interaction and provide detailed models for SAM binding the iron sulfur cluster via the carboxyl oxygen and amine of SAM with a sulfide-sulfonium interaction possibly providing a pathway for electron transfer.[2-5] EXAFS studies on LAM showed binding of SAM to the cluster and an interaction between the sulfonium of SAM and an iron of the cluster.[6] This work was followed by ENDOR studies to further characterize this interaction, which provided more evidence for interaction between SAM and the cluster.[7]

To date, there has been little work characterizing the interaction between SPL and AdoMet. In order to probe this interaction, a combination of equilibrium dialysis, ENDOR and Q-band EPR experiments are employed to resolve binding constants, bond coordinations and bond interactions.

Equilibrium dialysis has been widely used to obtain dissociation constants for small molecule binding to proteins. This method involves placing a thin membrane with a molecular weight cutoff in between two containers and placing the protein on one side of the membrane and the small molecule on the other side. The small molecule is able diffuse through the membrane and the protein is not; as such, if the small molecule binds to the protein one can measure the difference between the amount of protein on one side of the membrane versus the other side and calculate how much of the small molecule is bound to the protein. A variety of methods are available to measure the amount of small molecule including UV/Vis or radiolabeling.[8] Our experiment will use radiolabeled SAM to allow for easy quantification of SAM.

ENDOR spectroscopy has been applied to a variety of other iron sulfur cluster containing enzymes including aconitase[9-11] and nitrogenase[12] to probe the interaction with substrates. ENDOR spectroscopy examines the electron – nuclear hyperfine interactions which are generally too small to be observed by CW EPR. This can be employed in metalloproteins in which an electron spin (i.e. $S = \frac{1}{2}$) such as that of an iron sulfur cluster is in the vicinity of a magnetic nucleus such as ^1H, ^2H, ^{13}C, ^{14}N, ^{15}N, ^{17}O, ^{31}P or ^{33}S with $I > 0$. Hence, interactions that are too small to be observed with CW EPR can be detected by

ENDOR.[13] As seen with the PFL-AE and LAM, this technique will allow one

observe and model the interaction of SPL's iron sulfur cluster and isotopically

labeled SAM.

VIII.2 Experimental Methods

Materials

All chemicals used in this work were purchased commercially and were of

the highest purity. [2, 8, - ^3H] –ATP was purchased from GE Healthcare.

Individual Equilibrium Dispo-Dialyzer® 75 μL disposable kits were purchased

from the Nest Group Inc. for equilibrium dialysis. Isotopically labeled SAM

including ^2H, ^{13}C, ^{15}N and ^{17}O SAM had been previously synthesized in our lab.[3,4]

Synthesis of [2, 8,-^3H] SAM

SAM labeled with ^3H was synthesized by using the following reaction. A 5

mL reaction of 100 mM Tris HCl (pH 8.0), 50 mM KCl, 26 mM $MgCl_2$, 5.2 mM

adenosine triphosphate (ATP), 8% β-mercaptoethanol, 1 mM EDTA, 6.8 mM

methionine, 2.5 μL Inorganic pyrophosphatase and 500 μL SAM synthetase

crude lysate and 1 mCi [2, 8 - ^3H] – ATP stirred at room temperature for 16 hrs

and quenched with 500 μL 1 M HCl. The reaction was monitored by TLC to

completion and purified by loading onto a source 15s.6 cationic exchange

column. A linear gradient of MQ H_2O to 1 M HCl was used to elute the [2, 8 - ^3H]

SAM. The fractions containing SAM were lyophilized and redissolved in 50 mM

HEPES, 200 mM NaCl (pH 7.5).

Equilibrium dialysis of spore photoproduct lyase

Individual Equilibrium Dispo-Dialyzer® 75 µL disposable kits with a

molecular weight cutoff of 10,000 Da were used in this experiment. SPL at

varying concentrations (75 µM, 125 µM, 175 µM, 250 µM) were place on Side A

of the Dispo-Dialyzer® in a buffer containing 20 mM sodium phosphate, 500 mM

NaCl, 5% glycerol pH 8.0. Side B of the Dispo-Dialyzer® contained the same

buffer and 250 µM [*2, 8,-^{3}H*] SAM. All work was carried out in an anaerobic

mBraun box. These sample were made in triplicate with an additional three

samples prepared without protein as a control for SAM diffusion. All samples

were placed in a New Brunswick incubator/shaker and left for 2 hours at 100

RPM at 37 °C. Samples were removed from the shaker and the contents of each

side of the Dispo-Dialyzer® were pipetted into scintillation vials with 15 mL of

liquid scintillation fluid and run on a Beckman LS 6500 liquid scintillation counter.

Electron nuclear double resonance spectroscopy and Q-band EPR sample
preparation

SPL was purified as described in chapter 2 and concentrated to 550 µM.

All samples for ENDOR were prepared anaerobically in a mBraun box. 100 µL of

purified SPL was reduced with a final concentration 10 mM sodium dithionite and

10 mM DTT on ice for 10 minutes. After reduction, the SAM (either methyl ^{2}H,

methyl ^{13}C, amino ^{15}N, carboxyl ^{17}O or non-labeled SAM) was added to the SPL

sample and mixed. The sample was then transferred to custom made quartz tube

for 35 GHz EPR and immediately frozen with liquid nitrogen.

Q-band electron paramagnetic resonance

Q-band continuous wave electron paramagnetic resonance was carried

out at 35GHz, 2K, 20 dB, and 2.0 G modulation on a modified Varian E-110

spectrometer with a liquid helium immersion dewar.

Electron nuclear double resonance spectroscopy

Pulsed ENDOR spectra (35 GHz) were recorded on a spectrometer

described earlier,[14] equipped with a helium immersion dewar, and all the

measurements were carried out at approximately 2 K. Pulsed ENDOR

measurements employed the three-pulse Mims ENDOR sequence (π/2-τ-π/2-T-

π/2-τ-echo), where the RF was applied during the interval T.

For a nucleus (N) of spin $I = 1/2$ (^{13}C, ^{1}H, ^{15}N) interacting with a $S = \frac{1}{2}$

paramagnetic center, the first-order ENDOR spectrum for a single molecular

orientation is a doublet,

$$v_{\pm} = v_N \pm \frac{A}{2} \qquad (1)$$

centered at v_N, the Larmor frequency, and split by A, the orientation dependent

hyperfine constant, when $v_N > A/2$, as is true here for ^{1}H, ^{13}C, and ^{15}N nuclei.

Similarly, for a deuteron, ^{2}H (I = 1), or ^{14}N (I=1) and ^{17}O (I = 5/2) where ν_N >A/2, as is true here, the first-order ENDOR resonance condition can be written,

$$\nu_{\pm}(\pm) = \nu_D \pm \frac{A}{2} \pm \frac{3P}{2} \qquad (2)$$

where P, is the orientation-dependent quadrupolar splitting. This is the case with ^{2}H and ^{17}O nuclei in the present study. The full hyperfine tensor of a coupled nucleus, both principal values and orientation parameters (Euler angles) with respect to the g-tensor frame, is obtained by simulating the 2-D pattern of orientation-dependent ENDOR spectra recorded across the EPR envelope using the procedures and program described elsewhere.[15-19]

For a nucleus with hyperfine coupling, A, the Mims techniques have a response R that depends on the product, $A\tau$, according to the equation.

$$R \sim \left[1 - \cos(2\pi A \tau)\right] \qquad (3)$$

This function has zeroes, corresponding to minima in the ENDOR response (hyperfine suppression holes), at $A\tau = n$; $n = 0, 1, 2, ...$, and maxima at $A\tau = (2n + 1)/2$; $n = 0, 1, 2, ...,$[15, 16] The hyperfine couplings suppressed by the holes at $A= n/\tau$, $n = 1, 2, 3, ...$ can be adjusted by varying τ. However, the central, $n = 0$, hole at $\nu = \nu_N$ persists regardless. This can be of significance in distinguishing a tensor that is dominated by anisotropic interactions from one that is dominated by isotropic ones. The latter would never predict ENDOR intensity near ν_N, while

the former does so for certain orientations. By suppressing intensity near ν_N, the

$n = 0$. Mims hole diminishes the differences between the two cases.

VIII.3 Results and Discussion

Determination of the SAM-SPL dissociation constant

Equilibrium dialysis proved successful in obtaining a dissociation constant

(K_d) for SPL and SAM. Table VIII.1 shows the K_d results from experiments run at

various concentrations of SAM. Dissociation constants were calculated by using

formula (4).

$$K_d = [SAM] * [SPL] / [SPL-SAM] \qquad (4)$$

Sample Set	1	2	3	4
[SAM]	250 µM	250 µM	250 µM	250 µM
[SPL]	75 µM	125 µM	175 µM	250 µM
$K_{d\text{-SAM}}$	225 µM	175 µM	210 µM	185 µM

Table VIII.1 Table of dissociation constants calculated from varying amounts of SPL during equilibrium dialysis. This yielded an average K_d = 200 µM ± 25 µM.

Averaging the results from the different experiments yields a K_d = 200 µM ± 25

µM. By finding the dissociation constant for the SPL-SAM interaction, it can than

be compared to other K_ds of the radical SAM superfamily and provide insight into

the mechanism of SPL. Work on biotin synthase showed a low K_d similar to SPL,

150

with K_d= 100 ± 20 μM in the absence of dethiobiotin and K_d = 2.3 ± 2 μM in the presence of the substrate dethiobiotin.[20] As the substrate for SPL, SP, is not as easy to produce or quantify, no experiments were carried out in the presence of SP lesions. However, if SPL is similar to biotin synthase, an increase in binding affinity should be seen in the presence of it substrate, similar to that of biotin synthase. Synthetically produced SP would allow for the easy manipulation of the equilibrium dialysis experiments and such work is ongoing in our lab.

Initial Results from Q-band EPR of reduced SPL

Initial results from the Q-band EPR of reduced SPL shows the presence of a $[4Fe-4S]^{1+}$ cluster similar to that observed for the X-band EPR observed in chapter IV (Figure VIII.1 and 2). However, the addition of unlabeled SAM dramatically alters the shape of the EPR spectrum. Addition of the labeled SAMs produce spectra that are similar to the reduced SAM but also contains some high spin signals.

Initial ENDOR results

ENDOR data collection has yet to be completed for ENDOR spectroscopy for samples containing labeled SAM or unlabeled SAM. This work is still in progress and as of yet has revealed no signals due to low coupling between SPL and AdoMet. The absence of the ENDOR signal could be caused by a lack of SAM binding to the iron sulfur cluster or due to a weak signal strength.
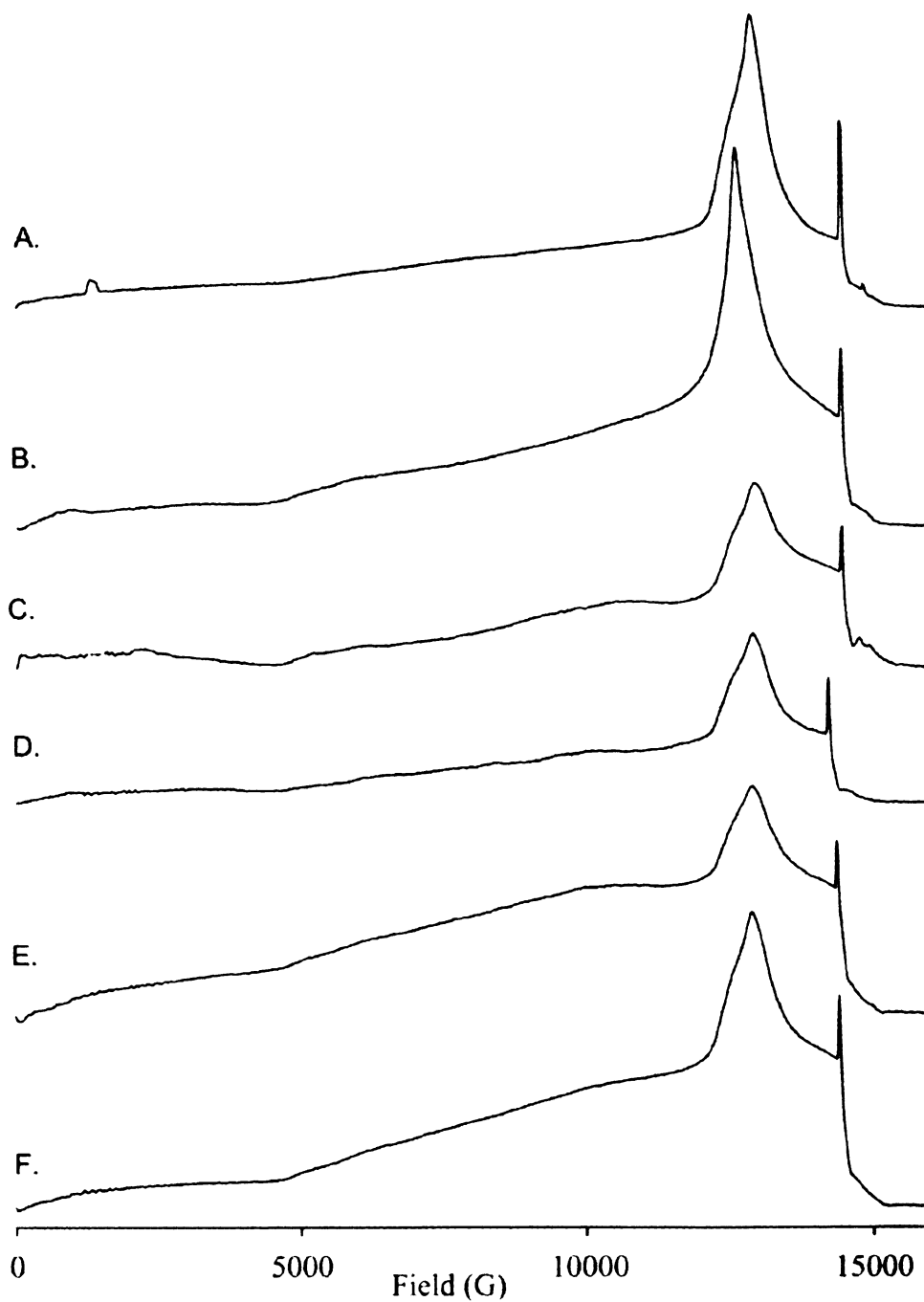
Figure VIII.1 35 GHz CW EPR absorbance spectra of SPL in the absence and presence of SAM A. Reduced SPL. B. Reduced SPL with non-labeled SAM. C-F. Reduced SPL with labeled SAM, (C.) ^{17}O SAM; (D.) ^{15}N SAM; (E.) methyl ^{13}C SAM; (F.) methyl ^{2}H SAM.
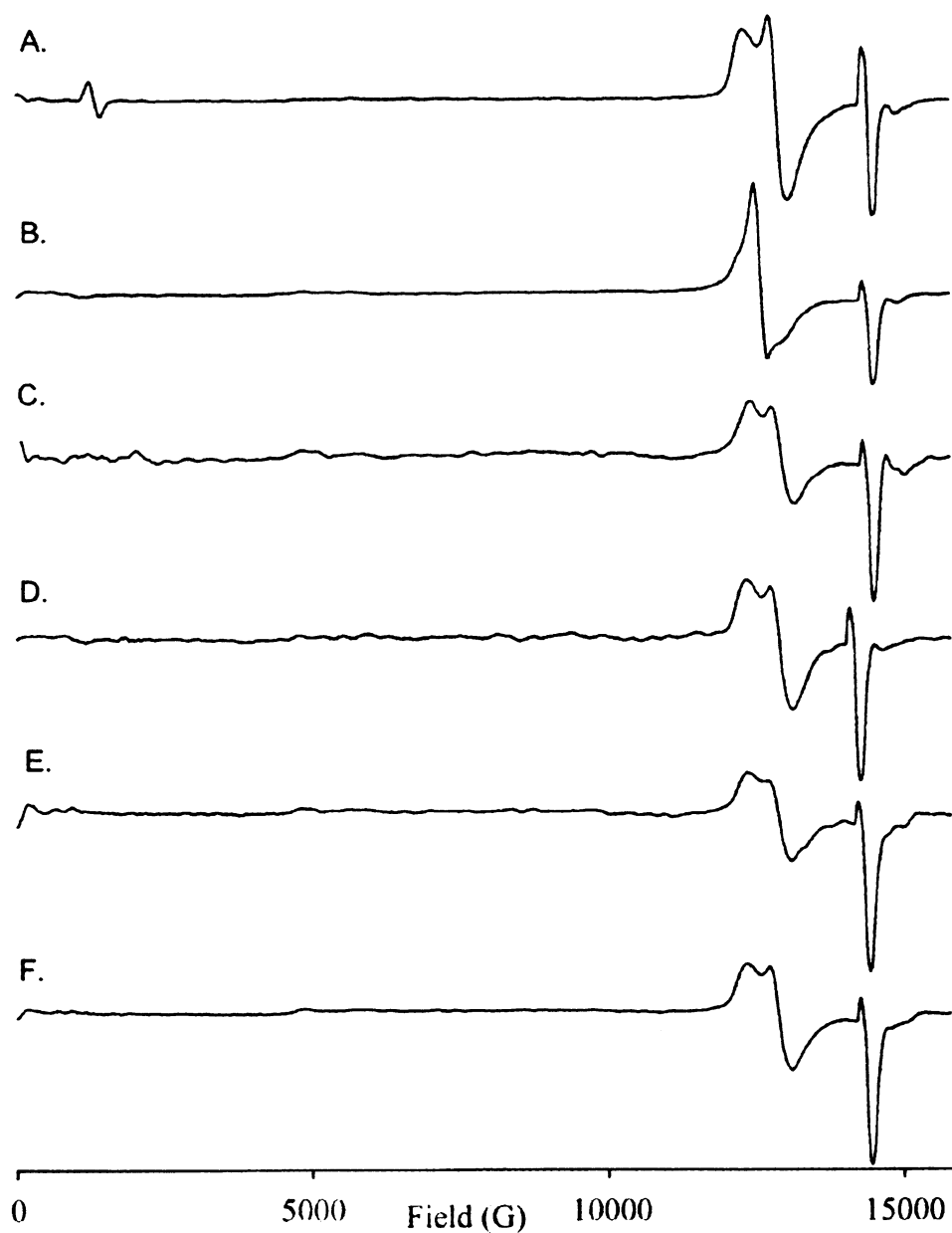
Figure VIII.2 35 GHz CW EPR derivative spectra of SPL in the absence and presence of SAM A. Reduced SPL. B. Reduced SPL with non-labeled SAM. C-F. Reduced SPL with labeled SAM, (C.) ^{17}O SAM; (D.) ^{15}N SAM; (E.) methyl ^{13}C SAM; (F.) methyl ^{2}H SAM.

VIII.4 Conclusions

Equilibrium dialysis experiments have shown SPL to have a dissociation constant with SAM of 200 ± 25 μM, which is in the range of that observed for BioB. Further experiments are needed using synthesized SP to see whether binding becomes tighter in the presence of substrate as it does in the case of BioB when dethiobiotin is added.[20] The relatively low binding affinity of SPL to SAM could be caused by the lack of substrate or the lack of DNA in the samples or both. Either of these additions might cause tighter binding of SPL to SAM. The expectation is that substrate binding alters the protein confirmation and allows tighter SAM binding.

Q-band EPR of SPL shows several interesting phenomenon that are difficult to explain without further experimentation. The observance of the much altered spectrum of reduced SPL with non-labeled SAM, which is not observed at X-band, is perplexing and could result from sample contamination or an altered SAM binding coordination.

No ENDOR signals have been observed to date and work is in progress.

VIII.5 References

1.   Cheek, J.; Broderick, J. B., Adenosylmethionine-dependent iron-sulfur enzymes: versatile clusters in a radical new role. *Journal of biological inorganic chemistry* **2001**, 6, (3), 209-26.

2.   Krebs, C.; Broderick, W. E.; Henshaw, T. F.; Broderick, J. B.; Huynh, B. H., Coordination of Adenosylmethionine to a Unique Iron Site of the [4Fe-4S] of Pyruvate Formate-Lyase Activating Enzyme: A Moessbauer Spectroscopic Study. *Journal of the American Chemical Society* **2002**, 124, (6), 912-913.

3.   Walsby, C. J.; Hong, W.; Broderick, W. E.; Cheek, J.; Ortillo, D.; Broderick, J. B.; Hoffman, B. M., Electron-Nuclear Double Resonance Spectroscopic Evidence That S-Adenosylmethionine Binds in Contact with the Catalytically Active [4Fe-4S]$^+$ Cluster of Pyruvate Formate-Lyase Activating Enzyme. *Journal of the American Chemical Society* **2002**, 124, (12), 3143-3151.

4.   Walsby, C. J.; Ortillo, D.; Broderick, W. E.; Broderick, J. B.; Hoffman, B. M., An Anchoring Role for FeS Clusters: Chelation of the Amino Acid Moiety of S-Adenosylmethionine to the Unique Iron Site of the [4Fe-4S] Cluster of Pyruvate Formate-Lyase Activating Enzyme. *Journal of the American Chemical Society* **2002**, 124, (38), 11270-11271.

5.   Walsby, C. J.; Ortillo, D.; Yang, J.; Nnyepi, M. R.; Broderick, W. E.; Hoffman, B. M.; Broderick, J. B., Spectroscopic Approaches to Elucidating Novel Iron-Sulfur Chemistry in the "Radical-SAM" Protein Superfamily. *Inorganic Chemistry* **2005**, 44, (4), 727-741.

6.   Cosper, N. J.; Booker, S. J.; Ruzicka, F.; Frey, P. A.; Scott, R. A., Direct FeS Cluster Involvement in Generation of a Radical in Lysine 2,3-Aminomutase. *Biochemistry* **2000**, 39, (51), 15668-15673.

7.   Cosper, M. M.; Cosper, N. J.; Hong, W.; Shokes, J. E.; Broderick, W. E.; Broderick, J. B.; Johnson, M. K.; Scott, R. A., Structural studies of the interaction of S-adenosylmethionine with the [4Fe-4S] clusters in biotin synthase and pyruvate formate-lyase activating enzyme. *Protein Science* **2003**, 12, (7), 1573-1577.

8.   Voet, D.; Voet, J. G., *Biochemistry*. 2nd ed.; John Wiley & Sons: New York, 1995.

9.   Werst, M. M.; Kennedy, M. C.; Houseman, A. L. P.; Beinert, H.; Hoffman, B. M., Characterization of the iron-sulfur [4Fe-4S]$^+$ cluster at the active site of aconitase by iron-57, sulfur-33, and nitrogen-14 electron nuclear double resonance spectroscopy. *Biochemistry* **1990**, 29, (46), 10533-40.

10. Telser, J.; Emptage, M. H.; Merkle, H.; Kennedy, M. C.; Beinert, H.; Hoffman, B. M., Oxygen-17 electron nuclear double resonance characterization of substrate binding to the 4-iron-4-sulfur ([4Fe-4S]$^{1+}$]) cluster of reduced active aconitase. *Journal of Biological Chemistry* **1986,** 261, (11), 4840-6.

11. Werst, M. M.; Kennedy, M. C.; Beinert, H.; Hoffman, B. M., Oxygen-17, proton, and deuterium electron nuclear double resonance characterization of solvent, substrate, and inhibitor binding to the iron-sulfur [4Fe-4S]$^{+}$ cluster of aconitase. *Biochemistry* **1990,** 29, (46), 10526-32.

12. Lee, H. I.; Benton, P. M. C.; Laryukhin, M.; Igarashi, R. Y.; Dean, D. R.; Seefeldt, L. C.; Hoffmann, B. M., The interstitial atom of the nitrogenase FeMo-cofactor: ENDOR and ESEEM show it is not an exchangeable nitrogen. *J. Am. Chem. Soc.* **2003,** 125, 5604-5605.

13. Que, L., *Physical Methods in Bioinorganic Chemistry*. University Science Books: Sausilito, CA, 2000.

14. Davoust, C. E. D., P. E.; Hoffman, B. M., *J. Magne. Reson.* **1996,** 119, 38.

15. Mims, W. B., *In Electron Spin-Echoes*. Plenum Press: New York, 1972.

16. Mims, W. B., *Proc. R. Soc. London B* **1965,** 283, 452.

17. Hoffman, B. M.; Venters, R. A., *J. Magn. Reson.* **1984,** 59, 110.

18. Hoffman, B. M.; Martinsen, J., *J. Magn. Reson.* **1985,** 62, 537.

19. Hoffman, B. M., *Acc. Chem. Res.* **1991,** 24, 164.

20. Ugulava, N. B.; Kendra, F. K.; Jarrett, J. T., Control of Adenosylmethionine-Dependent Radical Generation in Biotin Synthase: A Kinetic and Thermodynamic Analysis of Substrate Binding to Active and Inactive Forms of BioB. *Biochemistry* **2003,** 42, (9), 2708-2719.

CHAPTER IX

GENERAL CONCLUSIONS AND FUTURE DIRECTIONS

IX.1   The Iron Sulfur Cluster of SPL

Iron sulfur clusters have been found in a multitude of proteins and in nearly all forms of life on the planet.[1, 2] These clusters are involved in a diverse range of chemistry and the type and oxidation state of the cluster found in an enzyme can give important insight into the role the cluster plays in the protein. Previously published work on SPL has shown it to contain an iron sulfur cluster, however, this work was carried out with inactive protein after cluster reconstitution.[3] Our work reported herein is the first to examine the as-isolated active iron sulfur cluster of SPL.

UV/Vis spectroscopy of the purified SPL shows a spectrum characteristic of an iron sulfur cluster containing protein, with broad features between 300 and 600 nm, to which extinction coefficients at 410 nm and 450 nm of 11.9 and 10.5 $mM^{-1}cm^{-1}$ can be assigned. Addition of the reductant, sodium dithionite, causes a decrease in signal characteristic of a redox active iron sulfur cluster. EPR spectroscopy further confirmed the presence of an iron sulfur cluster and was able to give a more complete description of its state. EPR of the as isolated SPL showed a isotropic signal centered at g = 2.02 that is characteristic of a [3Fe-

4S]$^{1+}$ cluster. Spin quantification shows that this cluster accounted for ~35% of the iron present in the protein. Upon chemical reduction, there is a significant change in the EPR spectrum of SPL, a nearly axial signal is observed with g_z = 2.025, g_y = 1.928, and g_x = 1.890. This is characteristic of a [4Fe-4S]$^{1+}$ cluster. Addition of the enzymes cofactor SAM caused no change is the signal's shape but rather a reduction in intensity. The spin quantification of these spectra showed the [4Fe-4S]$^{1+}$ cluster to account for approximately of 54% and 11%, respectively of the iron present in the protein.

Mössbauer spectroscopy was also employed to look at the cluster states as EPR can only look at those states that have an unpaired electron. Mössbauer of the as isolated cluster yielded a result that 53% was in the [2Fe-2S]$^{2+}$ state and the rest is in the [3Fe-4S]$^{1+}$ state. Mössbauer of the chemically reduced SPL like the EPR spectrum, is dramatically altered and shows a mixture of 90% [4Fe-4S]$^{1+}$ and 10% [4Fe-4S]$^{2+}$. The large isomer shift observed in the spectrum of the reduced SPL indicates an electron rich environment. This electron rich environment would facilitate electron transfer from cluster to the C-S bond of SAM. This supports the proposal that SPL and the radical SAM superfamily in general use a [4Fe-4S]$^{1+}$ cluster to deliver an electron to AdoMet, cleaving the C-S bond to form a putative adenosyl radical and methionine.

IX.2 Catalytic activity of SPL

Previous reports of SPL did not provide a specific activity of the enzyme[3-6] and other reports of SPL activity with SP not incorporated into a DNA helix,[7] show a somewhat low activity. In this report, we provide a specific activity of SPL with the SP lesion in a DNA backbone of plasmid DNA and correlate this activity to the amount of $[4Fe-4S]^{1+}$ cluster present.

Our initial time course assays for SPL provide an activity of 0.33 μmol SP repaired/min/mg SPL. Although earlier publications do not specify a specific activity for SPL, by looking at the results we were able to calculate a specific activity for some of these experiment and it is almost 1000 fold lower than what we have calculated here, possibly because of low Fe-S cluster content and aerobic conditions in their work.[6] They also carried out their assay overnight, which may have been longer than necessary to repair the DNA.

Despite the high activity of SPL shown above, EPR studies have shown that it is very difficult to reduce the cluster 100% even with a substantial amount of chemical reductant added. Therefore, we reduced SPL prior to use in the assay and monitored the reduction by EPR. This protein was then used in repair assays. Not surprisingly, by reducing the protein before use in repair assays, an increase in activity to 1.33 μMol SP repaired/min/mg SPL was seen and 2.4 μmol SP repaired/min/mg when corrected for the amount of $[4Fe-4S]^{1+}$ cluster. There are several implications of these observations. With the enzyme showing an increase in activity corresponding to an increase in the amount of reduced

cluster, it is reasonable to conclude that the $[4Fe-4S]^{1+}$ cluster is the active state

of SPL. This conclusion is supported by the evidence for other members of the

radical SAM superfamily using the $[4Fe-4S]^{1+}$ cluster as the active cluster form.[8,

9] It also consistent with a mechanism in which an electron from the electron rich

iron sulfur cluster is transferred to the electron deficient sulfonium atom of

AdoMet to cause homolytic cleavage of the C-S bond to form the putative

adenosyl radical and initiate radical catalysis.

IX.3   Mechanism of SPL

While many of the enzymes in the radical SAM superfamily utilize AdoMet

as a substrate including biotin synthase[10] and pyruvate formate lyase activating

enzyme[8], another well characterized enzyme, lysine 2,3-aminomutase[11], utilizes

SAM as a catalytic cofactor. Mehl and Begley first published in 1999 a

mechanism in which SPL was used as a catalytic cofactor.[12] This mechanism

was later supported by evidence from Cheek and Broderick showing that tritium

transfers from SP C-6 to SAM during SP repair.[13]

The mechanism proposed in Scheme VI.1 also predicts that a hydrogen

atom from a 5'-deoxyadenosine intermediate is abstracted by the product

thymine radical (Scheme VI.1). If correct, this predicts that the label from 5'-

tritiated SAM should be transferred to repaired thymine. To support this, we

synthesized AdoMet that was labeled at the 5'- position and looked for

incorporation into thymine after SP repair. A peak was observed at the location of

thymine after HPLC separation of the repair reaction; the quantity of label transfer was consistent with an isotope affect of ~15.8, based on the specific activity of SPL and the amount of tritium incorporated into the SAM. This transfer from SAM to thymine during repair further supports the mechanism proposed.

Based on the mechanism originally proposed by Mehl and Begley, AdoMet acts as a cofactor, if this is true, no SAM should be cleaved irreversibly to 5'-deoxyadenosine and methionine. Studies in this report show that after multiple turnover and SP repair, only a small fraction of SAM is cleaved even after 24 hours. This evidence of essentially no irreversible SAM cleavage in addition to other studies in our lab that show a single SAM can repair upwards of 400 SP lesions[13, 14] strongly supports a repair mechanism in which SAM is utilized as a cofactor.

Other mechanistic studies described in this work examined the isotope effect of initial H atom abstraction from the C-6 ring of thymine. By labeling the SP at C-6 position and looking at the amount of tritium transfer at 0%, 25%, 50% and 100% repair we observe an isotope affect of ~15-17, showing that initial H atom abstraction to be a slow step in the reaction pathway. Furthermore, we have calculated the amount of label transfer expected from our labeled C-6 SP to SAM if 100% of the SP is repaired and 100% of the tritium is transferred from SP to SAM. We observe that only 50% of the total amount of label is transferred from the C-6 labeled SP to SAM. One of the predictions that could be made from this result is that SP is formed in a non-stereospecific manner. If this is the case, then the C-6 tritium label will have a stereochemistry that is 50% R and 50% S. It then

follows that SPL stereospecifically abstracts the tritium from either 100% of the R isomer or 100% of the S isomer, leaving 50% of the label in the repaired thymine and 50% of the label gets transferred to SAM. In this scenario, SP is formed non-stereospecifically, and SPL repairs SP stereospecifically.

Our overall conclusion is that experimental evidence in our lab supports the original mechanism proposed by Mehl and Begley[12] in which the H atom is abstracted from the C-6 of thymine stereospecifically by the 5'-deoxyadenosyl radical created by reductive cleavage of AdoMet. The subsequent C-6 radical undergoes a radical mediated β-scission, causing the C-C bond to break and leaving a radical on the methyl group. This radical re-abstracts a hydrogen from the 5'-deoxyadenosine to reform the 5'-deoxyadenosyl radical which in turn can interact with methionine to reform SAM.

IX.4   Interaction of DNA and SPL

Most proteins that act upon DNA, either as promoters, inhibitors, replicators or repairers first bind to the DNA and than find the specific sequence or base pair(s) where they will perform their task.[15] Often times this non-specific interaction is what allows the enzyme to quickly act upon the DNA base pairs of interest.[15] SPL has been shown to be no different and reports herein have shown it capable of binding to DNA in the absence of spore photoproduct with or without the enzymes cofactors, SAM and an iron sulfur cluster.

As SPL has C-terminal homology to the repair enzyme DNA photolyase and amino acid residues consistent with a helix-turn-helix DNA binding motif

similar to DNA photolyase[16], it is likely that SPL binds non-specifically to the DNA via this motif. Studies with DNA photolyase have shown the protein binding to DNA via the helix-turn-helix motif of the C-terminus with the damaged DNA bases flipped out of the DNA double helix and into the protein's active site.[17] This is likely the same mechanism by which SPL recognizes the damaged lesion as well, with the thymine bases flipped out of the helix and into the active site near SAM.

IX.5   An Overview of Spore Photoproduct Repair

Evidence provided above and similarities to other DNA repair enzymes and enzymes in the radical SAM superfamily can provide us with a hypothesis for a complete picture of SPL-catalyzed repair of the spore photoproduct lesion.

After the sporulation and production of the SASPs, which binds to the chromosomal DNA with a high affinity under spore like conditions (i.e. pH ~6.5 with dipicolinic acid and Ca^{2+}), the DNA converts to an A-like conformation.[18-21] Exposure to ultra-violet light, while in the spore form, causes the DNA lesion spore photoproduct to form, possibly because of the conformation change provided by SASPs binding the DNA.[22, 23]

When conditions favor spore germination, the pH of the spore changes back to ~7.5 and the SASP is degraded[24], causing it to unbind the DNA, which changes the conformation back to B. SPL can then non-specifically bind to the DNA via a helix-turn-helix motif at the C-terminus and begin searching for SP lesions. Similar to cyclobutane dimers and 6'-4' photoproducts[16, 17], it is likely

that the damaged dimer is flipped out of the DNA helix where SPL can recognize and bind to the SP lesion. The SP dimer is positioned close to the active site of SPL near SAM and the $[4Fe-4S]^{1+}$ cluster. Once in position, the Fe-S cluster donates an electron to the C-S bond of AdoMet and causes homolytic SAM cleavage, creating a 5'-deoxyadenosyl radical.

The newly formed radical species abstracts a hydrogen from the C-6 ring position of thymine, which than attacks the methylene bridge of the SP lesion. The methylene bridge is cleaved and a radical is formed on the methyl group. This radical reabstracts a hydrogen from 5'-deoxyadenosine to reform the adenosyl radical and can then interact with methionine to remake AdoMet. This is illustrated in Scheme VI.1. With the lesion repaired, SPL can move along the helix again to repair more SP lesions.

IX.6   Implications For DNA Repair And Similarities To DNA Photolyase

In addition to being consistent with our current understanding of SPL, the mechanistic proposal from the previous section (IX.5) displays intriguing parallels to the proposed mechanism for DNA photolyase. In both cases, radical chemistry is used to cleave a covalent pyrimidine dimer, with the DNA photolyase using radical anion chemistry and SPL using neutral radical chemistry. These two enzymes, however, use very different mechanisms by which to initiate the radical chemistry as follows: NADH, a secondary cofactor, and light in the case of DNA photolyase, and an iron sulfur cluster and AdoMet in the case of SPL. Thus, radical chemistry is not only a significant source of DNA damage but is also an

important means of repairing DNA damage *in vivo*. It is intriguing that such vastly different cofactors are utilized to perform what is quite similar chemistry. By analogy to what Beinert[25] has proposed for other enzyme systems, perhaps the F-S/AdoMet cofactor combination found in SPL is a primitive "holdover" from more anaerobic times, and the NADH and light-driven reaction is a more modern adaptation.

IX.7 Further Experiments: Protein Crystallography

A fundamental tool when examining enzymes and proteins is x-ray crystallography. By first crystallizing a protein out of solution and than exposing it to x-rays and viewing their diffraction through the crystal, a pattern emerges that can be solved to obtain the three dimensional structure of the protein. This technique has been widely applied to both organic and inorganic materials as well as proteins to solve their three dimensional atomic structures. X-ray crystallography has been responsible for the majority of known protein structures.[26]

Crystallization of macro-molecules such as proteins is not a trivial manner and can require extensive manipulation of buffering conditions and different crystallization techniques. For the crystallization to be successful, the protein in question must be free of contaminants and in a homogeneous state. After crystallization, the crystals produced must generally be of a resolution of 4 Å or better to allow for the successful solution of the 3-D structure.[26]

Work on the protein crystallization of SPL is currently under way. Samples of purified SPL were prepared with an iron content of 3.0 Fe/protein and 5 mM AdoMet as stated in Chapter II followed by concentration to 25 mg/mL. These samples are currently undergoing crystallization studies with our collaborators in the Drennan lab at MIT. Currently, no suitable crystals have been obtained although some poor crystals of SPL have resulted but can not be used for X-ray diffraction. If successful, the crystal structure would confirm the probe of an interaction between SAM and the iron sulfur cluster as well as examine the presence of the helix-turn-helix binding motif.

IX.8   Further Experiments: Synthesis of Synthetic Spore Photoproduct

It is both difficult and time consuming to create the tritiated SP in the pUC18 plasmid that is used for repair assays in this work. In addition it is difficult to control the amount of SP produced and used in each activity assay. It is therefore very desirable to produce a synthetic spore photoproduct.

Work on the synthesis of spore photoproduct was initially carried out in the Begley lab[27], however, these experiments did not provide any evidence for repair activity using SPL. More recent studies have shown repair of a synthesized SP lesion but the activity was relatively low and SPL could only repair one of the two isomers produced.[28] Neither of these reports incorporated a phosphate group in between the dimers or incorporation of SP into a DNA strand, making them far from ideal substrate models for SP. New reports have shown SPL to repair the

166

synthetically produced SP with a phosphate linker but still have not incorporated it into a DNA strand to produce an ideal model of the SP lesion.[29]

Work is, therefore, in progress in our lab to synthesize an SP lesion and incorporate it into a DNA strand and to use this for further studies of SPL, including kinetic and mechanistic assays as well as spectroscopic studies. A synthetic SP lesion could also be used in coordination with X-ray crystallization studies to obtain a structure with a bound DNA substrate similar to what was obtained with DNA photolyase and a cyclobutane dimer.[17]

IX.9   Further Experiments: EXAFS studies of SPL

Extended X-ray absorption fine structure spectroscopy has been carried out on several members of the radical SAM superfamily, including LAM[30, 31], PFL-AE[32] and biotin synthase[32]. In the studies with LAM, EXAFS has shown and interaction between the Fe of the cluster and selenium used in the place of sulfur in AdoMet.[31] However, work on both PFL-AE and biotin synthase, did not show this interaction[32], leading to the possibility that members of the radical SAM superfamily that use AdoMet as a catalytic cofactor interact with AdoMet differently than those that use it as a substrate.

It would therefore be interesting to apply EXAFS to SPL and see if the interaction between the selenium and Fe exists as it does for LAM and if this correlates to AdoMet's role as a catalytic cofactor in these enzymes. Currently, we have synthesized a suitable amount of seleno-SAM by using seleno-

methionine in our synthesis reaction in the place of methionine and have produced ~20 mg for use. However, EXAFS have not been carried out because of the difficulty in obtaining a sufficiently high concentration of SPL for the experiment. It is expected that a concentration of at least 1 mM SPL would be needed to observe the interaction with EXAFS and this has not been obtained.

IX.10 Further Experiments: DNA Binding Studies

Past studies have shown SPL to bind to the SP lesion by DNA footprinting[6] however this work was carried out with protein that was either reconstituted or did not contain a stoichiometric amount of iron. Work carried out in this report has shown SPL to bind non-specifically to DNA regardless of cluster content or the presence of SAM. While both of these studies are interesting, further work is needed to fully characterize the SPL-DNA interaction.

Experiments that could be conducted include gel shift assays on DNA oligomers that contain a single SP lesion or multiple SP lesions and if this increases SPL's binding affinity. Apo-SPL also could be used to see if the lack of the iron sulfur cluster lowers the affinity to the SP lesion.

IX.11 References

1. Beinert, H.; Holm, R. H.; Munck, E., Iron-sulfur clusters: nature's modular, multipurpose structures. *Science* **1997**, 277, (5326), 653-659.

2. Beinert, H., Iron-sulfur proteins: ancient structures, still full of surprises. *J. Biol. Inorg. Chem.* **2000**, 5, 2-15.

3. Rebeil, R.; Nicholson, W. L., The subunit structure and catalytic mechanism of the Bacillus subtilis DNA repair enzyme spore photoproduct lyase. *Proceedings of the National Academy of Sciences of the United States of America* **2001**, 98, (16), 9038-43.

4. Fajardo-Cavazos, P.; Salazar, C.; Nicholson, W. L., Molecular cloning and characterization of the Bacillus subtilis spore photoproduct lyase (spl) gene, which is involved in repair of UV radiation-induced DNA damage during spore germination. *Journal of Bacteriology* **1993**, 175, (6), 1735-44.

5. Rebeil, R.; Sun, Y.; Chooback, L.; Pedraza-Reyes, M.; Kinsland, C.; Begley, T. P.; Nicholson, W. L., Spore photoproduct lyase from Bacillus subtilis spores is a novel iron-sulfur DNA repair enzyme which shares features with proteins such as class III anaerobic ribonucleotide reductases and pyruvate-formate lyases. *Journal of Bacteriology* **1998**, 180, (18), 4879-85.

6. Slieman, T. A.; Rebeil, R.; Nicholson, W. L., Spore photoproduct (SP) lyase from Bacillus subtilis specifically binds to and cleaves SP (5-thyminyl-5,6-dihydrothymine) but not cyclobutane pyrimidine dimers in UV-irradiated DNA. *Journal of Bacteriology* **2000**, 182, (22), 6412-7.

7. Friedel, M. G.; Berteau, O.; Pieck, J. C.; Atta, M.; Ollagnier-de-Choudens, S.; Fontecave, M.; Carell, T., The spore photoproduct lyase repairs the 5S- and not the 5R-configured spore photoproduct DNA lesion. *Chemical Communications* **2006**, (4), 445-447.

8. Henshaw, T. F.; Cheek, J.; Broderick, J. B., The [4Fe-4S]1+ Cluster of Pyruvate Formate-Lyase Activating Enzyme Generates the Glycyl Radical on Pyruvate Formate-Lyase: EPR-Detected Single Turnover. *Journal of the American Chemical Society* **2000**, 122, (34), 8331-8332.

9. Hinckley, G. T.; Ruzicka, F. J.; Thompson, M. J.; Blackburn, G. M.; Frey, P. A., Adenosyl coenzyme and pH dependence of the [4Fe-4S]2+/1+ transition in lysine 2,3-aminomutase. *Archives of Biochemistry and Biophysics* **2003**, 414, (1), 34-39.

10. Jarrett, J. T., The novel structure and chemistry of iron-sulfur cluster in the adenosylmethionie-dependent radical enzyme biotin synthase. *Archives of Biochemistry and Biophysics* **2003**, 433, 312-321.

11.   Lieder, K. W.; Booker, S.; Ruzicka, F. J.; Beinert, H.; Reed, G. H.; Frey, P. A., S-Adenosylmethionine-Dependent Reduction of Lysine 2,3-Aminomutase and Observation of the Catalytically Functional Iron-Sulfur Centers by Electron Paramagnetic Resonance. *Biochemistry* **1998**, 37, (8), 2578-2585.

12.   Mehl, R. A.; Begley, T. P., Mechanistic Studies on the Repair of a Novel DNA Photolesion: The Spore Photoproduct. *Organic Letters* **1999**, 1, (7), 1065-1066.

13.   Cheek, J.; Broderick, J. B., Direct H Atom Abstraction from Spore Photoproduct C-6 Initiates DNA Repair in the Reaction Catalyzed by Spore Photoproduct Lyase: Evidence for a Reversibly Generated Adenosyl Radical Intermediate. *Journal of the American Chemical Society* **2002**, 124, (12), 2860-2861.

14.   Buis, J. M.; Cheek, J.; Kalliri, E.; Broderick, J. B., Characterization fo an active spore photoproduct lyase, a DNA repair enzyme in the radical sam superfamily. *Journal of Biological Chemistry* **2006**, In Press.

15.   Halford, S. E.; Marko, J. F., How do site-specific DNA-binding proteins find their targets? *Nucleic Acids Research* **2004**, 32, (10), 3040-3052.

16.   Sancar, A., Structure and Function of DNA Photolyase and Cryptochrome Blue-Light Photoreceptors. *Chemical Reviews* **2003**, 103, (6), 2203-2237.

17.   Mees, A.; Klar, T.; Gnau, P.; Hennecke, U.; Eker, A. P. M.; Carell, T.; Essen, L.-O., Crystal structure of a photolyase bound to a CPD-like DNA lesion after in situ repair. *Science* **2004**, 306, (5702), 1789-1793.

18.   Fairhead, H.; Setlow, P., Binding of DNA to a/b-type small, acid-soluble proteins from spores of Bacillus or Clostridium species prevents formation of cytosine dimers, cytosine-thymine dimers, and bipyrimidine photoadducts after UV irradiation. *Journal of Bacteriology* **1992**, 174, (9), 2874-80.

19.   Douki, T.; Setlow, B.; Setlow, P., Effects of the binding of a/b-type small, acid-soluble spore proteins on the photochemistry of DNA in spores of Bacillus subtilis and in vitro. *Photochemistry and Photobiology* **2005**, 81, (Jan./Feb.), 163-169.

20.   Kosman, J.; Setlow, P., Effects of carboxy-terminal modifications and pH on binding of a Bacillus subtilis small, acid-soluble spore protein to DNA. *Journal of Bacteriology* **2003**, 185, (20), 6095-6103.

21.   Setlow, B.; Setlow, P., Dipicolinic acid greatly enhances production of spore photoproduct in bacterial spores upon UV irradiation. *Applied and Environmental Microbiology* **1993**, 59, (2), 640-3.

22. Setlow, P. *Studies on the role of SASP in heat and radiation resistance of bacterial spores and on regulation of a SASP specific protease*; Health Cent.,Univ. Farmington,CT, USA.: 1990;

23. Mohr, S. C.; Sokolov, N. V. H. A.; He, C.; Setlow, P., Binding of small acid-soluble spore proteins from Bacillus subtilis changes the conformation of DNA from B to A. *Proceedings of the National Academy of Sciences of the United States of America* **1991**, 88, (1), 77-81.

24. Sanchez-Salas, J. L.; Santiago-Lara, M. L.; Setlow, B.; Sussman, M. D.; Setlow, P., Properties of Bacillus megaterium and Bacillus subtilis mutants which lack the protease that degrades small, acid-soluble proteins during spore germination. *Journal of Bacteriology* **1992**, 174, (3), 807-14.

25. Beinert, H., Iron-sulfur proteins: ancient structures, still full of surprises. *Journal of Biological Inorganic Chemistry* **2000**, 5, 2-15.

26. Drenth, J., *Principles of Protein X-Ray Crystallography*. Springer-Verlag Inc: New York, 1999.

27. Nicewonger, R.; Begley, T. P., Synthesis of the spore photoproduct. *Tetrahedron Letters* **1997**, 38, (6), 935-936.

28. Friedel, M. G.; Berteau, O.; Pieck, J. C.; Atta, M.; Ollagnier-de-Choudens, S.; Fontecave, M.; Carell, T., The spore photoproduct lyase repairs the 5S- and not the 5R-configured spore photoproduct DNA lesion. *Chem. Commun.* **2006**, 4, 445-447.

29. Chandor, A.; Berteau, O.; Douki, T.; Gasparutto, D.; Sanakis, Y.; Ollagnier-de-Choudens, S.; Atta, M.; Fontecave, M., Dinucleotide spore photoproduct: A minimal substrate of the DNA repair spore photoproduct lyase enzyme from bacillus subtilis. *J. Biol. Chem.* **2006**, In Press.

30. Chen, D.; Walsby, C.; Hoffman, B. M.; Frey, P. A., Coordination and Mechanism of Reversible Cleavage of S-Adenosylmethionine by the [4Fe-4S] Center in Lysine 2,3-Aminomutase. *Journal of the American Chemical Society* **2003**, 125, (39), 11788-11789.

31. Cosper, N. J.; Booker, S. J.; Ruzicka, F.; Frey, P. A.; Scott, R. A., Direct FeS Cluster Involvement in Generation of a Radical in Lysine 2,3-Aminomutase. *Biochemistry* **2000**, 39, (51), 15668-15673.

32. Cosper, M. M.; Cosper, N. J.; Hong, W.; Shokes, J. E.; Broderick, W. E.; Broderick, J. B.; Johnson, M. K.; Scott, R. A., Structural studies of the interaction of S-adenosylmethionine with the [4Fe-4S] clusters in biotin synthase and pyruvate formate-lyase activating enzyme. *Protein Science* **2003**, 12, (7), 1573-1577.

171